

Learning to Control: The iUzawa-Net for Nonsmooth Optimal Control of Linear PDEs*

Yongcun Song[†] Xiaoming Yuan[‡] Hangrui Yue[§] Tianyou Zeng[¶]

Abstract. We propose an optimization-informed deep neural network approach, named iUzawa-Net, aiming for the first solver that enables real-time solutions for a class of nonsmooth optimal control problems of linear partial differential equations (PDEs). The iUzawa-Net unrolls an inexact Uzawa method for saddle point problems, replacing classical preconditioners and PDE solvers with specifically designed learnable neural networks. We prove universal approximation properties and establish the asymptotic ε -optimality for the iUzawa-Net, and validate its promising numerical efficiency through nonsmooth elliptic and parabolic optimal control problems. Our techniques offer a versatile framework for designing and analyzing various optimization-informed deep learning approaches to optimal control and other PDE-constrained optimization problems. The proposed learning-to-control approach synergizes model-based optimization algorithms and data-driven deep learning techniques, inheriting the merits of both methodologies.

Keywords: Optimal control, PDE, operator learning, deep neural network, universal approximation theorem, nonsmooth optimization, infinite-dimensional optimization, inexact Uzawa method

AMS subject classifications: 49M41, 35Q93, 35Q90, 68T07, 65K05, 41A30

1 Introduction

Optimal control models governed by partial differential equations (PDEs) are crucial for studying complex systems in various areas. Typical examples include optimal design in aerodynamics [46], precision control in chemical processes [12], the development of targeted drug delivery systems in medicine [10], performance optimization in digital twins [2], data assimilation in weather forecasting [17], and stable control in robotic swarms [74], just to name a few. In practice, nonsmoothness naturally arises in optimal control models, see e.g. [30, 42, 45, 66], as constraints and nonsmooth regularizations are often imposed on the control variables to ensure certain desired properties, such as boundedness [42], sparsity [63], and discontinuity [61]. The nonsmooth structure and PDE constraints preclude direct application of standard optimization algorithms, such as conjugate gradient and quasi-Newton methods. Furthermore, emerging applications increasingly demand efficient or even real-time solutions. In this context, classical numerical methods struggle due to the high-dimensional and ill-conditioned algebraic systems arising from mesh-based discretizations, which are computationally expensive to solve. These challenges necessitate carefully designed and problem-specific numerical methods for nonsmooth optimal control problems, especially in real-time scenarios.

1.1 Model

Let $\Omega \subset \mathbb{R}^d$ with $d \geq 1$ be a bounded domain with Lipschitz boundary. We consider the following general optimal control problem initiated in [42] with a linear PDE constraint:

$$\min_{u \in U, y \in Y} \frac{1}{2} \|y - y_d\|_Y^2 + \frac{1}{2} \langle u, Nu \rangle_U + \theta(u), \quad \text{s.t. } y = S(u + f), \quad (1.1)$$

where U and Y are Hilbert spaces; $u \in U$ and $y \in Y$ are the control and state variables, respectively; and $N : U \rightarrow U$ is a linear, bounded, self-adjoint, and positive definite operator with $\langle u, Nu \rangle_U \geq c_0 \|u\|_U^2$ for

*February 13, 2026.

[†]Division of Mathematical Sciences, School of Physical and Mathematical Sciences, Nanyang Technological University, 21 Nanyang Link, 637371, Singapore. This author was supported by the NTU Start-Up Grant. Email: yongcun.song@ntu.edu.sg

[‡]Department of Mathematics, The University of Hong Kong, Pok Fu Lam, Hong Kong SAR, China. This author was partially supported by the Croucher Senior Fellowship. Email: xmyuan@hku.hk

[§]School of Mathematical Sciences, Nankai University, Tianjin 300071, China. This author was supported by the National Natural Science Foundation of China (No. 12301399). Email: yuehangrui@gmail.com

[¶]Department of Mathematics, The University of Hong Kong, Pok Fu Lam, Hong Kong SAR, China. This author was supported by Hong Kong PhD Fellowship Scheme. Email: logic@connect.hku.hk

some constant $c_0 > 0$. The constraint $y = S(u + f)$ represents a well-posed linear PDE defined on Ω with $S : U \rightarrow Y$ being the corresponding linear solution operator and $f \in U$ being an uncontrollable source term¹. We denote by $S^* : Y \rightarrow U$ the adjoint operator of S , which is assumed to be well-defined. The function $y_d \in Y$ represents a given desired state, and the functional $\theta : U \rightarrow \mathbb{R} \cup \{+\infty\}$ is assumed to be convex, lower semicontinuous, proper but *nonsmooth*, which imposes a constraint or regularization on the control variable. Throughout the remainder of this work, we fix $U = L^2(\Omega)$ and $Y = L^2(\Omega)$ for simplicity of presentation.

We treat y_d and f as *parameters* of the problem (1.1), and focus on the challenging scenario where (1.1) needs to be solved *repeatedly* for *many different* parameter instances, and thus real-time solution of each case of (1.1) with fixed $(y_d, f)^\top$ is required². This scenario arises in numerous important applications, including predictive control of PDEs [13, 14], real-time optimal control [6, 8], and numerical studies of optimal control problems [7, 19]. In particular, emerging applications such as digital twins [2, 22, 23, 70] impose stringent real-time requirements on the solution of the underlying virtual models, of which (1.1) constitutes a representative example. Clearly, achieving such demands is typically beyond the capacity of traditional numerical methods, whose common aim is to solve (1.1) with a fixed $(y_d, f)^\top$ via a sequence of iterations while each one usually costs considerable time. This necessitates the development of efficient algorithms capable of solving (1.1) in real time for varying problem parameters $(y_d, f)^\top$.

1.2 Classical Numerical Methods for Problem (1.1)

In the literature, numerous numerical methods have been developed for solving various specific cases of (1.1). Algorithms like semismooth Newton (SSN) methods [67], primal-dual active set methods [36], and interior point methods [68] generally achieve superlinear convergence rate, but entail solving complex subproblems at each iteration, which are often computationally expensive. More recently, first-order algorithms have been applied to solving (1.1), including the alternating direction method of multipliers (ADMM) [20], the primal-dual method [60], the proximal gradient method [56, 55], the Peaceman–Rachford method [19], and the inexact Uzawa method [59]. These algorithms typically incur lower computational cost per iteration, which makes them attractive for large-scale problems. Note that their convergence rate is at most linear, meaning that achieving high-accuracy solutions may require a large number of iterations.

All the above algorithms rely heavily on mesh-based discretization schemes for implementation, e.g., finite element methods (FEMs) and finite difference methods (FDMs). Such discretizations give rise to large-scale algebraic systems or optimization subproblems at each iteration, which typically require iterative solvers, resulting in nested (multi-layer) iterations. Moreover, the condition numbers of the resulting subproblems often deteriorate as the mesh is refined, making their numerical solutions computationally demanding or even prohibitive. To mitigate the aforementioned difficulties, various preconditioned numerical methods have been developed in the literature, see, e.g., [29, 48, 50, 54, 59, 64, 65]. The effectiveness and efficiency of these algorithms critically depend on the appropriate choice of preconditioners. In particular, the design of effective preconditioners requires a delicate balance between computational cost and convergence enhancement. It must account for the specific mathematical structure of the problem at hand, often necessitating case-by-case analysis and sophisticated problem-dependent design.

It is noteworthy that classical numerical methods are capable of computing highly accurate solutions. However, they are typically designed for the problem (1.1) with fixed parameters y_d and f , and any change in the parameters necessitates solving (1.1) from scratch. In such cases, classical methods become computationally expensive and are unable to produce real-time solutions.

1.3 Physics-Informed Neural Networks and Operator Learning for Problem (1.1)

Several deep learning approaches applicable to solving (1.1) have been proposed, including physics-informed neural networks (PINNs) [18, 37, 61] and operator-learning-based methods [60, 62], which differ from classical numerical methods in that they are generally mesh-free, easy to implement, and flexible to adapt to various concrete examples of (1.1). In [37], the hard-constraint PINNs were proposed for solving control-constrained

¹We adopt the conventional formulation in which u and f are treated as distinct variables, representing the controllable and uncontrollable parts of the PDE parameter, rather than absorbing f into u through a change of variables.

²For simplicity, we focus on the parameters y_d and f . Our methodology can be easily generalized if other parameters in (1.1) are considered, e.g., the boundary values and initial values.

optimal control problems with interfaces. In [61], PINNs were incorporated within the ADMM for solving the resulting optimal control subproblem in each ADMM iteration. In [18], a Prox-PINNs framework was proposed for solving general elliptic variational inequalities, which covers (1.1) as a special case. Several operator-learning-enhanced primal-dual approaches were proposed in [60, 62] for solving (1.1) with $N = \alpha I$ for some $\alpha > 0$, with [60] focusing on linear PDE constraints and [62] addressing nonlinear PDE constraints. They embed deep-learning-based PDE solvers within traditional primal-dual algorithms, accelerating the solution of PDE subproblems by replacing classical iterative PDE solvers with forward passes of deep neural networks. The combination of computational efficiency, accuracy, and generalization ability makes operator learning particularly suitable for tasks requiring frequent, computationally intensive evaluations.

Notably, the PINNs-based methods discussed above require training a neural network from scratch for solving (1.1) with each different problem parameter $(y_d, f)^\top$. For operator learning methods, current approaches embed neural surrogate models as subroutines for solving PDE subproblems into traditional optimization algorithms, which still require manual design of the stepsizes and preconditioners. The resulting algorithms usually require a large number of iterations to converge, as indicated in [37, 62]. Additionally, operator learning methods for PDEs, such as Fourier Neural Operators (FNOs) [40], could in principle be used to learn the mapping from the problem parameters $(y_d, f)^\top$ to the optimal control u^* . However, these operator learning methods are purely data-driven and do not exploit the mathematical structure of (1.1). As a result, they often lack interpretability and achieve only limited accuracy in solving (1.1), as validated in Section 6.

1.4 Optimization-Informed Neural Networks

Optimization-informed neural networks, also known as algorithm unrolling for finite-dimensional models, originated in [21] as data-driven methods for solving optimization problems. The core idea of algorithm unrolling is to design a neural network where each layer mirrors an iteration of a traditional optimization algorithm. The resulting neural network can be viewed as being unrolled from traditional optimization algorithms; hence, the interpretability and robustness of its architecture can be increased. In particular, all the hyperparameters in the blueprint optimization algorithms, such as stepsizes and preconditioners, are treated as learnable parameters in the neural networks and are automatically optimized during the training process.

Various algorithm-unrolled neural networks have been proposed for finite-dimensional optimization problems, including the learned iterative shrinkage-thresholding algorithm (LISTA) [21], unrolled proximal gradient descent methods [31], unrolled ADMM [71, 72], and unrolled primal-dual methods [1, 39]. Notably, in these neural networks, only a few layers are required to achieve satisfactory numerical accuracy, in contrast to their blueprint optimization algorithms that often require relatively many iterations. We refer to [24, 57, 58] for a comprehensive review of the recent advances in algorithm unrolling for finite-dimensional problems and its various applications.

A straightforward application of the above works to (1.1) requires discretizing the underlying infinite-dimensional input and output function spaces into finite-dimensional ones. However, neural network models trained on a specific discretization generally do not generalize well to other discretizations, which can significantly degrade the numerical accuracy. Consequently, developing optimization-informed neural networks that are capable of operating directly in infinite-dimensional settings with PDE constraints becomes a problem of significant interest and importance, yet limited work has been done in this direction. In [35], the authors proposed a generative neural operator for approximating mappings from the space of convex and Gâteaux differentiable functions to Hilbert spaces, which can be applied to solve parameterized unconstrained convex optimization problems. However, this method requires evaluating the objective functional and performing adaptive sampling in each forward pass. In (1.1), evaluating the objective functional entails solving PDEs, which makes such forward passes prohibitively expensive and renders this approach impractical. To the best of our knowledge, there is currently no optimization-informed neural network architecture that is practically effective for solving the PDE-constrained optimal control problem (1.1).

1.5 Methodology

We propose an optimization-informed neural network architecture, termed **iUzawa-Net**, for efficiently solving the optimal control problem (1.1). Structurally, the **iUzawa-Net** is composed by stacking layers that mirror an inexact Uzawa method for solving (1.1). This approach generalizes the unrolling technique introduced in [21] to infinite-dimensional settings, while incorporating recent advances in deep learning for approximating mappings between function spaces. As a result, the **iUzawa-Net** serves as a neural surrogate model for the *solution operator* of (1.1), defined as the parameter-to-control mapping

$$T : Y \times U \rightarrow U, \quad (y_d, f)^\top \mapsto u^*, \quad (1.2)$$

where u^* is the optimal control of (1.1) corresponding to the problem parameter $(y_d, f)^\top$. After training, we perform an efficient forward pass of the trained surrogate model to approximate $T(y_d, f)$ for each input parameters y_d and f , hence numerically solving (1.1) in real-time. In the following, we briefly outline the design of the **iUzawa-Net** and detail its implementation in Section 2.

1.5.1 An inexact Uzawa method for (1.1)

We start with the saddle-point problem reformulation of (1.1):

$$\min_{u \in U} \max_{p \in Y} \frac{1}{2} \langle u, Nu \rangle_U + \theta(u) + \langle p, Su \rangle_Y - \frac{1}{2} \|p\|_Y^2 - \langle p, y_d - Sf \rangle_Y, \quad (1.3)$$

where $p \in Y$ is the associated Fenchel dual variable. It is well-known that, for any given $(y_d, f)^\top \in Y \times U$, (1.3) admits a solution $(u^*, p^*) \in U \times Y$ by the Fenchel-Rockafellar duality [4, Section 15.3], and the solution is unique due to the strict convexity and concavity of (1.3) with respect to u and p , respectively. Hence, the solution operator T in (1.2) is well-defined. Furthermore, (1.3) admits the following necessary and sufficient optimality condition:

$$0 \in Nu^* + \partial\theta(u^*) + S^*p^*, \quad 0 = Su^* - p^* - (y_d - Sf). \quad (1.4)$$

Inspired by [9, 16, 59], we consider the following inexact Uzawa algorithm for (1.1):

$$\begin{cases} u^{k+1} = (Q_A + \partial\theta)^{-1} ((Q_A - N) u^k - S^* p^k), \\ p^{k+1} = p^k + Q_S^{-1} (Su^{k+1} - p^k + Sf - y_d), \end{cases} \quad (1.5)$$

where $Q_A : U \rightarrow U$ and $Q_S : Y \rightarrow Y$ are two self-adjoint positive definite operators preconditioning on N and $SN^{-1}S^* + I$, respectively. The convergence of (1.5) is guaranteed for any choice of preconditioners satisfying $Q_A \succeq N$ and $Q_S \succeq SN^{-1}S^* + I$; this follows from a straightforward extension of the analysis in [59].

To implement (1.5), one needs to construct the preconditioners Q_A and Q_S and solve two PDEs $z^k = S^*p^k$ and $y^{k+1} = Su^{k+1}$ at each iteration. With suitable choices of Q_A and Q_S , the inexact Uzawa method (1.5) efficiently solves (1.1) with fixed y_d and f . In practice, the scheme (1.5) involves a trade-off between the algebraic measurement of convergence speed in terms of the outer iterations and the computational cost of each inner iteration. Balancing these effects relies on carefully designing the preconditioners Q_A and Q_S , which typically requires problem-dependent tuning.

1.5.2 iUzawa-Net: an overview

The **iUzawa-Net** is designed by converting the iterative structure of (1.5) into a multi-layer neural network, which allows the numerically challenging operators S^* and S , as well as the preconditioners Q_A and Q_S , to be parameterized as trainable neural sub-networks. To this end, we specify $Q_A = N + \tau I$ with some $\tau \geq 0$, and the iterative scheme (1.5) reduces to

$$\begin{cases} u^{k+1} = (N + \tau I + \partial\theta)^{-1} (\tau u^k - S^* p^k), \\ p^{k+1} = p^k + Q_S^{-1} (Su^{k+1} - p^k + Sf - y_d). \end{cases} \quad (1.6)$$

Then, we employ two learnable neural networks $\mathcal{S}^k : U \rightarrow Y$ and $\mathcal{A}^k : Y \rightarrow U$ to approximate the solution operator S and its adjoint S^* , respectively, in the k -th iteration of (1.6). Simultaneously, we construct two

learnable deep surrogate models $\mathcal{Q}_A^k : U \rightarrow U$ and $\mathcal{Q}_S^k : Y \rightarrow Y$ to approximate the operators $(N + \tau I + \partial\theta)^{-1}$ and \mathcal{Q}_S^{-1} . By treating the k -th iteration of (1.6) with the surrogate operators as the k -th layer of the **iUzawa-Net**, and stacking the first L layers together, we obtain the following neural network architecture:

$$\left\{ \begin{array}{l} \mathcal{T}(y_d, f; \theta_{\mathcal{T}}) = u^L, \end{array} \right. \quad (1.7a)$$

$$\left\{ \begin{array}{l} u^{k+1} = \mathcal{Q}_A^k(\tau u^k - \mathcal{A}^k p^k), \\ p^{k+1} = p^k + \mathcal{Q}_S^k(\mathcal{S}^k(u^{k+1} + f) - p^k - y_d), \end{array} \right. \quad \forall k = 0, \dots, L-1, \quad (1.7b)$$

$$\left\{ \begin{array}{l} u^0 = 0, \quad p^0 = 0. \end{array} \right. \quad (1.7c)$$

Here, $\mathcal{T}(y_d, f; \theta_{\mathcal{T}})$ denotes the proposed **iUzawa-Net**; $\theta_{\mathcal{T}}$ denotes the collection of trainable parameters in \mathcal{S} , \mathcal{A} , \mathcal{Q}_A and \mathcal{Q}_S ; and u^L provides an approximation to the optimal control u^* associated with the parameters y_d and f . For notational simplicity, we denote by u^{k+1} and p^{k+1} both the iterates generated by the inexact Uzawa method in (1.6) and the outputs of the k -th layer of the **iUzawa-Net** in (1.7). The abuse of notation should not cause confusion, as the meaning is clear from the context.

In implementation, the parameter $\tau > 0$ can be chosen arbitrarily by users. We employ neural networks in operator learning for PDEs (e.g., FNO or DeepONet [44]) as the architectures for the PDE solution operators \mathcal{S}^k and \mathcal{A}^k . The module \mathcal{Q}_S^k is specifically constructed to approximate a symmetric positive definite preconditioner. For \mathcal{Q}_A^k , we consider the important case in which $(N + \tau I + \partial\theta)^{-1}$ acts pointwise on its input³, and we design the architecture of \mathcal{Q}_A^k accordingly to capture this structural property. The specific architectures of all modules are described in detail in Section 2. A schematic of the full network architecture of the **iUzawa-Net** is provided in Figure 2.3.

1.5.3 Theoretical results of the **iUzawa-Net**

We first follow the established literature on neural network approximation theory (e.g., [33, 49]) and show that, under mild conditions, the solution operator T defined in (1.2) can be approximated to arbitrary accuracy on any compact set by an **iUzawa-Net** with two layers. This result implies that the **iUzawa-Net** serves as a *universal approximator* for the class of solution operators of (1.1). Nevertheless, it does not guarantee two properties that are expected to be satisfied by optimization-informed neural networks, namely *algorithm tracking* and *weight tying*, whose definitions will be detailed in Definitions 4.1 and 5.1. Informally, algorithm tracking implies that the layer outputs of the **iUzawa-Net** can be interpreted as inexact iterates of the inexact Uzawa method (1.5), and weight tying means that the layers in (1.7) share identical parameters. Both properties are naturally expected in an optimization-informed neural network based on (1.5) with fixed stepsize and preconditioners. The lack of these properties reveals that the above approximation result does not guarantee that the network preserves the underlying optimization structure.

To bridge this gap, we develop an analysis framework that unifies tools from optimization and neural network approximation theory, and establish the following results. First, we demonstrate that for any layer number $L \in \mathbb{N}$, there exists an **iUzawa-Net** that is algorithm tracking. Based on this result and from an optimization perspective, we establish the *asymptotic ε -optimality* of the class of algorithm tracking **iUzawa-Nets** in the sense that, for any $\varepsilon > 0$, there exists $L \in \mathbb{N}$ such that, for all $k \geq L$, $(u^{k+1}, p^{k+1})^\top$ remains in an ε -neighbourhood of the optimal pair $(u^*, p^*)^\top$. This, in turn, yields a universal approximation result in terms of the depth of the class of **iUzawa-Nets** that are algorithm tracking. We further show that under some additional regularity assumptions on (1.1), for any *bounded* set, there exists an algorithm tracking and weight tying **iUzawa-Net** that attains asymptotic ε -optimality on it. This result provides theoretical justification for the module-sharing design adopted in implementation, which substantially reduces model complexity while still achieving satisfactory numerical accuracy. Notably, this result holds without requiring compactness, which is of crucial advantage as compactness assumptions are restrictive in infinite-dimensional spaces.

³This setting covers a broad range of applications. In many of these cases, closed-form expressions of $(N + \tau I + \partial\theta)^{-1}$ are not available, which motivates the use of a learned neural network to approximate it.

1.6 Contributions

The **iUzawa-Net** demonstrated in Section 1.5 provides a unified framework that integrates classical iterative methods with modern deep learning techniques for solving (1.1). Computationally:

- The **iUzawa-Net** involves only a single offline training phase; during inference, obtaining a numerical solution of (1.1) for a new set of input parameters requires only a forward pass of the neural network. This facilitates real-time solutions for (1.1) by avoiding nested iterations in traditional numerical methods.
- The **iUzawa-Net** enables data-driven preconditioner design within a single end-to-end trainable manner, which offers accelerated convergence and improved adaptability across different problem settings. Notably, this brings the additional benefit that given sufficient data, the solution operator of (1.1) can be learned even without the explicit knowledge of S and θ .

Theoretically:

- We prove several universal approximation theorems of the proposed **iUzawa-Net** under mild assumptions. In particular, under mild regularity assumptions, one of the results allows approximating the solution operator of (1.1) to arbitrary accuracy with shared layer parameters on bounded sets, avoiding the compactness requirement in conventional universal approximation results.
- Compared with existing works, our analysis framework unifies tools from optimization and neural network approximation theory, which is of independent interest and provides a framework for designing and analyzing optimization-informed neural networks in infinite-dimensional spaces.

In summary, our approach differs from existing methods for (1.1) by simultaneously achieving numerical efficiency, ease of implementation, structural interpretability, and rigorous theoretical guarantees.

1.7 Organization

The rest of this paper is organized as follows. In Section 2, we present the design of the neural network architectures for the learnable modules in the **iUzawa-Net**. We then prove a universal approximation theorem for the **iUzawa-Net** in Section 3. In Section 4, we show that the outputs of the **iUzawa-Net** approximate the optimal control of (1.1) with guaranteed accuracy after passing through sufficiently many layers, which results in a new universal approximation result for the **iUzawa-Net**. In Section 5, some new approximation results under additional regularity assumptions are presented. Several numerical experiments are presented in Section 6 to demonstrate the efficiency, accuracy, and generalization ability of the proposed **iUzawa-Net**. In particular, we compare the results of the **iUzawa-Net** with the reference ones obtained by FEM-based traditional algorithms and other deep learning methods. We conclude in Section 7.

2 iUzawa-Net: Modules Design and Training

In this section, we detail the implementation of the **iUzawa-Net** defined in (1.7). We first elaborate on the constructions of neural network architectures for the learnable modules \mathcal{S}^k , \mathcal{A}^k , \mathcal{Q}_S^k , and \mathcal{Q}_A^k in (1.7). Subsequently, we present the full architecture and a training framework for the **iUzawa-Net**.

2.1 Neural Network Architecture for \mathcal{S}^k and \mathcal{A}^k

For illustration, we apply the FNO [40] as the structure of the neural networks \mathcal{S}^k and \mathcal{A}^k , which is an operator learning framework designed for approximating PDE solution operators. For completeness, we provide a brief overview of the specific FNO architecture adopted in this work; we refer the reader to [34, 40] for a comprehensive discussion.

Recall that the optimal control problem (1.1) is defined on a bounded domain $\Omega \subset \mathbb{R}^d$. Without loss of generality, we assume that the closure $\overline{\Omega} \subset (0, 2\pi)^d$, hence $\overline{\Omega}$ can be embedded into the interior of the d -dimensional torus \mathbb{T}^d . We identify Ω as a subset of \mathbb{T}^d through this embedding. The architecture for \mathcal{S}^k is defined as:

$$\mathcal{S}^k(u) = (\mathcal{Q} \circ \mathcal{K}_{\text{FNO}} \circ \mathcal{P})(\mathcal{E}(u))|_{\Omega}, \quad (2.1)$$

where $\mathcal{E} : L^2(\Omega) \rightarrow L^2(\mathbb{T}^d)$ is a linear and bounded extension operator satisfying $\mathcal{E}(u)|_{\Omega} = u$ for all $u \in L^2(\Omega)$; $\mathcal{P} : L^2(\mathbb{T}^d) \rightarrow L^2(\mathbb{T}^d; \mathbb{R}^{m_p})$ is a pointwise lifting operator defined by $\mathcal{P}(v)(x) = Pv(x)$ with a lifting dimension m_p and a learnable linear transformation $P : \mathbb{R} \rightarrow \mathbb{R}^{m_p}$. Similarly, $\mathcal{Q} : L^2(\mathbb{T}^d; \mathbb{R}^{m_p}) \rightarrow L^2(\mathbb{T}^d)$ is a pointwise

projection operator satisfying $\mathcal{Q}(v)(x) = Qv(x)$ for some learnable linear transformation $Q : \mathbb{R}^{m_p} \rightarrow \mathbb{R}$. The operator $\mathcal{K}_{\text{FNO}} : L^2(\mathbb{T}^d; \mathbb{R}^{m_p}) \rightarrow L^2(\mathbb{T}^d; \mathbb{R}^{m_p})$ represents a series of Fourier layers defined by

$$\begin{cases} \mathcal{K}_{\text{FNO}}(v) = v^{(L)}, \\ v^{(\ell+1)} = \sigma(\mathcal{F}^{-1}(\mathcal{R}_\ell \cdot \mathcal{F}_{k_{\max}}(v^{(\ell)})) + W_\ell v^{(\ell)}), \quad \forall \ell = 0, \dots, L-1, \\ v^{(0)} = v, \end{cases} \quad (2.2)$$

where L is the number of the Fourier layers. Here, $\mathcal{F}_{k_{\max}}$ denotes the Fourier transform truncated to the lowest k_{\max} Fourier modes in each coordinate; \mathcal{F}^{-1} denotes the inverse Fourier transform; $\mathcal{R}_\ell : (\mathbb{Z} \cap [-k_{\max}, k_{\max}])^d \rightarrow \mathbb{C}^{m_p \times m_p}$ is a learnable complex-valued weights on the Fourier domain; $W_\ell \in \mathbb{R}^{m_p \times m_p}$ is a learnable pointwise linear transformation acting on the original domain; and σ is a nonlinear activation function acting pointwise. The composition $\mathcal{Q} \circ \mathcal{K}_{\text{FNO}} \circ \mathcal{P} : L^2(\mathbb{T}^d) \rightarrow L^2(\mathbb{T}^d)$ is referred to as an FNO in the literature. In implementation, if the input u is discretized on a uniform grid \mathcal{D} within the domain Ω , both $\mathcal{F}_{k_{\max}}$ and \mathcal{F}^{-1} can be computed efficiently using the fast Fourier transform (FFT). We employ an identical neural network architecture for \mathcal{A}^k with a distinct set of learnable parameters.

The FNO architecture incorporates both global transformations in the frequency domain and local, pointwise transformations in the physical domain. This structure is particularly capable of capturing the nonlocal dependencies inherent in PDE solution operators S and S^* . Furthermore, it has been shown that FNOs are universal approximators for the class of continuous operators [33] and possess the discretization invariance property [34], allowing the trained model to generalize across different mesh resolutions.

2.2 Neural Network Architecture for \mathcal{Q}_S^k

Since the convergence of (1.5) merely requires Q_S to be self-adjoint and the condition $Q_S \succeq SN^{-1}S^* + I$, the choice of Q_S is generally not unique. Leveraging such flexibility, we design \mathcal{Q}_S^k , the approximator of Q_S , with a single-layer, purely linear structure to reduce the parameter complexity of the **iUzawa-Net**. Despite its simplicity, this design guarantees that \mathcal{Q}_S^k is self-adjoint and positive definite, which are essential properties for the asymptotic ε -optimality of the **iUzawa-Net** discussed in Section 4.

We assume that $\bar{\Omega} \subset (0, 2\pi)^d$ and identify the bounded domain Ω as a subset of \mathbb{T}^d as in Section 2.1. Our design relies on the following result.

Proposition 2.1. *Let $\kappa \in L^2(\mathbb{T}^d; \mathbb{R}^{m \times m})$ and $W \in \mathbb{R}^{m \times m}$ for some positive integer m . For any $v \in L^2(\mathbb{T}^d; \mathbb{R}^m)$, define the linear operator $\mathcal{K} : L^2(\mathbb{T}^d; \mathbb{R}^m) \rightarrow L^2(\mathbb{T}^d; \mathbb{R}^m)$ by*

$$\mathcal{K}(v)(x) = Wv(x) + \int_{\mathbb{T}^d} \kappa(x-y)v(y)dy, \quad \forall v \in L^2(\mathbb{T}^d; \mathbb{R}^m), \quad \text{for a.e. } x \in \Omega. \quad (2.3)$$

If $W = V^\top V$ for some $V \in \mathbb{R}^{m \times m}$ and κ takes the form

$$\kappa(y) = \int_{\mathbb{T}^d} \phi(z-y)^\top \phi(z) dz$$

for some $\phi \in L^2(\mathbb{T}^d; \mathbb{R}^{m \times m})$, then \mathcal{K} is bounded, self-adjoint, and positive semidefinite.

For notational convenience, we define the following convolution operation for matrix-valued functions on \mathbb{T}^d :

$$(v_1 * v_2)(x) := \int_{\mathbb{T}^d} v_1(x-y)v_2(y) dy, \quad \forall v_1 \in L^2(\mathbb{T}^d; \mathbb{R}^{m_1 \times m_2}), v_2 \in L^2(\mathbb{T}^d; \mathbb{R}^{m_2 \times m_3}), \quad (2.4)$$

where the product in the integration is the standard matrix product. It then follows that

$$\kappa(x-y) = \int_{\mathbb{T}^d} \phi(z-x)^\top \phi(z-y) dz = (\phi_-^\top * \phi)(x-y), \quad (2.5)$$

where $\phi_-^\top(x) := \phi(-x)^\top$. Note that the operation $*$ defined in (2.4) is associative. Motivated by Proposition 2.1 and (2.5), we apply \mathcal{K} in (2.3) to define the following architecture for \mathcal{Q}_S^k :

$$\begin{aligned} \mathcal{Q}_S^k(u) &= (\mathcal{P}^\top \circ \mathcal{K} \circ \mathcal{P})(\mathcal{E}(u))|_\Omega + \gamma u, \quad \forall u \in L^2(\Omega), \\ \mathcal{K}(v)(x) &= (V^\top V v(x) + (\phi_-^\top * \phi * v)(x)), \quad \forall v \in L^2(\mathbb{T}^d; \mathbb{R}^{m_p}), \quad \text{for a.e. } x \in \mathbb{T}^d, \end{aligned} \quad (2.6)$$

where $\mathcal{E} : L^2(\Omega) \rightarrow L^2(\mathbb{T}^d)$ is a linear and bounded extension operator satisfying $\mathcal{E}(u)|_\Omega = u$ for all $u \in L^2(\Omega)$; $\mathcal{P} : L^2(\mathbb{T}^d) \rightarrow L^2(\mathbb{T}^d; \mathbb{R}^{m_p})$ is a pointwise lifting operator satisfying $\mathcal{P}(v)(x) = Pv(x)$ for some learnable linear transformation $P : \mathbb{R} \rightarrow \mathbb{R}^{m_p}$; $\mathcal{P}^\top : L^2(\mathbb{T}^d; \mathbb{R}^{m_p}) \rightarrow L^2(\mathbb{T}^d)$ is defined by $\mathcal{P}^\top(v)(x) = P^\top v(x)$; $\phi \in L^2(\mathbb{T}^d; \mathbb{R}^{m_p \times m_p})$ and $V \in \mathbb{R}^{m_p \times m_p}$ are learnable parameters.⁴ Utilizing Proposition 2.1, it can be verified that \mathcal{Q}_S^k defined in (2.6) is linear, bounded, self-adjoint, and positive definite for all $\gamma > 0$. We remark that the term γu with hyperparameter $\gamma > 0$ not only ensures that \mathcal{Q}_S^k is strictly positive definite, but also serves a role similar to a residual connection [27] in the neural network.

Note that $\mathcal{F}(\phi)(k)$ is nonzero only if $k \in \mathbb{Z}^d$. Also, the convolution theorem applies to the definition (2.4), i.e.,

$$\mathcal{F}(v_1 * v_2)(k) = \mathcal{F}(v_1)(k) \mathcal{F}(v_2)(k), \quad \forall v_1 \in L^2(\mathbb{T}^d; \mathbb{R}^{m_1 \times m_2}), v_2 \in L^2(\mathbb{T}^d; \mathbb{R}^{m_2 \times m_3}), k \in \mathbb{Z}^d,$$

where the product on the right-hand side is complex-valued matrix multiplication. We are thus motivated to parameterize the convolution kernel ϕ directly in the Fourier domain via $\Phi := \mathcal{F}(\phi)$. In particular, we have $\mathcal{F}(\phi_-^\top * \phi * v) = \mathcal{F}(\phi_-^\top) \cdot \mathcal{F}(\phi) \cdot \mathcal{F}(v)$, where the dot symbol denotes pointwise product of functions; and

$$\mathcal{F}(\phi_-^\top)(k) = \int_{\mathbb{T}^d} \phi(-x)^\top e^{-i\langle k, x \rangle} dx = \int_{\mathbb{T}^d} \phi(-x)^\top \overline{e^{-i\langle k, -x \rangle}} dx = \int_{\mathbb{T}^d} \overline{\phi(x)^\top e^{-i\langle k, x \rangle}} dx = \Phi(k)^*, \quad \forall k \in \mathbb{Z}^d,$$

where the star in the last equality denotes the Hermitian transpose. Substituting this into (2.6) and denoting $\tilde{u} = \mathcal{E}(u)$, we obtain the following explicit expression for \mathcal{Q}_S^k :

$$\mathcal{Q}_S^k(u)(x) = P^\top V^\top V P u(x) + \mathcal{F}^{-1} \left(\Phi^* \cdot \Phi \cdot \mathcal{F}(P \tilde{u}(\cdot)) \right) \Big|_\Omega (x) + \gamma u(x), \quad \forall u \in L^2(\Omega), \quad \text{for a.e. } x \in \Omega, \quad (2.7)$$

where P , V , and Φ are trainable parameters. We illustrate the architecture of \mathcal{Q}_S^k in Figure 2.1.

In implementation, we first discretize the torus \mathbb{T}^d as a finite set \mathcal{D} with cardinality $|\mathcal{D}|$. The input $u \in L^2(\Omega)$ is extended periodically as a function in $L^2(\mathbb{T}^d)$, and then represented as a vector in $\mathbb{R}^{|\mathcal{D}|}$. For the extension operation, zero-padding is sufficient for computational purposes, while theoretical analysis may require \mathcal{E} to preserve Sobolev regularity, see e.g., Proposition 3.7. We adopt a finite-dimensional parameterization of Φ by truncating it to a maximal number of modes k_{\max} in each coordinate. To ensure that $\mathcal{Q}_S^k u$ is real-valued, we impose the constraint $\Phi(k) = \overline{\Phi(-k)}$ for all $k \in \mathbb{Z}^d$. Hence, we directly parameterize Φ as a complex-valued tensor in $\mathbb{C}^{(k_{\max}+1)^d \times m_p \times m_p}$. The Fourier transforms in (2.7) are correspondingly implemented as discrete Fourier transforms. In particular, the FFT is applicable when \mathcal{D} is a uniform grid, which reduces computational complexity; see e.g., [40].

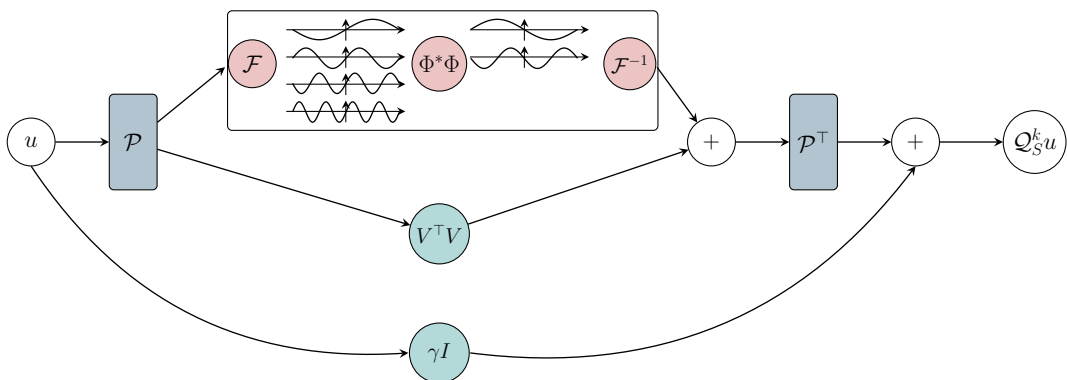


Figure 2.1: The neural network architecture of \mathcal{Q}_S^k .

2.3 Neural Network Architecture for \mathcal{Q}_A^k

We focus on the specific case where N and θ satisfy the following pointwise assumption.

⁴Note that (2.3) is similar to a single Fourier layer in FNO with a different parameterization strategy that ensures positive definite.

Assumption 2.2. *We make the following assumptions:*

(i) *The operator $N : L^2(\Omega) \rightarrow L^2(\Omega)$ acts as a multiplication operator:*

$$N(u)(x) = \lambda(x)u(x) \quad \text{a.e. in } \Omega,$$

where $\lambda \in L^\infty(\Omega)$ satisfies $\lambda(x) \geq c_0 > 0$ a.e. in Ω .

(ii) *There exist an integer $m \geq 1$, a closed set $E \subset \mathbb{R}^m$ and a function $\psi_\xi : \mathbb{R}^m \rightarrow \mathbb{R} \cup \{+\infty\}$ parameterized by $\xi \in E$, such that ψ_ξ is convex, lower semicontinuous, and proper for all $\xi \in E$. The functional $\theta : L^2(\Omega) \rightarrow \mathbb{R} \cup \{+\infty\}$ is given by*

$$\theta(u) = \int_{\Omega} \psi_{\mu(x)}(u(x)) dx, \quad \forall u \in L^2(\Omega),$$

for some $\mu \in L^\infty(\Omega; \mathbb{R}^m)$ satisfying $\mu(x) \in E$ a.e. in Ω . Here, the integral is interpreted as $+\infty$ if the integrand equals $+\infty$ over a subset of Ω with positive measure.

Though formulated abstractly, Assumption 2.2 covers many practical scenarios. Notable examples include:

(i) *Control-constrained optimal control problems:* $N = \lambda I$ for some $\lambda > 0$ and $\theta(u) = I_{U_{ad}}(u)$, where

$$U_{ad} = \{u \in L^2(\Omega) \mid u_a(x) \leq u(x) \leq u_b(x) \text{ a.e. in } \Omega\} \quad (2.8)$$

for some $u_a, u_b \in L^\infty(\Omega)$, and $I_{U_{ad}}(\cdot)$ is the indicator functional of the set U_{ad} . In this case, Assumption 2.2 (i) holds with $\lambda(x) = \lambda$, and Assumption 2.2 (ii) holds with

$$m = 2, \quad E = \{\xi := (\xi_1, \xi_2) \in \mathbb{R}^2 : \xi_1 \leq \xi_2\}, \quad \psi_\xi(r) = I_{[\xi_1, \xi_2]}(r), \quad \mu(x) = (u_a(x), u_b(x))^\top.$$

(ii) *Sparse optimal control problems:* $N = \lambda I$ for some $\lambda > 0$ and $\theta(u) = \beta \|u\|_{L^1(\Omega)} + I_{U_{ad}}(u)$ for some $\beta \geq 0$ and U_{ad} defined in (2.8). In this case, Assumption 2.2 (i) holds with $\lambda(x) = \lambda$, and Assumption 2.2 (ii) holds with

$$\begin{aligned} m &= 3, \quad E = \{\xi := (\xi_1, \xi_2, \xi_3) \in \mathbb{R}^3 : \xi_1 \leq \xi_2, \xi_3 \geq 0\}, \\ \psi_\xi(r) &= \xi_3|r| + I_{[\xi_1, \xi_2]}(r), \quad \mu(x) = (u_a(x), u_b(x), \beta)^\top. \end{aligned}$$

In these cases, it suffices to apply a pointwise operator to approximate $(N + \tau I + \partial \theta)^{-1}$; this observation will be generalized in Lemma 4.9. To motivate a reasonable network architecture, denoting σ as the ReLU activation function, we observe that

$$\begin{aligned} ((\lambda + \tau)I + \partial I_{U_{ad}})^{-1}(u)(x) &= \text{proj}_{[u_a(x), u_b(x)]} \left(\frac{1}{\lambda + \tau} u(x) \right) \\ &= u_b(x) - \sigma \left(u_b(x) - u_a(x) - \sigma \left(\frac{1}{\lambda + \tau} u(x) - u_a(x) \right) \right), \end{aligned} \quad (2.9)$$

$$\begin{aligned} ((\lambda + \tau)I + \partial (\beta \| \cdot \|_{L^1(\Omega)} + I_{U_{ad}}))^{-1}(u)(x) &= \text{proj}_{[u_a(x), u_b(x)]} \left(\left[\frac{|u(x)| - \beta}{\lambda + \tau} \right]_+ \text{sgn} \left(\frac{1}{\lambda + \tau} u(x) \right) \right) \\ &= u_b(x) - \sigma \left(u_b(x) - u_a(x) - \sigma \left(\sigma \left(\frac{u(x) - \beta}{\lambda + \tau} \right) - \sigma \left(\frac{-u(x) - \beta}{\lambda + \tau} \right) - u_a(x) \right) \right), \\ &= u_b(x) - \sigma \left(u_b(x) - u_a(x) - \sigma \left((1 \ -1) \sigma \left(\frac{1}{\lambda + \tau} \begin{pmatrix} 1 \\ -1 \end{pmatrix} u(x) - \frac{\beta}{\lambda + \tau} \begin{pmatrix} 1 \\ 1 \end{pmatrix} \right) - u_a(x) \right) \right), \end{aligned} \quad (2.10)$$

both of which can be parameterized as several layers of neural networks with input $(u(x), \mu(x))^\top$, ReLU activation function, and concatenated skip connections [32]. Generalizing this observation to the cases where $\lambda(x)$ is non-constant, we propose the following neural network architecture for \mathcal{Q}_A^k :

$$(\mathcal{Q}_A^k(u))(x) = \mathcal{N}(u(x), \mu(x), \lambda(x)) \quad \text{a.e. in } \Omega, \quad (2.11)$$

where $\mathcal{N} : \mathbb{R}^{m+2} \rightarrow \mathbb{R}$ is a neural network defined by

$$\begin{cases} \mathcal{N}(r, \xi, \eta) = W_L \cdot (v^{(L-1)}, r, \xi, \eta)^\top + b_L, \\ v^{(l)} = \sigma \left(W_l \cdot (v^{(l-1)}, r, \xi, \eta)^\top + b_l \right), \quad l = 1, 2, \dots, L-1, \\ v^{(0)} = W_0 \cdot (r, r, \xi, \eta)^\top. \end{cases} \quad (2.12)$$

Here, $r \in \mathbb{R}$, $\xi \in \mathbb{R}^m$, $\eta \in \mathbb{R}$, L is the number of layers, W_l and b_l are the weight matrices and bias vectors of the l -th layer, respectively, and σ is the ReLU activation function. We allow the vector $(r, \xi, \eta)^\top$ to be fed into each hidden layer, thereby facilitating concatenated skip connections from the input to every hidden layer. The architecture of \mathcal{Q}_A^k is illustrated in Figure 2.2.

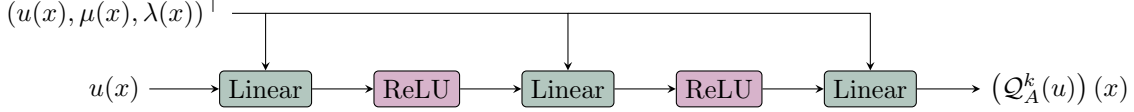


Figure 2.2: The neural network architecture of \mathcal{Q}_A^k .

In implementation, if $\lambda(x)$ or $\mu(x)$ is constant over Ω , we simplify \mathcal{Q}_A^k by omitting the constant parameters from the input. For instance, if λ is constant, the reduced architecture reads as

$$(\mathcal{Q}_A^k(u))(x) = \mathcal{N}(u(x), \mu(x)), \quad \text{a.e. } x \in \Omega, \quad (2.13)$$

where $\mathcal{N} : \mathbb{R}^{m+1} \rightarrow \mathbb{R}$ is a neural network defined by

$$\begin{cases} \mathcal{N}(r, \xi) = W_L \cdot (v^{(L-1)}, r, \xi)^\top + b_L, \\ v^{(l)} = \sigma \left(W_l \cdot (v^{(l-1)}, r, \xi)^\top + b_l \right), \quad l = 1, 2, \dots, L-1, \\ v^{(0)} = W_0 \cdot (r, r, \xi)^\top, \end{cases} \quad (2.14)$$

for some weights $\{W_\ell\}_{\ell=0}^L$ and biases $\{b_\ell\}_{\ell=1}^L$.

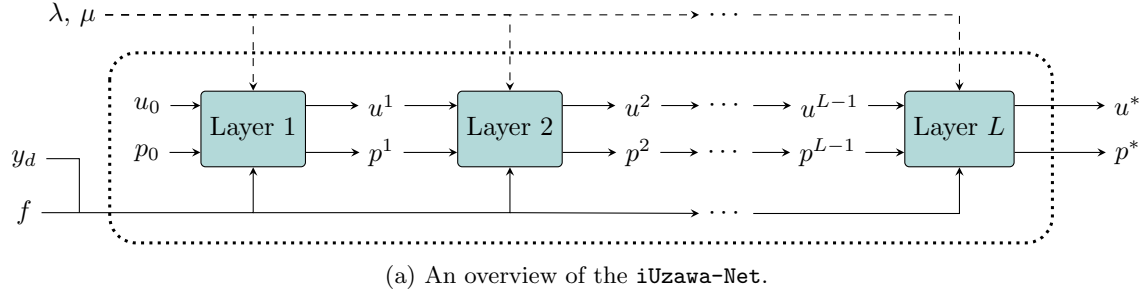
2.4 Full Architecture and Training Framework of the iUzawa-Net

With the constructions of \mathcal{S}^k , \mathcal{A}^k , \mathcal{Q}_S^k , and \mathcal{Q}_A^k detailed in Sections 2.1-2.3, the **iUzawa-Net** defined in (1.7) becomes fully implementable. These neural modules collectively specify all learnable parameters in the **iUzawa-Net**, replacing the preconditioners and PDE solution operators required by the inexact Uzawa iteration (1.6). Our design ensures that each layer of the **iUzawa-Net** is optimization-informed and structurally mirrors one iteration of (1.6). A schematic illustration of the **iUzawa-Net**, highlighting the interaction among \mathcal{S}^k , \mathcal{A}^k , \mathcal{Q}_S^k , and \mathcal{Q}_A^k within each layer, is provided in Figure 2.3. The terms u^0 and p^0 correspond to the initialization of (1.6). For simplicity, we fix $u^0 = 0$ and $p^0 = 0$ throughout this work.

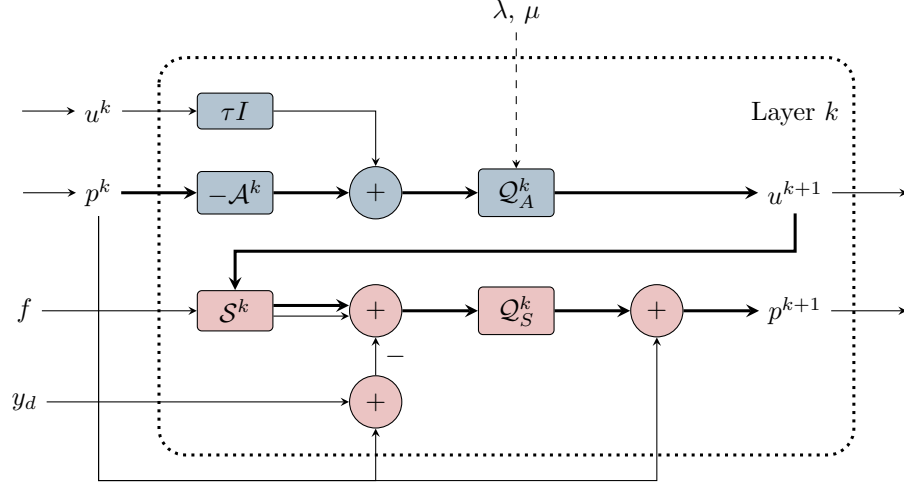
To train the **iUzawa-Net**, we generate a dataset $\{((y_d)_i, f_i)^\top, u_i^*\}_{i=1}^N$, where $(y_d)_i, f_i$ are the parameters of (1.1) and u_i^* is the corresponding optimal control. Each u_i^* can be obtained from real-world observations or computed using traditional numerical solvers or deep learning-based methods. The **iUzawa-Net** is trained by minimizing the following relative L^2 -error loss:

$$\mathcal{L}(\theta_{\mathcal{T}}) = \frac{1}{N} \sum_{i=1}^N \frac{\|\mathcal{T}((y_d)_i, f_i; \theta_{\mathcal{T}}) - u_i^*\|_{L^2(\Omega)}^2}{\max \left\{ \|u_i^*(x)\|_{L^2(\Omega)}^2, \varepsilon_L \right\}}, \quad (2.15)$$

where $\varepsilon_L > 0$ is a small constant to ensure stability. In implementation, the L^2 -norms in (2.15) are approximated discretely, which will be detailed by the numerical experiments in Section 6. This end-to-end training approach facilitates data-driven preconditioner training mechanism and enables real-time inference of the optimal control for new problem parameters y_d and f , effectively compensating for the initial computational cost in data generation and training.



(a) An overview of the iUzawa-Net.



(b) A single layer of the iUzawa-Net.

Figure 2.3: An overview of the iUzawa-Net (1.7).

3 Universal Approximation of the iUzawa-Net

In this section, we prove that the iUzawa-Net (1.7) admits the universal approximation property for the class of solution operators of (1.1) under Assumption 2.2. Specifically, we show that the solution operator T defined in (1.2) can be approximated to arbitrary accuracy on any compact set by an iUzawa-Net with two layers. For simplicity, we assume that Ω is a spatial domain, and remark that the subsequent analysis extends directly to spatio-temporal domains.

3.1 Preliminaries

In this subsection, we present some preliminary results related to (1.1) and its optimality system (1.4), which will be utilized in the subsequent analysis.

Lemma 3.1. *Let $N : U \rightarrow U$ and $\theta : U \rightarrow \mathbb{R} \cup \{+\infty\}$ be defined as in (1.1). Then the operator $(N + \partial\theta)^{-1} : U \rightrightarrows U$ is single-valued. Furthermore, for any $v_1, v_2 \in U$, let $u_1 = (N + \partial\theta)^{-1}(v_1)$ and $u_2 = (N + \partial\theta)^{-1}(v_2)$. Then*

$$\langle v_1 - v_2, u_1 - u_2 \rangle_U \geq c_0 \|u_1 - u_2\|_U^2, \quad (3.1)$$

where $c_0 > 0$ is the coercivity constant of N . Consequently, $(N + \partial\theta)^{-1}$ is Lipschitz continuous with Lipschitz constant c_0^{-1} .

Proof. Since θ is convex, lower semicontinuous, and proper, and N is coercive, it follows from [15, Lemma 1] and [5, Theorem 2.3] that $(N + \partial\theta)^{-1}$ is single-valued. Moreover, the operator $\partial\theta$ is maximally monotone [4, Theorem 20.25]. Hence, for any $v_1, v_2 \in U$, if $u_1 = (N + \partial\theta)^{-1}(v_1)$, and $u_2 = (N + \partial\theta)^{-1}(v_2)$, the monotonicity of $\partial\theta$ implies

$$\langle v_1 - v_2, u_1 - u_2 \rangle_U \geq \langle N(u_1 - u_2), u_1 - u_2 \rangle_U. \quad (3.2)$$

Applying the coercivity of N to the right hand side and the Cauchy-Schwarz inequality to the left hand side, we obtain

$$\|v_1 - v_2\|_U \|u_1 - u_2\|_U \geq \langle v_1 - v_2, u_1 - u_2 \rangle_U \geq \langle N(u_1 - u_2), u_1 - u_2 \rangle_U \geq c_0 \|u_1 - u_2\|_U^2.$$

This establishes (3.1). The Lipschitz continuity follows immediately by dividing both sides by $c_0 \|u - \tilde{u}\|_U$ (assuming $u \neq \tilde{u}$, as the case $u = \tilde{u}$ is trivial). \square

Lemma 3.2. *The solution operator T of (1.1) is a mapping of $Sf - y_d$, i.e.,*

$$T(y_d, f) = T_0(Sf - y_d)$$

for some operator $T_0 : Y \rightarrow U$. Moreover, T_0 is Lipschitz continuous with Lipschitz constant $c_0^{-1} \|S\|$.

Proof. The existence of T_0 is a direct consequence of the optimality condition (1.4), whose solution $(u^*, p^*)^\top$ depends on (y_d, f) only through $Sf - y_d$. Let $z_1, z_2 \in Y$ and denote $u_i^* = T_0(z_i)$ for $i = 1, 2$. By (1.4), there exists $p_i^* \in Y$ such that

$$\begin{cases} 0 \in Nu_i^* + \partial\theta(u_i^*) + S^*p_i^*, \\ 0 = Su_i^* - p_i^* + z_i. \end{cases} \quad (3.3)$$

By Lemma 3.1, $(N + \partial\theta)^{-1}$ is single-valued. Hence (3.3) is equivalent to

$$(S \circ (N + \partial\theta)^{-1} \circ S^* + I)(-p_i^*) + z_i = 0, \quad (3.4)$$

where $I : Y \rightarrow Y$ denotes the identity operator. It follows from (3.4) and (3.1) that

$$\begin{aligned} & \langle z_1 - z_2, p_1^* - p_2^* \rangle_Y \\ &= \|p_1^* - p_2^*\|_Y^2 - \langle (S \circ (N + \partial\theta)^{-1} \circ S^*)(-p_1^*) - (S \circ (N + \partial\theta)^{-1} \circ S^*)(-p_2^*), p_1^* - p_2^* \rangle_Y \\ &= \|p_1^* - p_2^*\|_Y^2 + \langle (N + \partial\theta)^{-1}(-S^*p_1^*) - (N + \partial\theta)^{-1}(-S^*p_2^*), -S^*(p_1^* - p_2^*) \rangle_U \\ &\geq \|p_1^* - p_2^*\|_Y^2 + c_0 \|(N + \partial\theta)^{-1}(-S^*p_1^*) - (N + \partial\theta)^{-1}(-S^*p_2^*)\|_U^2 \\ &\geq \|p_1^* - p_2^*\|_Y^2. \end{aligned}$$

Hence $\|p_1^* - p_2^*\|_Y \leq \|z_1 - z_2\|_Y$. Applying Lemma 3.1 again yields

$$\begin{aligned} \|u_1^* - u_2^*\|_U &= \|(N + \partial\theta)^{-1}(-S^*p_1^*) - (N + \partial\theta)^{-1}(-S^*p_2^*)\|_U \\ &\leq c_0^{-1} \|S^*\| \|p_1^* - p_2^*\|_Y \\ &\leq c_0^{-1} \|S^*\| \|z_1 - z_2\|_Y. \end{aligned}$$

\square

Remark 3.3. *Though T is a mapping of $Sf - y_d$, we insist on designing the *iUzawa-Net* as an operator with input $(y_d, f)^\top$ rather than $Sf - y_d$, since evaluating Sf requires an additional PDE solve.*

We now state, without proof, the following universal approximation theorems for fully-connected neural networks (FCNNs) and FNOs. Note that Proposition 3.4 follows directly from [49, Theorem 3.1], the Tietze extension theorem, and the fact that uniform convergence of an \mathbb{R}^n -valued function is equivalent to uniform convergence in each of its coordinates. The compactness of the image in Proposition 3.5 is guaranteed by the fact that FNOs maps $H^s(\Omega)$ continuously into $H^s(\Omega)$ for any $s \geq 0$, which holds by noticing the followings: the extension operator \mathcal{E} in Proposition 3.5 and the restriction operator $H^s(\mathbb{T}^d) \rightarrow H^s(\Omega)$ are continuous; all the pointwise operations in (2.1)–(2.2) are Lipschitz; and the Fourier transforms in (2.2) are truncated to finitely many Fourier modes.

Proposition 3.4 (c.f. [49, Theorem 3.1]). *Let $F \subset \mathbb{R}^m$ be a closed set and $g : F \rightarrow \mathbb{R}^n$ be a continuous function. If $\sigma : \mathbb{R} \rightarrow \mathbb{R}$ is continuous and not a polynomial, then for any compact set $K \subset F$ and any $\varepsilon > 0$, there exists a fully connected neural network $\mathcal{N}_{FC} : \mathbb{R}^m \rightarrow \mathbb{R}^n$ with activation function σ , such that*

$$\sup_{x \in K} \|g(x) - \mathcal{N}_{FC}(x)\| < \varepsilon.$$

Proposition 3.5 (c.f. [33, Theorem 9]). *Let $s_1, s_2 \geq 0$ and $\Omega \subset \mathbb{R}^d$ be a bounded domain with Lipschitz boundary satisfying $\overline{\Omega} \subset (0, 2\pi)^d$. Let $G : H^{s_1}(\Omega) \rightarrow H^{s_2}(\Omega)$ be a continuous operator and $K \subset H^{s_1}(\Omega)$ be a compact set. Then for any $\varepsilon > 0$, there exist a continuous embedding $\mathcal{E} : H^{s_1}(\Omega) \rightarrow H^{s_1}(\mathbb{T}^d)$ and an FNO $\mathcal{G} : H^{s_1}(\mathbb{T}^d) \rightarrow H^{s_2}(\mathbb{T}^d)$, such that*

$$\sup_{v \in K} \|G(v) - (\mathcal{G} \circ \mathcal{E}(v))|_{\Omega}\|_{H^{s_2}(\Omega)} < \varepsilon.$$

Furthermore, if $s_2 \leq s_1$, the image $(\mathcal{G} \circ \mathcal{E})(K)|_{\Omega}$ is compact in $H^{s_2}(\Omega)$.

As a direct consequence of Proposition 3.4, the universal approximation property also holds for the neural network architecture defined in (2.12), since the architecture in (2.12) encompasses standard FCNNs (e.g., by setting the weights of the concatenated skip connections to zero).

Lemma 3.6. *Let m be any positive integer, $F \subset \mathbb{R}^{m+2}$ be a closed set, $g : F \rightarrow \mathbb{R}$ be a continuous function, and $\sigma(x) = \max\{0, x\}$ be the ReLU activation function. Then for any compact set $K \subset F$ and any $\varepsilon > 0$, there exists a neural network $\mathcal{N} : \mathbb{R}^{m+2} \rightarrow \mathbb{R}$ with the architecture defined in (2.12), such that*

$$\sup_{(r, \xi, \eta)^{\top} \in K} \|g(r, \xi, \eta) - \mathcal{N}(r, \xi, \eta)\| < \varepsilon.$$

For the neural network \mathcal{Q}_S^k constructed in (2.7), we establish the following properties regarding its approximation capabilities and regularity.

Proposition 3.7. *For any hyperparameter $\gamma > 0$, the following assertions hold:*

- (i) *For any $\tilde{\gamma} \geq \gamma$, there exists a neural network \mathcal{Q}_S of the form (2.7) such that $\mathcal{Q}_S = \tilde{\gamma}I$.*
- (ii) *For any linear, bounded, self-adjoint, and positive definite operator Q_S , there exists \mathcal{Q}_S of the architecture (2.7) such that the difference $\mathcal{Q}_S - Q_S$ is linear, bounded, self-adjoint, and positive.*
- (iii) *For any $s \geq 0$, there exists an bounded linear extension operator $\mathcal{E}_s : L^2(\Omega) \rightarrow L^2(\mathbb{T}^d)$, such that if \mathcal{Q}_S is defined by (2.7) with $\mathcal{E} = \mathcal{E}_s$ and Φ is supported on finitely many truncated Fourier modes, then \mathcal{Q}_S maps $H^s(\Omega)$ continuously into $H^s(\Omega)$.*

Proof. To prove (i), let $P = e_1 \in \mathbb{R}^{m_p}$ be the first standard basis vector, $V = \sqrt{\tilde{\gamma} - \gamma}I$, and $\Phi = 0$. Then for any $u \in L^2(\Omega)$,

$$\mathcal{Q}_S^k(u)(x) = P^{\top} V^{\top} V P((\mathcal{E}u)(x)) + \gamma u(x) = e_1^{\top} (\tilde{\gamma} - \gamma) I e_1 u(x) + \gamma u(x) = (\tilde{\gamma} - \gamma) u(x) + \gamma u(x) = \tilde{\gamma} u(x), \quad \text{a.e. in } \Omega.$$

For (ii), since Q_S is bounded and self-adjoint, taking sufficiently large $\tilde{\gamma}$ in (i) guarantees that $\mathcal{Q}_S - Q_S$ is bounded, self-adjoint, and positive semidefinite.

We now establish (iii). By [33, Lemma 41], for any $s \geq 0$, there exists a bounded linear extension operator $\bar{\mathcal{E}}_s : H^s(\Omega) \rightarrow H^s(\mathbb{T}^d)$. Since $H^s(\Omega)$ is dense in $L^2(\Omega)$, and the embedding $H^s(\mathbb{T}^d) \hookrightarrow L^2(\mathbb{T}^d)$ is dense and continuous, $\bar{\mathcal{E}}_s$ extends uniquely to a bounded linear mapping $\mathcal{E}_s : L^2(\Omega) \rightarrow L^2(\mathbb{T}^d)$, which maps $H^s(\Omega)$ continuously into $H^s(\Omega)$ since $\mathcal{E}_s|_{H^s(\Omega)} = \bar{\mathcal{E}}_s$. Now assume that \mathcal{Q}_S is defined by the architecture in (2.7) with $\mathcal{E} = \mathcal{E}_s$ and Φ being supported on finitely many Fourier modes. Note also that the restriction operator $H^s(\mathbb{T}^d) \rightarrow H^s(\Omega)$ is continuous and all the pointwise operations in (2.7) are Lipschitz. It thus follows that \mathcal{Q}_S^k maps $H^s(\Omega)$ into $H^s(\Omega)$ continuously. \square

3.2 Universal Approximation of the iUzawa-Net

We now establish a universal approximation property of the **iUzawa-Net**, highlighting its capacity to approximate the solution operator of (1.1) with theoretical guarantees.

Theorem 3.8. *Let $T : Y \times U \rightarrow U$ be the solution operator of (1.1). For any compact set $K \subset Y \times U$ and $\varepsilon > 0$, there exists a two-layer **iUzawa-Net** $\mathcal{T}(y_d, f; \theta_{\mathcal{T}})$ defined in (1.7), such that*

$$\sup_{(y_d, f)^{\top} \in K} \|T(y_d, f) - \mathcal{T}(y_d, f; \theta_{\mathcal{T}})\|_U \leq \varepsilon.$$

Proof. For any two-layer **iUzawa-Net** \mathcal{T} , we have $\mathcal{T}(y_d, f; \theta_{\mathcal{T}}) = u^2$, where u^2 is the second-layer output defined in (1.7). It follows that

$$u^2 = \mathcal{Q}_A^1(-\mathcal{A}^1(-\mathcal{Q}_S^0(\mathcal{S}^0(\mathcal{Q}_A^0(-\mathcal{A}^0(p^0)) + f) - y_d)) + \tau \mathcal{Q}_A^0(-\mathcal{A}^0(p^0))).$$

We take an FNO $\mathcal{A}^0 : Y \rightarrow U$ with all-zero parameter (hence $\mathcal{A}^0 = 0$). Following Lemma 3.6, we choose a neural network $\mathcal{N} : \mathbb{R} \rightarrow \mathbb{R}$ of the form (2.12) to approximate the zero mapping on the compact set $\{0\}$ with error $\varepsilon_1/|\Omega|^{1/2}$. Let \mathcal{Q}_A be defined as in (2.11) with the constructed \mathcal{N} . It follows that

$$\|\mathcal{Q}_A^0(-\mathcal{A}^0(p^0))\|_U < \varepsilon_1. \quad (3.5)$$

The compactness of K implies that its projections onto U and Y , denoted by K_U and K_Y , are compact. Define $K_0 = \{\mathcal{Q}_A^0(-\mathcal{A}^0(p^0))\}$ and $K_1 = K_U + K_0$. Then both K_0 and K_1 are compact. By Proposition 3.5, there exists an FNO \mathcal{S}^0 such that

$$\sup_{v \in K_1} \|Sv - \mathcal{S}^0(v)\|_Y < \varepsilon_2,$$

and hence for any $f \in K_U$,

$$\begin{aligned} \|Sf - \mathcal{S}^0(\mathcal{Q}_A^0(-\mathcal{A}^0(p^0)) + f)\|_Y &\leq \|Sf - S(\mathcal{Q}_A^0(-\mathcal{A}^0(p^0)) + f)\|_Y \\ &\quad + \|S(\mathcal{Q}_A^0(-\mathcal{A}^0(p^0)) + f) - \mathcal{S}^0(\mathcal{Q}_A^0(-\mathcal{A}^0(p^0)) + f)\|_Y \\ &< \|S\|\varepsilon_1 + \varepsilon_2. \end{aligned} \quad (3.6)$$

By Lemma 3.2, $T(y_d, f) = T_0(Sf - y_d)$ for some continuous $T_0 : Y \rightarrow U$. Thus Proposition 3.5 guarantees an FNO \mathcal{A}^1 such that

$$\sup_{z \in K_2} \|-T_0(-z) - \mathcal{A}^1(z)\|_U < \varepsilon_3, \quad (3.7)$$

where $K_2 := -\mathcal{S}^0 K_1 + K_Y$ is compact by Proposition 3.5. From Proposition 3.7, we take any $\gamma < 1$ in (2.7) and choose $\mathcal{Q}_S^0 = I$. It follows from Lemma 3.2, (3.6) and (3.7) that

$$\begin{aligned} &\|T_0(Sf - y_d) - ((-\mathcal{A}^1) \circ (-\mathcal{Q}_S^0))(\mathcal{S}^0(\mathcal{Q}_A^0(-\mathcal{A}^0(p^0)) + f) - y_d)\|_U \\ &\leq \|T_0(Sf - y_d) - T_0(\mathcal{S}^0(\mathcal{Q}_A^0(-\mathcal{A}^0(p^0)) + f) - y_d)\|_U \\ &\quad + \|T_0(\mathcal{S}^0(\mathcal{Q}_A^0(-\mathcal{A}^0(p^0)) + f) - y_d) + \mathcal{A}^1(-(\mathcal{S}^0(\mathcal{Q}_A^0(-\mathcal{A}^0(p^0)) + f) - y_d))\|_U \\ &< c_0^{-1}\|S\|(\|S\|\varepsilon_1 + \varepsilon_2) + \varepsilon_3. \end{aligned}$$

Finally, we take \mathcal{Q}_A^1 to approximate the identity operator over the compact set

$$K_3 := -\mathcal{A}^1(K_2) + \tau K_0,$$

with accuracy

$$\sup_{v \in K_3} \|v - \mathcal{Q}_A^1 v\|_U < \varepsilon_4.$$

Let $\bar{v} = ((-\mathcal{A}^1) \circ (-\mathcal{Q}_S^0))(\mathcal{S}^0(\mathcal{Q}_A^0(-\mathcal{A}^0(p^0)) + f) - y_d)$, then $\bar{v} \in -\mathcal{A}^1(K_2)$ and thus $\bar{v} + \tau \mathcal{Q}_A^0(-\mathcal{A}^0(p^0)) \in K_3$. As a result, we have

$$\begin{aligned} \|u^2 - T(y_d, f)\|_U &= \|\mathcal{Q}_A^1(\bar{v}) + \tau \mathcal{Q}_A^0(-\mathcal{A}^0(p^0)) - T_0(Sf - y_d)\|_U \\ &\leq \|\mathcal{Q}_A^1(\bar{v}) - \bar{v}\| + \|\bar{v} - T_0(Sf - y_d)\| + \|\tau \mathcal{Q}_A^0(-\mathcal{A}^0(p^0))\| \\ &< (c_0^{-1}\|S\|^2 + \tau)\varepsilon_1 + c_0^{-1}\|S\|\varepsilon_2 + \varepsilon_3 + \varepsilon_4 =: \varepsilon, \end{aligned}$$

for any $(y_d, f) \in K$. The result follows immediately by choosing $\varepsilon_1, \varepsilon_2, \varepsilon_3, \varepsilon_4$ sufficiently small. \square

It is important to note that Theorem 3.8 does not imply universal approximation for arbitrary mappings between Hilbert spaces, since the approximable operators are restricted to those depending only on $Sf - y_d$. While the design of the **iUzawa-Net** restricts the class of approximable operators, it embeds the intrinsic mathematical structure of the optimal control problem (1.1) into the network. Consequently,

the **iUzawa-Net** fundamentally distinguishes itself from standard black-box operator learning approaches, leveraging its optimization-informed nature to enhance both interpretability and robustness.

The proof of Theorem 3.8 constructs a network where modules like \mathcal{A}^1 and \mathcal{Q}_A^0 do not correspond to their counterparts S^* or $(N + \tau I + \partial\theta)^{-1}$ in the blueprint optimization algorithm (1.5), but rather serve as generic approximators. Such a configuration does not adhere to the optimization-informed design principle of the **iUzawa-Net**. To address this, we provide stronger approximation results in Sections 4 and 5, which guarantees that the learnable modules approximate their respective target operators and, more importantly, ensures that the layer outputs of the **iUzawa-Net** faithfully track the iterates of the inexact Uzawa method.

4 Asymptotic ε -Optimality of the **iUzawa-Net** Layer Outputs

In this section, we prove the existence of an **iUzawa-Net** $\mathcal{T}(y_d, f; \theta_{\mathcal{T}})$ whose layer outputs closely approximate inexact iterates of (1.5). We formally define this property as *algorithm tracking*.

Definition 4.1. Let $Q_A = N + \tau I$ for some $\tau \geq 0$ and Q_S be a fixed linear, bounded, self-adjoint, and positive definite operator. For any $K \subset Y \times U$ and $\delta > 0$, we say that an **iUzawa-Net** is *algorithm tracking with respect to K and δ* , or simply (K, δ) -tracking, if for any input $(y_d, f)^\top \in K$ and initialization $(p^0, u^0)^\top \in K \cup \{0\}$, its k -th layer output u^k and p^k satisfy

$$\bar{u}^{k+1} = (Q_A + \partial\theta)^{-1} (\tau u^k - S^* p^k), \quad (4.1a)$$

$$p^{k+1} = p^k + Q_S^{-1} (S\bar{u}^{k+1} - p^k + Sf - y_d), \quad (4.1b)$$

$$u^{k+1} \in \{u \in U : \|u - \bar{u}^{k+1}\|_U \leq \delta\}, \quad (4.1c)$$

$$p^{k+1} \in \{p \in Y : \|p - \bar{p}^{k+1}\|_Y \leq \delta\}, \quad (4.1d)$$

for any $k = 0, \dots, L-1$.

We require $(p^0, u^0)^\top \in K \cup \{0\}$ since we are mainly interested in those **iUzawa-Net** with $u^0 = p^0 = 0$. Utilizing (4.1), which defines an inexact algorithm of (1.5), we show that the layer outputs of \mathcal{T} enter and stay in a neighborhood of the optimal control u^* after sufficiently many layers. In particular, Theorem 4.13 establishes an asymptotic ε -optimality result for the layer outputs of the **iUzawa-Net**. As a corollary, this yields a new universal approximation theorem for the **iUzawa-Net** under the algorithm tracking requirement. Unlike the general result in Theorem 3.8, this theorem ensures theoretical consistency with the optimization-informed architecture, as the network is shown to track the optimization trajectory.

Our analysis proceeds in two steps. First, we analyze the optimization algorithm (4.1) itself, proving that its sequence eventually enters and remains within a neighborhood of the optimal control u^* . Second, we show that for any compact $K \subset U \times Y$ and $\delta > 0$, there exists an **iUzawa-Net** that is (K, δ) -tracking, by showing that its internal neural networks \mathcal{S}^k , \mathcal{A}^k , \mathcal{Q}_A^k and \mathcal{Q}_S^k approximate their corresponding operators with sufficient accuracy on appropriately constructed compact sets. Combining these results together yields the asymptotic ε -optimality of the **iUzawa-Net** layer outputs.

4.1 Inexact Iterations of (1.5) and Asymptotic ε -Optimality

In the remaining part of this subsection, we fix $Q_A = N + \tau I$ and Q_S such that the operators

$$Q_A - N, \quad Q_S - (I + SN^{-1}S^*) \quad \text{are positive semidefinite,} \quad (4.2)$$

and consider *any* inexact iterates $\{u^k\}_{k=0}^\infty, \{p^k\}_{k=0}^\infty$ that satisfy (4.1) for all $k \geq 0$ (note that $\{u^k\}_{k=0}^\infty$ and $\{p^k\}_{k=0}^\infty$ are not necessarily layer outputs of an **iUzawa-Net**). For convenience, we denote $w, \bar{w} \in U \times Y$ and two bounded linear self-adjoint operators $Q : U \times Y \rightarrow U \times Y$ and $R : U \times Y \rightarrow U \times Y$ as

$$w = \begin{pmatrix} u \\ p \end{pmatrix}, \quad \bar{w} = \begin{pmatrix} \bar{u} \\ \bar{p} \end{pmatrix}, \quad Q(u, p) = \begin{pmatrix} (Q_A - N) u \\ Q_S p \end{pmatrix}, \quad R(u, p) = \begin{pmatrix} (Q_A - N) u \\ (Q_S - \frac{1}{2}(I + SN^{-1}S^*)) p \end{pmatrix}.$$

We take the inner product $\langle \cdot, \cdot \rangle_{U \times Y}$ on $U \times Y$ as the canonical one induced by the Cartesian product. It is clear that Q and R are positive semidefinite, which introduces the following seminorms on $U \times Y$:

$$\|w\|_Q^2 := \langle Qw, w \rangle_{U \times Y}, \quad \|w\|_R^2 := \langle Rw, w \rangle_{U \times Y}.$$

Similar notations to the above will be used to denote the seminorms induced by other positive semidefinite operators. We use $\sigma_0(\cdot)$ to denote the infimum of the spectrum modulus of a given operator.

We begin by showing that \bar{w}^{k+1} is a contractive iterate with respect to w^k for all $k \geq 0$. The following Lemma 4.2 is a direct extension of [25, Theorem 4.4] and [59, Theorem 3.3] to the infinite-dimensional setting. We provide a detailed proof for completeness.

Lemma 4.2. *Let $\{w^k\}_{k=0}^\infty$ and $\{\bar{w}^k\}_{k=1}^\infty$ satisfy (4.1). Let $w^* = (u^*, p^*)^\top$ be the unique solution to (1.1). For any $k \geq 0$, it holds that*

$$\|\bar{w}^{k+1} - w^*\|_Q^2 \leq \|w^k - w^*\|_Q^2 - \|\bar{w}^{k+1} - w^k\|_R^2. \quad (4.3)$$

Proof. By (4.1), it is easy to verify that

$$\begin{cases} Q_A(u^k - \bar{u}^{k+1}) - Nu^k - S^*p^k \in \partial\theta(\bar{u}^{k+1}), \\ Q_S(p^k - \bar{p}^{k+1}) + S\bar{u}^{k+1} - p^k + (Sf - y_d) = 0. \end{cases} \quad (4.4)$$

Since w^* solves (1.1), it follows from the optimality condition (1.4) that

$$\begin{cases} -Nu^* - S^*p^* \in \partial\theta(u^*), \\ Su^* - p^* + (Sf - y_d) = 0. \end{cases} \quad (4.5)$$

From the monotonicity of $\partial\theta$, we have

$$\begin{aligned} & \langle (Q_A - N)(u^k - \bar{u}^{k+1}) - N(\bar{u}^{k+1} - u^*) - S^*(p^k - p^*), \bar{u}^{k+1} - u^* \rangle_U \geq 0, \\ & Q_S(p^k - \bar{p}^{k+1}) + S(\bar{u}^{k+1} - u^*) - (p^k - p^*) = 0. \end{aligned}$$

It follows that

$$\begin{aligned} & \langle Q(w^k - \bar{w}^{k+1}), \bar{w}^{k+1} - w^* \rangle_{U \times Y} \\ &= \langle (Q_A - N)(u^k - \bar{u}^{k+1}), \bar{u}^{k+1} - u^* \rangle_U + \langle Q_S(p^k - \bar{p}^{k+1}), \bar{p}^{k+1} - p^k + p^k - p^* \rangle_Y \\ &\geq \langle (Q_A - N)(u^k - \bar{u}^{k+1}), \bar{u}^{k+1} - u^* \rangle_U + \langle -S(\bar{u}^{k+1} - u^*) + (p^k - p^*), \bar{p}^{k+1} - p^k + p^k - p^* \rangle_Y \\ &\geq \langle N(\bar{u}^{k+1} - u^*) + S^*(p^k - p^*), \bar{u}^{k+1} - u^* \rangle_U - \|p^k - \bar{p}^{k+1}\|_{Q_S}^2 \\ &\quad - \langle S(\bar{u}^{k+1} - u^*), p^k - p^* \rangle_Y + \|p^k - p^*\|_Y^2 \\ &= \langle N(\bar{u}^{k+1} - u^*), \bar{u}^{k+1} - u^* \rangle_U + \langle S(\bar{u}^{k+1} - u^*), p^k - \bar{p}^{k+1} \rangle_Y \\ &\quad - \langle p^k - p^*, p^k - \bar{p}^{k+1} \rangle_Y + \|p^k - p^*\|_Y^2. \end{aligned} \quad (4.6)$$

Since N is bounded, self-adjoint, and positive definite over the Hilbert space U , it admits a bounded, self-adjoint, and positive definite square root. Utilizing this square root and applying the Cauchy-Schwarz inequality, we have for all $\omega > 0$ that

$$\begin{aligned} & \langle S(\bar{u}^{k+1} - u^*), p^k - \bar{p}^{k+1} \rangle_Y \geq -\omega \|\bar{u}^{k+1} - u^*\|_N^2 - \frac{1}{4\omega} \|p^k - \bar{p}^{k+1}\|_{SN^{-1}S^*}^2, \\ & \langle p^k - p^*, p^k - \bar{p}^{k+1} \rangle_Y \leq \omega \|p^k - p^*\|_Y^2 + \frac{1}{4\omega} \|p^k - \bar{p}^{k+1}\|_Y^2. \end{aligned} \quad (4.7)$$

Take $\omega = 1$ in (4.7). Together with (4.6), we obtain

$$\langle Q(w^k - \bar{w}^{k+1}), \bar{w}^{k+1} - w^* \rangle_{U \times Y} \geq -\frac{1}{4} \|p^k - \bar{p}^{k+1}\|_{SN^{-1}S^*}^2 - \frac{1}{4} \|p^k - \bar{p}^{k+1}\|_Y^2 = -\frac{1}{4} \|p^k - \bar{p}^{k+1}\|_{I + SN^{-1}S^*}^2.$$

Therefore, we have

$$\begin{aligned} \|w^k - w^*\|_Q^2 &= \|w^k - \bar{w}^{k+1}\|_Q^2 + \|\bar{w}^{k+1} - w^*\|_Q^2 + 2 \langle Q(w^k - \bar{w}^{k+1}), \bar{w}^{k+1} - w^* \rangle_{U \times Y} \\ &\geq \|w^k - \bar{w}^{k+1}\|_Q^2 + \|\bar{w}^{k+1} - w^*\|_Q^2 - \frac{1}{2} \|p^k - \bar{p}^{k+1}\|_{SN^{-1}S^* + I}^2 \\ &= \|\bar{w}^{k+1} - w^*\|_Q^2 + \|w^k - \bar{w}^{k+1}\|_R^2. \end{aligned}$$

□

Next, we bound $\|\bar{w}^k - w^*\|_{U \times Y}$ using the properties of the following set-valued mapping:

$$\varphi : U \times Y \rightrightarrows U \times Y, \quad \varphi(w) = \begin{pmatrix} \varphi_1(w) \\ \varphi_2(w) \end{pmatrix} := \begin{pmatrix} Nu + \partial\theta(u) + S^*p \\ -Su + p - (Sf - y_d) \end{pmatrix}. \quad (4.8)$$

Note that $0 \in \varphi(w^*)$ by the optimality conditions (1.4).

Lemma 4.3. *There exists some $\kappa_0 > 0$ such that for any $w_1, w_2 \in U \times Y$, it holds that*

$$\kappa_0 \cdot \text{dist}(\varphi(w_1), \varphi(w_2)) \geq \|w_1 - w_2\|_{U \times Y}. \quad (4.9)$$

Proof. The inequality trivially holds if $\varphi(w_1)$ or $\varphi(w_2)$ is empty, where the distance in (4.9) is infinity. Otherwise, take any $\zeta_1 := (\xi_1, \eta_1)^\top \in \varphi(w_1)$ and $\zeta_2 := (\xi_2, \eta_2)^\top \in \varphi(w_2)$. It is easy to verify that

$$-S(N + \partial\theta)^{-1}(\xi_i - S^*p_i) + p_i - (Sf - y_d) = \eta_i, \quad i = 1, 2. \quad (4.10)$$

Rewrite (4.10) with $i = 2$ as

$$-S(N + \partial\theta)^{-1}(\xi_1 - S^*p_2) + p_2 - (Sf - y_d) = \eta_2 + r, \quad (4.11)$$

where $r \in Y$ is defined by

$$r = S(N + \partial\theta)^{-1}(\xi_2 - S^*p_2) - S(N + \partial\theta)^{-1}(\xi_1 - S^*p_2).$$

By the Cauchy-Schwarz inequality, (4.10) with $i = 1$, (4.11), and a similar argument to the proof of Lemma 3.2, we have

$$\|\eta_1 - (\eta_2 + r)\|_Y \|p_1 - p_2\|_Y \geq \langle \eta_1 - (\eta_2 + r), p_1 - p_2 \rangle_Y \geq \|p_1 - p_2\|_Y^2. \quad (4.12)$$

By Lemma 3.1 and the boundedness of S , we have

$$\|r\|_Y \leq c_0^{-1} \|S\| \|\xi_1 - \xi_2\|_U,$$

and hence

$$\|\eta_1 - (\eta_2 + r)\|_Y \leq \|\eta_1 - \eta_2\|_Y + c_0^{-1} \|S\| \|\xi_1 - \xi_2\|_U.$$

In view of (4.12), we obtain

$$\|p_1 - p_2\|_Y \leq \|\eta_1 - \eta_2\|_Y + c_0^{-1} \|S\| \|\xi_1 - \xi_2\|_U. \quad (4.13)$$

Next, observe that

$$u_i = (N + \partial\theta)^{-1}(\xi_i - S^*p_i), \quad i = 1, 2.$$

Again, similar to the proof of Lemma 3.2, it follows from (4.13) that

$$\|u_1 - u_2\|_U \leq c_0^{-1} \left(\left(1 + c_0^{-1} \|S\|^2 \right) \|\xi_1 - \xi_2\|_U + \|S\| \|\eta_1 - \eta_2\|_Y \right). \quad (4.14)$$

Hence, from (4.13) and (4.14) we have

$$\begin{aligned} \|w_1 - w_2\|_{U \times Y} &= \left(\|u_1 - u_2\|_U^2 + \|p_1 - p_2\|_Y^2 \right)^{1/2} \\ &\leq \left(2 \left(\left(c_0^{-1} \left(1 + c_0^{-1} \|S\|^2 \right) \right)^2 + \left(c_0^{-1} \|S\| \right)^2 \right) \|\xi_1 - \xi_2\|_U^2 + 2 \left(\left(c_0^{-1} \|S\| \right)^2 + 1 \right) \|\eta_1 - \eta_2\|_Y^2 \right)^{1/2} \\ &\leq \left(2 \max \left\{ \left(c_0^{-1} \left(1 + c_0^{-1} \|S\|^2 \right) \right)^2 + \left(c_0^{-1} \|S\| \right)^2, \left(c_0^{-1} \|S\| \right)^2 + 1 \right\} \right)^{1/2} \|\zeta_1 - \zeta_2\|_{U \times Y} \\ &=: \kappa_0 \|\zeta_1 - \zeta_2\|_{U \times Y}. \end{aligned} \quad (4.15)$$

Since $\zeta_1 \in \varphi(w_1)$ and $\zeta_2 \in \varphi(w_2)$ are taken arbitrarily, we conclude that

$$\|w_1 - w_2\|_{U \times Y} \leq \kappa_0 \cdot \text{dist}(\varphi(w_1), \varphi(w_2)).$$

□

Lemma 4.4. Let $\{w^k\}_{k=0}^\infty$ and $\{\bar{w}^{k+1}\}_{k=0}^\infty$ satisfy (4.1). Let $w^* = (u^*, p^*)^\top$ be the unique solution to (1.1). Then for any $k \geq 0$, it holds that

$$\|\bar{w}^{k+1} - w^*\|_Q \leq \kappa \|\bar{w}^{k+1} - w^k\|_R \quad (4.16)$$

for some constant $\kappa > 0$.

Proof. Note that (4.1) implies

$$Q(w^k - \bar{w}^{k+1}) - \begin{pmatrix} S^*(p^k - \bar{p}^{k+1}) \\ p^k - \bar{p}^{k+1} \end{pmatrix} \in \varphi(\bar{w}^{k+1}). \quad (4.17)$$

By (4.17), Lemma 4.3, and the fact that $0 \in \varphi(w^*)$, we have

$$\begin{aligned} \|\bar{w}^{k+1} - w^*\|_Q^2 &\leq \|Q\| \|\bar{w}^{k+1} - w^*\|_{U \times Y}^2 \\ &\leq \kappa_0^2 \|Q\| \cdot \text{dist}^2(\varphi(w^*), \varphi(\bar{w}^{k+1})) \\ &\leq \kappa_0^2 \|Q\| \cdot \text{dist}^2(0, \varphi(\bar{w}^{k+1})) \\ &\leq \kappa_0^2 \|Q\| \left\| Q(w^k - \bar{w}^{k+1}) - \begin{pmatrix} S^*(p^k - \bar{p}^{k+1}) \\ p^k - \bar{p}^{k+1} \end{pmatrix} \right\|_{U \times Y}^2 \\ &\leq \kappa_0^2 \|Q\| \left(\|(Q_A - N)(u^k - \bar{u}^{k+1}) - S^*(p^k - \bar{p}^{k+1})\|_U^2 + \|(Q_S - I)(p^k - \bar{p}^{k+1})\|_Y^2 \right) \\ &\leq \kappa_0^2 \|Q\| \left(2 \|Q_A - N\| \|u^k - \bar{u}^{k+1}\|_{Q_A - N}^2 + 2 \|p^k - \bar{p}^{k+1}\|_{SS^*}^2 \right. \\ &\quad \left. + \|Q_S - I\| \|p^k - \bar{p}^{k+1}\|_{Q_S - I}^2 \right). \end{aligned} \quad (4.18)$$

Since N is bounded and continuously invertible, by (4.2) we have

$$\begin{aligned} 2 \left(Q_S - \frac{1}{2}I - \frac{1}{2}SN^{-1}S^* \right) &\succeq \left(Q_S - \frac{1}{2}I - \frac{1}{2}SN^{-1}S^* \right) + \left(\frac{1}{2}I + \frac{1}{2}SN^{-1}S^* \right) = Q_S \\ &\succeq Q_S - I, \\ 2 \left(Q_S - \frac{1}{2}I - \frac{1}{2}SN^{-1}S^* \right) &\succeq 2 \left(\frac{1}{2}I + \frac{1}{2}SN^{-1}S^* \right) \succeq \sigma_0(N^{-1})SS^* = \|N\|^{-1}SS^*, \end{aligned} \quad (4.19)$$

where the notation \succeq means that the operator on its left hand side minus the operator on its right hand side is positive semidefinite. Combining (4.18) and (4.19), we conclude that

$$\|\bar{w}^{k+1} - w^*\|_Q^2 \leq 2\kappa_0^2 \|Q\| \max \left\{ \|Q_A - N\|, 2\|N\| + \|Q_S - I\| \right\} \|\bar{w}^{k+1} - w^k\|_R^2,$$

and thus complete the proof with

$$\begin{aligned} \kappa &:= 2\kappa_0^2 \|Q\| \max \left\{ \|Q_A - N\|, 2\|N\| + \|Q_S - I\| \right\} \\ &= 2\kappa_0^2 \cdot \max \left\{ \|Q_A - N\|, \|Q_S\| \right\} \cdot \max \left\{ \|Q_A - N\|, 2\|N\| + \|Q_S - I\| \right\}. \end{aligned}$$

□

With the above lemmas, we are now in a position to establish the asymptotic ε -optimality of (4.1).

Proposition 4.5. Let $\{w^k\}_{k=0}^\infty$ and $\{\bar{w}^k\}_{k=1}^\infty$ satisfy (4.1). Let $w^* = (u^*, p^*)^\top$ be the unique solution to (1.1). There exist constants $0 < \rho < 1$ and $c > 0$ independent of δ , such that

$$\|w^{k+1} - w^*\|_Q \leq \rho \|w^k - w^*\|_Q + c\delta. \quad (4.20)$$

In particular, for any $\varepsilon > 0$, there exist $\delta_0 = C\varepsilon$ with $C > 0$ independent of ε and $L = O(\log(1/\varepsilon))$, such that for any $\delta < \delta_0$ and $k \geq L$, the iterates $\{w^k\}_{k=0}^\infty$ of (4.1) satisfy

$$\|w^k - w^*\|_{U \times Y} < \varepsilon. \quad (4.21)$$

Proof. Combining Lemma 4.2 and Lemma 4.4 yields

$$\|\bar{w}^{k+1} - w^*\|_Q^2 \leq \frac{\kappa^2}{1 + \kappa^2} \|w^k - w^*\|_Q^2. \quad (4.22)$$

By (4.22), (4.1c) and (4.1d), we have

$$\begin{aligned} \|w^{k+1} - w^*\|_Q &\leq \|\bar{w}^{k+1} - w^*\|_Q + \|w^{k+1} - \bar{w}^{k+1}\|_Q \leq \rho \|w^k - w^*\|_Q + (2\|Q\|)^{1/2}\delta \\ &= \rho \|w^k - w^*\|_Q + c\delta, \end{aligned} \quad (4.23)$$

where

$$\rho = (\kappa^2/(1 + \kappa^2))^{1/2} \in (0, 1), \quad c = (2\|Q\|)^{1/2} = (2 \max \{\|Q_A - N\|, \|Q_S\|\})^{1/2} > 0.$$

Note that both ρ and c are independent of δ .

Now we fix some $\delta > 0$. Consider any

$$\varepsilon_1 > \left(\frac{2}{1 - \rho} + 1 \right) c\delta, \quad (4.24)$$

and define

$$\tilde{\rho} = \rho + \frac{c\delta}{\varepsilon_1 - c\delta}.$$

Note that $\rho < \tilde{\rho} < \frac{1+\rho}{2} \in (0, 1)$. For each iterate w^k , by (4.23) and the definitions of ε_1 and $\tilde{\rho}$, it is easy to verify the followings:

- If $\|w^k - w^*\|_Q \geq \varepsilon_1 - c\delta$, then $\|w^{k+1} - w^*\|_Q \leq \tilde{\rho} \|w^k - w^*\|_Q$;
- If $\|w^k - w^*\|_Q < \varepsilon_1 - c\delta$, then $\|w^{k+1} - w^*\|_Q < \varepsilon_1$.

Hence, all the iterates $\{w^k : k \geq L - 1\}$ with

$$L = \left\lceil \log_{\tilde{\rho}} \frac{\varepsilon_1 - c\delta}{\|w^0 - w^*\|_Q} \right\rceil + 2 \leq \left\lceil \left(\log \frac{1 + \rho}{2} \right)^{-1} \log \frac{\varepsilon_1}{(2 - \rho) \|w^0 - w^*\|_Q} \right\rceil + 2 = O \left(\log \left(\frac{1}{\varepsilon_1} \right) \right) \quad (4.25)$$

satisfy $\|w^k - w^*\|_Q < \varepsilon_1$. Since ρ does not depend on δ , the constant in $O(\log(1/\varepsilon_1))$ does not depend on δ .

Next, we bound $\|w^k - w^*\|_{U \times Y}$ from $\|w^{k-1} - w^*\|_Q$ for any ε_1 satisfying (4.24). Note that $Q_S \succeq I + SN^{-1}S^*$ and hence $\sigma_0(Q_S) \geq 1$, where $\sigma_0(Q_S)$ is the infimum of the spectrum of Q_S . Clearly, Q_S is linear, bounded, self-adjoint, and coercive, hence it admits a bounded inverse Q_S^{-1} with $\|Q_S^{-1}\| = \sigma_0(Q_S)^{-1}$. By the above discussions, there exists $L = O(\log(1/\varepsilon_1))$ defined in (4.25) such that for all $k \geq L - 1$,

$$\begin{aligned} \|u^k - u^*\|_{Q_A - N} &\leq \|w^k - w^*\|_Q < \varepsilon_1, \\ \|p^k - p^*\|_Y &\leq \sigma_0(Q_S)^{-1/2} \|p^k - p^*\|_{Q_S} \leq \sigma_0(Q_S)^{-1/2} \|w^k - w^*\|_Q < \sigma_0(Q_S)^{-1/2} \varepsilon_1. \end{aligned} \quad (4.26)$$

Since $Q_A - N$ is positive semidefinite, Q_A is positive definite. Applying Lemma 3.1 to Q_A shows that $(Q_A + \partial\theta)^{-1}$ is Lipschitz with constant $\sigma_0(Q_A)^{-1} \leq c_0^{-1}$. Thus, from (4.1a) we have

$$\begin{aligned} \|\bar{u}^{k+1} - u^*\|_U &\leq \sigma_0(Q_A)^{-1} (\|(Q_A - N)(u^k - u^*)\|_U + \|S^*(p^k - p^*)\|_Y) \\ &\leq \sigma_0(Q_A)^{-1} \left(\|Q_A - N\|^{1/2} \|u^k - u^*\|_{Q_A - N} + \|S\| \|p^k - p^*\|_Y \right) \\ &< \sigma_0(Q_A)^{-1} \left(\|Q_A - N\|^{1/2} + \sigma_0(Q_S)^{-1/2} \|S\| \right) \varepsilon_1. \end{aligned} \quad (4.27)$$

Therefore, for any $k \geq L$, it follows from (4.26), (4.27) and (4.1c)–(4.1d) that

$$\begin{aligned}
\|w^k - w^*\|_{U \times Y} &\leq \|\bar{w}^k - w^*\|_{U \times Y} + \|\bar{w}^k - w^k\|_{U \times Y} \\
&= \left(\|\bar{u}^k - u^*\|_U^2 + \|\bar{p}^k - p^*\|_Y^2 \right)^{1/2} + \left(\|\bar{u}^k - u^k\|_U^2 + \|\bar{p}^k - p^k\|_Y^2 \right)^{1/2} \\
&< \left(\sigma_0(Q_A)^{-2} \left(\|Q_A - N\|^{1/2} + \sigma_0(Q_S)^{-1/2} \|S\| \right)^2 + \sigma_0(Q_S)^{-1} \right)^{1/2} \varepsilon_1 + \sqrt{2}\delta \\
&< \left(\left(\sigma_0(Q_A)^{-2} \left(\|Q_A - N\|^{1/2} + \sigma_0(Q_S)^{-1/2} \|S\| \right)^2 + \sigma_0(Q_S)^{-1} \right)^{1/2} + \frac{\sqrt{2}(1-\rho)}{(3-\rho)c} \right) \varepsilon_1 \\
&\leq \left(\left(c_0^{-2} \left(\|Q_A - N\|^{1/2} + \|S\| \right)^2 + 1 \right)^{1/2} + \frac{\sqrt{2}(1-\rho)}{(3-\rho)c} \right) \varepsilon_1 \\
&:= C_1 \varepsilon_1,
\end{aligned} \tag{4.28}$$

where $C_1 > 0$ is a constant independent of ε_1 and δ .

For any $\varepsilon > 0$, take

$$\varepsilon_1 = \varepsilon/C_1, \quad \delta_0 = \frac{1-\rho}{(3-\rho)cC_1} \varepsilon =: C\varepsilon.$$

Clearly $C > 0$ is independent of ε . It is easy to verify that any $\delta < \delta_0$ satisfies (4.24), hence (4.28) implies for any $k \geq L$ that $\|w^k - w^*\|_{U \times Y} < \varepsilon$, where L is defined as in (4.25). Finally, recall that the constant in the big-O notation in (4.25) is independent of δ , which concludes the proof. \square

Remark 4.6. Note that (4.20) remains valid even when $\delta = 0$, which verifies the linear convergence rate of (1.5) for the specific model (1.1). Note from (4.25) and (4.28) that the constant in $L = O(\log(1/\varepsilon))$ and C depends only on the choice of the preconditioners Q_A and Q_S in (4.1). This observation will be crucial for establishing the uniformity of the constants C and L in Theorem 4.13, the asymptotic ε -optimality result of the *iUzawa-Net*.

4.2 Universal Approximation of \mathcal{Q}_A^k

Since \mathcal{S}^k and \mathcal{A}^k are implemented as FNOs, their universal approximation properties follow directly from Proposition 3.5. In addition, by Proposition 3.7, the operator \mathcal{Q}_S^k can be realized as sufficiently positive definite operator, which is already adequate for our purposes. Consequently, \mathcal{Q}_A^k is the only component whose approximation properties require further analysis among all network modules in the *iUzawa-Net*. In this subsection, we prove that under Assumption 2.2 and some additional mild conditions, the neural network architecture \mathcal{Q}_A^k defined in (2.11)–(2.12) can approximate $(N + \tau I + \partial\theta)^{-1}$ to arbitrary accuracy on any compact set. We begin with the following continuity assumption on the subgradient of ψ_ξ defined in Assumption 2.2, which is required to apply Proposition 3.4 in the subsequent analysis.

Assumption 4.7. Let E and ψ be defined as in Assumption 2.2. Denote $\text{gph } \partial\psi_\xi$ as the graph of $\partial\psi_\xi$ [52]. We assume that the set-valued mapping $\xi \mapsto \text{gph } \partial\psi_\xi$ is continuous; or equivalently, for any $\xi \in E$ and any sequence $\{\xi_n\} \subset E$ with $\xi_n \rightarrow \xi$, the set-valued mappings $\partial\psi_{\xi_n}$ converge to $\partial\psi_\xi$ in the sense of graph limit, i.e.,

$$\text{g-lim sup}_{n \rightarrow \infty} \partial\psi_{\xi_n} \subset \partial\psi_\xi \subset \text{g-lim inf}_{n \rightarrow \infty} \partial\psi_{\xi_n}, \tag{4.29}$$

where the graphical outer limit g-lim sup and graphical inner limit g-lim inf are defined as in [52, Definition 5.32]⁵.

Remark 4.8. The notations of graphical convergence and graphical outer/inner limit are standard and widely adopted in variational analysis. The condition (4.29) is a mild assumption that requires ψ_ξ to be parameterized by ξ in a graphically continuous manner with respect to its subdifferential. Since ψ_ξ is a mapping from \mathbb{R} to \mathbb{R} , (4.29) is verifiable for many practical cases, including the examples given in Section 2.3.

⁵For any two set-valued mappings $\varphi_1 : X \rightrightarrows Y$ and $\varphi_2 : X \rightrightarrows Y$, we follow the convention in [52] and denote $\varphi_1 \subset \varphi_2$ if and only if $\varphi_1(x) \subset \varphi_2(x)$ for any $x \in X$.

We claim that the mapping $(N + \tau I + \partial\theta)^{-1}$ acts pointwise on its input. Furthermore, under Assumption 4.7, we show that this pointwise action is continuous by some technical variational analysis arguments.

Lemma 4.9. *Assume that N and θ satisfy Assumption 2.2 and let λ , c_0 , E and μ be defined as therein. Then there exists a function $\phi : \mathbb{R} \times E \times [c_0, \infty) \rightarrow \mathbb{R}$, such that for any $v \in L^2(\Omega)$, we have*

$$(N + \tau I + \partial\theta)^{-1}(v)(x) = \phi(v(x), \mu(x), \lambda(x)), \quad \text{a.e. in } \Omega, \quad (4.30)$$

and $\phi(v(\cdot), \mu(\cdot), \lambda(\cdot)) \in L^2(\Omega)$. Moreover, $\phi(s, \xi, \eta)$ is Lipschitz continuous in the variable s with a uniform Lipschitz constant for all $(\xi, \eta)^\top \in E \times [c_0, \infty)$. If Assumption 4.7 holds in addition, then ϕ is continuous on $\mathbb{R} \times E \times [c_0, \infty)$.

Proof. Fix any $\bar{v} \in L^2(\Omega)$ and denote $\bar{u} = (N + \tau I + \partial\theta)^{-1}(\bar{v})$. We have

$$\bar{u} = \arg \min_{u \in L^2(\Omega)} \left\{ \frac{1}{2} \int_{\Omega} (\lambda(x) + \tau) |u(x)|^2 - \bar{v}(x)u(x) + \psi(u(x), \mu(x)) dx \right\}.$$

Clearly, the above optimization problem can be equivalently decomposed into pointwise minimization problems, i.e., $\bar{u}(x)$ satisfies

$$\bar{u}(x) = \arg \min_{r \in \mathbb{R}} \left\{ \frac{1}{2} (\lambda(x) + \tau) r^2 - \bar{v}(x)r + \psi(r, \mu(x)) \right\}, \quad \text{a.e. in } \Omega.$$

Thus, $(N + \tau I + \partial\theta)^{-1}(\bar{v})(x)$ satisfies (4.30) with

$$\phi(s, \xi, \eta) = \arg \min_{r \in \mathbb{R}} \left\{ \frac{1}{2} (\eta + \tau) r^2 - sr + \psi(r, \xi) \right\}, \quad \text{for } s \in \mathbb{R}, \xi \in \mathbb{R}^m, \eta \geq c_0.$$

We have $\phi(v(\cdot), \mu(\cdot), \lambda(\cdot)) \in L^2(\Omega)$ since $(N + \tau I + \partial\theta)^{-1}$ maps $L^2(\Omega)$ into $L^2(\Omega)$. Moreover, note that

$$\phi(s, \xi, \eta) = ((\eta + \tau)I + \partial\psi_\xi)^{-1}(s). \quad (4.31)$$

Hence, applying Lemma 3.1 to $(\eta + \tau)I$ and ψ_ξ , we see that $\phi(s, \xi, \eta)$ is Lipschitz continuous in s for all $(\xi, \eta)^\top \in E \times [c_0, \infty)$ with a uniform Lipschitz constant $(c_0 + \tau)^{-1}$.

Denote the set-valued mappings $\Xi_\xi = \partial\psi_\xi$ and $H_\eta = (\eta + \tau)I$ for any $\xi \in E$ and $\eta \geq c_0$. Thus (4.29) becomes

$$\text{g-lim sup}_{n \rightarrow \infty} \Xi_{\xi_n} \subset \Xi_\xi \subset \text{g-lim inf}_{n \rightarrow \infty} \Xi_{\xi_n}. \quad (4.32)$$

and (4.31) becomes

$$\phi(s, \xi, \eta) = (\Xi_\xi + H_\eta)^{-1}(s). \quad (4.33)$$

We now show that under (4.32), for any $(\bar{\xi}, \bar{\eta})^\top \in E \times [c_0, \infty)$ and any sequence $\{(\xi_n, \eta_n)^\top\} \subset E \times [c_0, \infty)$ with $(\xi_n, \eta_n)^\top \rightarrow (\bar{\xi}, \bar{\eta})^\top$, we have

$$\text{g-lim sup}_{n \rightarrow \infty} (\Xi_{\xi_n} + H_{\eta_n}) \subset \Xi_{\bar{\xi}} + H_{\bar{\eta}} \subset \text{g-lim inf}_{n \rightarrow \infty} (\Xi_{\xi_n} + H_{\eta_n}). \quad (4.34)$$

By [52, Proposition 5.33], for any $\bar{r} \in \mathbb{R}$, we have

$$\begin{aligned} \left(\text{g-lim sup}_{n \rightarrow \infty} (\Xi_{\xi_n} + H_{\eta_n}) \right) (\bar{r}) &= \bigcup_{\{r_n \rightarrow \bar{r}\}} \limsup_{n \rightarrow \infty} (\Xi_{\xi_n}(r_n) + H_{\eta_n}(r_n)), \\ \left(\text{g-lim inf}_{n \rightarrow \infty} (\Xi_{\xi_n} + H_{\eta_n}) \right) (\bar{r}) &= \bigcup_{\{r_n \rightarrow \bar{r}\}} \liminf_{n \rightarrow \infty} (\Xi_{\xi_n}(r_n) + H_{\eta_n}(r_n)), \end{aligned} \quad (4.35)$$

where the unions are taken over all sequences $\{r_n\} \subset \mathbb{R}$ such that $r_n \rightarrow \bar{r}$, and the outer limit \limsup and the inner limit \liminf are defined in [52, Definition 4.1]. Since $(\eta_n + \tau)r_n \rightarrow (\bar{\eta} + \tau)\bar{r}$ for any $r_n \rightarrow \bar{r}$, by the definition of H_η , we have

$$\limsup_{n \rightarrow \infty} H_{\eta_n}(r_n) = \liminf_{n \rightarrow \infty} H_{\eta_n}(r_n) = H_\eta(\bar{r}). \quad (4.36)$$

Applying [52, Theorem 4.26] to the addition operator $A : \mathbb{R} \times \mathbb{R} \rightarrow \mathbb{R}, (x, y) \mapsto x + y$, which satisfies $|A(x, y)| \rightarrow \infty$ when $|(x, y)| \rightarrow \infty$, we obtain that for any $r_n \rightarrow \bar{r}$,

$$\begin{aligned} \limsup_{n \rightarrow \infty} (\Xi_{\xi_n}(r_n) + H_{\eta_n}(r_n)) &= A \left(\limsup_{n \rightarrow \infty} (\Xi_{\xi_n}(r_n) \times H_{\eta_n}(r_n)) \right) \\ &\subset A \left(\limsup_{n \rightarrow \infty} \Xi_{\xi_n}(r_n) \times \limsup_{n \rightarrow \infty} H_{\eta_n}(r_n) \right) \\ &= H_{\bar{\eta}}(\bar{r}) + \limsup_{n \rightarrow \infty} \Xi_{\xi_n}(r_n), \end{aligned} \quad (4.37)$$

where the last equality follows from (4.36). Similarly,

$$\begin{aligned} \liminf_{n \rightarrow \infty} (\Xi_{\xi_n}(r_n) + H_{\eta_n}(r_n)) &\supset A \left(\liminf_{n \rightarrow \infty} (\Xi_{\xi_n}(r_n) \times H_{\eta_n}(r_n)) \right) \\ &= A \left(\liminf_{n \rightarrow \infty} \Xi_{\xi_n}(r_n) \times \liminf_{n \rightarrow \infty} H_{\eta_n}(r_n) \right) \\ &= H_{\bar{\eta}}(\bar{r}) + \liminf_{n \rightarrow \infty} \Xi_{\xi_n}(r_n). \end{aligned} \quad (4.38)$$

Take the union over all sequences $r_n \rightarrow \bar{r}$ in (4.37) and (4.38). It follows from (4.32), (4.35), and [52, Proposition 5.33] that

$$\begin{aligned} \left(\text{g-lim sup}_{n \rightarrow \infty} (\Xi_{\xi_n} + H_{\eta_n}) \right) (\bar{r}) &\subset \bigcup_{\{r_n \rightarrow \bar{r}\}} \left(H_{\bar{\eta}}(\bar{r}) + \limsup_{n \rightarrow \infty} \Xi_{\xi_n}(r_n) \right) \\ &= H_{\bar{\eta}}(\bar{r}) + \bigcup_{\{r_n \rightarrow \bar{r}\}} \limsup_{n \rightarrow \infty} \Xi_{\xi_n}(r_n) \\ &= H_{\bar{\eta}}(\bar{r}) + \left(\text{g-lim sup}_{n \rightarrow \infty} \Xi_{\xi_n} \right) (\bar{r}) \\ &\subset (\Xi_{\bar{\xi}} + H_{\bar{\eta}}) (\bar{r}), \end{aligned}$$

and similarly,

$$\left(\text{g-lim inf}_{n \rightarrow \infty} (\Xi_{\xi_n} + H_{\eta_n}) \right) (\bar{r}) \supset (\Xi_{\bar{\xi}} + H_{\bar{\eta}}) (\bar{r}),$$

which proves (4.34).

We are now ready to establish the continuity of ϕ at any $(\bar{s}, \bar{\xi}, \bar{\eta})^\top \in \mathbb{R} \times E \times [c_0, \infty)$ under (4.29) (or equivalently, under (4.32)). Recall that ϕ takes the form (4.33). Since ψ_ξ is convex, lower semicontinuous, and proper for any $\xi \in E$, $\Xi_{\bar{\xi}} = \partial\psi_{\bar{\xi}}$ is closed valued [51, Section 23]. By (4.34) and [52, Theorem 5.37], we have for any $(\xi_n, \eta_n)^\top \rightarrow (\bar{\xi}, \bar{\eta})^\top$ that

$$\limsup_{n \rightarrow \infty} (\Xi_{\xi_n} + H_{\eta_n})^{-1}(\bar{s}) \subset (\Xi_{\bar{\xi}} + H_{\bar{\eta}})^{-1}(\bar{s}).$$

Hence, by (4.33) and the definition of \limsup , any limit point of the sequence $\{\phi(\bar{s}, \xi_n, \eta_n)\}_{n=1}^\infty$ is $\phi(\bar{s}, \bar{\xi}, \bar{\eta})$. We claim that $\{\phi(\bar{s}, \xi_n, \eta_n)\}_{n=1}^\infty$ is bounded. If not, there exists an unbounded subsequence of $\{\phi(\bar{s}, \xi_n, \eta_n)\}_{n=1}^\infty$, and assume without loss of generality that $|\phi(\bar{s}, \xi_n, \eta_n)| \rightarrow \infty$. Again, by [52, Theorem 5.37],

$$(\Xi_{\bar{\xi}} + H_{\bar{\eta}})^{-1}(\bar{s}) \subset \bigcap_{\omega > 0} \liminf_{n \rightarrow \infty} (\Xi_{\xi_n} + H_{\eta_n})^{-1}(\bar{B}(\bar{s}, \omega)).$$

where $\bar{B}(\bar{s}, \omega)$ denotes the closed ball centered at \bar{s} with radius ω . Hence by (4.33), for any $\omega > 0$, there exists a sequence $\{s_n\}_{n=1}^\infty \subset \bar{B}(\bar{s}, \omega)$ such that $\phi(s_n, \xi_n, \eta_n) \rightarrow \phi(\bar{s}, \bar{\xi}, \bar{\eta})$ as $n \rightarrow \infty$. In particular, there exists $s_n \rightarrow \bar{s}$ such that $\phi(s_n, \xi_n, \eta_n) \rightarrow \phi(\bar{s}, \bar{\xi}, \bar{\eta})$. Together with the Lipschitz continuity of $\phi(\cdot, \xi_n, \eta_n)$ and the uniformity of the Lipschitz constant, this contradicts $|\phi(\bar{s}, \xi_n, \eta_n)| \rightarrow \infty$. Therefore, $\{\phi(\bar{s}, \xi_n, \eta_n)\}_{n=1}^\infty$ is bounded with every convergent subsequence converging to $\phi(\bar{s}, \bar{\xi}, \bar{\eta})$, which implies that

$$\lim_{n \rightarrow \infty} \phi(\bar{s}, \xi_n, \eta_n) = \phi(\bar{s}, \bar{\xi}, \bar{\eta}). \quad (4.39)$$

Since the above argument holds for any sequence $\{(\xi_n, \eta_n)^\top\} \subset E \times [c_0, \infty)$ with $(\xi_n, \eta_n)^\top \rightarrow (\bar{\xi}, \bar{\eta})^\top$, we have that $\phi(\bar{s}, \xi, \eta)$ being continuous in $(\xi, \eta)^\top$ on $E \times [c_0, \infty)$ for any $\bar{s} \in \mathbb{R}$. Finally, the joint continuity of ϕ follows from the Lipschitz continuity in s and the continuity in $(\xi, \eta)^\top$. \square

Lemma 4.10. *Assume that Assumption 2.2 holds, and let λ , μ , E and c_0 be defined as therein. Let $\phi : \mathbb{R} \times E \times [c_0, \infty) \rightarrow \mathbb{R}$ be a continuous function such that $\phi(s, \xi, \eta)$ is Lipschitz continuous in s with a uniform Lipschitz constant $L_\phi > 0$ for all $\xi \in E$ and $\eta \in [c_0, \infty)$, and $\phi(u(\cdot), \mu(\cdot), \lambda(\cdot)) \in L^2(\Omega)$ for any $u \in L^2(\Omega)$. Assume that $G : L^2(\Omega) \rightarrow L^2(\Omega)$ satisfies*

$$G(u)(x) = \phi(u(x), \mu(x), \lambda(x)), \quad \text{a.e. in } \Omega, \quad \forall u \in L^2(\Omega). \quad (4.40)$$

Then for any compact $K \subset L^2(\Omega)$ and $\varepsilon > 0$, there exists a neural network $\mathcal{N} : \mathbb{R}^{m+2} \rightarrow \mathbb{R}$ as given in (2.12), such that the neural network $\mathcal{G} : L^2(\Omega) \rightarrow L^2(\Omega)$ defined by

$$\mathcal{G}(u(x)) = \mathcal{N}(u(x), \mu(x), \lambda(x)), \quad \text{a.e. in } \Omega, \quad \forall u \in L^2(\Omega) \quad (4.41)$$

satisfies

$$\sup_{u \in K} \|G(u) - \mathcal{G}(u)\|_{L^2(\Omega)} < \varepsilon. \quad (4.42)$$

Moreover, the image $\mathcal{G}(K)$ is compact in $L^2(\Omega)$.

Proof. Fix any compact $K \subset L^2(\Omega)$ and $\varepsilon > 0$. Denote by $\nu(x) := (\mu(x), \lambda(x))^\top \in L^\infty(\Omega; \mathbb{R}^{m+1})$. For any $u \in L^2(\Omega)$ and $r > 0$, define $u_r : \Omega \rightarrow \mathbb{R}$ (up to a measure zero set) by

$$u_r(x) = \begin{cases} u(x), & |u(x)| \leq r, \\ 0, & |u(x)| > r, \end{cases} \quad \text{a.e. in } \Omega. \quad (4.43)$$

Consider the mapping $\pi_r : L^2(\Omega) \rightarrow \mathbb{R}$ defined by $\pi_r(u) = \|u - u_r\|_{L^2(\Omega)}$. By the dominated convergence theorem, we have $\lim_{r \rightarrow \infty} \pi_r(u) = 0$. It is clear that π_r is continuous and $r \mapsto \pi_r(u)$ is monotone for each $u \in L^2(\Omega)$. Since K is compact, it follows from Dini's theorem that

$$\lim_{r \rightarrow \infty} \sup_{u \in K} \|u - u_r\|_{L^2(\Omega)} = 0.$$

In particular, there exists $R_0 > 0$ independent of u , such that $R_0 \geq \|\nu\|_{L^\infty(\Omega; \mathbb{R}^{m+1})}$ and

$$\|u - u_{R_0}\|_{L^2(\Omega)}^2 < \frac{\varepsilon^2}{4L_\phi^2}, \quad \text{for all } u \in K. \quad (4.44)$$

We now approximate $G(u)$ by a neural network satisfying (2.11). Define the constants

$$R_1 := \|\nu\|_{L^\infty(\Omega; \mathbb{R}^{m+1})}, \quad M_0 := \text{ess sup}_{x \in \Omega} |\phi(0, \nu(x))|,$$

and two compact sets

$$\mathcal{K}_1 := [-R_0, R_0] \subset \mathbb{R}, \quad \mathcal{K}_2 = E \times [c_0, R_1] \subset \mathbb{R}^{m+1}.$$

Note that $R_1 \leq R_0$, $\nu(x) \in \mathcal{K}_2$ a.e. on Ω , and $M_0 < \infty$ (since K_2 is compact and $\phi(0, \cdot)$ is continuous on K_2 by Lemma 4.9). By Lemma 3.6, there exists a neural network $\mathcal{N}_0 : \mathbb{R}^{m+2} \rightarrow \mathbb{R}$ of the form (2.12), such that

$$\sup_{s \in \mathcal{K}_1, \zeta \in \mathcal{K}_2} |\phi(s, \zeta) - \mathcal{N}_0(s, \zeta)| < \frac{\varepsilon}{2|\Omega|^{1/2}}. \quad (4.45)$$

Define the neural network $\mathcal{N} : \mathbb{R}^{m+2} \rightarrow \mathbb{R}$ with ReLU activation function σ by

$$\mathcal{N}(s, \zeta) = \mathcal{N}_0(R_0 \mathbf{1} - \sigma(2R_0 \mathbf{1} - \sigma((s, \zeta)^\top + R_0 \mathbf{1}))),$$

where $\mathbf{1} \in \mathbb{R}^{m+2}$ is the all-one vector. Note that \mathcal{N} also has the structure defined in (2.12). Since $R_1 \leq R_0$, we have

$$\mathcal{N}(s, \zeta) = \mathcal{N}_0(\text{proj}_{[-R_0, R_0]^{m+2}}(s, \zeta)) = \mathcal{N}_0(\text{proj}_{\mathcal{K}_1}(s), \zeta), \quad \forall s \in \mathbb{R}, \zeta \in \mathcal{K}_2. \quad (4.46)$$

For any $u \in K$, define the sets $E_u^+ := \{x \in \Omega : u(x) > R_0\}$ and $E_u^- := \{x \in \Omega : u(x) < -R_0\}$. By the set decomposition $\Omega = E_u^+ \cup E_u^- \cup (\Omega \setminus (E_u^+ \cup E_u^-))$, we have

$$\begin{aligned} & \|G(u) - \mathcal{G}(u)\|_{L^2(\Omega)}^2 \\ &= \int_{E_u^+} |\phi(u(x), \nu(x)) - \mathcal{N}(u(x), \nu(x))|^2 dx + \int_{E_u^-} |\phi(u(x), \nu(x)) - \mathcal{N}(u(x), \nu(x))|^2 dx \\ &\quad + \int_{\Omega \setminus (E_u^+ \cup E_u^-)} |\phi(u(x), \nu(x)) - \mathcal{N}(u(x), \nu(x))|^2 dx \\ &=: \text{(I)} + \text{(II)} + \text{(III)}. \end{aligned}$$

For (I), from (4.45), (4.46), the Lipschitz continuity of ϕ in s , and the fact that $\nu(x) \in \mathcal{K}_2$ a.e. in Ω , we have

$$\begin{aligned} \text{(I)} &\leq \int_{E_u^+} \left(2|\phi(u(x), \nu(x)) - \phi(R_0, \nu(x))|^2 + 2|\phi(R_0, \nu(x)) - \mathcal{N}(u(x), \nu(x))|^2 \right) dx \\ &= 2 \int_{E_u^+} |\phi(u(x), \nu(x)) - \phi(R_0, \nu(x))|^2 dx + 2 \int_{E_u^+} |\phi(R_0, \nu(x)) - \mathcal{N}_0(R_0, \nu(x))|^2 dx \\ &\leq 2L_\phi^2 \int_{E_u^+} |u(x) - u_{R_0}(x)|^2 dx + 2|E_u^+| \cdot \frac{\varepsilon^2}{4|\Omega|} \\ &\leq 2L_\phi^2 \|u - u_{R_0}\|_{L^2(E_u^+)}^2 + \frac{|E_u^+|}{2|\Omega|} \cdot \varepsilon^2. \end{aligned}$$

Similarly,

$$\text{(II)} \leq 2L_\phi^2 \|u - u_{R_0}\|_{L^2(E_u^-)}^2 + \frac{|E_u^-|}{2|\Omega|} \cdot \varepsilon^2.$$

For (III), we have $|u(x)| \leq R_0$ on $\Omega \setminus (E_u^+ \cup E_u^-)$, and hence by (4.45),

$$\begin{aligned} \text{(III)} &= \int_{\Omega \setminus (E_u^+ \cup E_u^-)} |\phi(u(x), \nu(x)) - \mathcal{N}_0(u(x), \nu(x))|^2 dx \\ &\leq \frac{|\Omega \setminus (E_u^+ \cup E_u^-)|}{4|\Omega|} \cdot \varepsilon^2. \end{aligned}$$

Combining the estimates of (I), (II) and (III), it follows from (4.44) that

$$\begin{aligned} \|G(u) - \mathcal{G}(u)\|_{L^2(\Omega)}^2 &= \text{(I)} + \text{(II)} + \text{(III)} \\ &\leq 2L_\phi^2 \|u - u_{R_0}\|_{L^2(\Omega)}^2 + \frac{2|E_u^+| + 2|E_u^-| + |\Omega \setminus (E_u^+ \cup E_u^-)|}{4|\Omega|} \cdot \varepsilon^2 \\ &\leq \frac{\varepsilon^2}{2} + \frac{\varepsilon^2}{2} = \varepsilon^2. \end{aligned}$$

Since the above inequality is valid for all $u \in K$, we conclude that (4.42) holds.

Next, for proving the compactness of $\mathcal{G}(K)$, it suffices to show the continuity of \mathcal{G} on K . Take any $\varepsilon' > 0$. For any $u, v \in K$, we have

$$\begin{aligned} \|\mathcal{G}(u) - \mathcal{G}(v)\|_{L^2(\Omega)}^2 &= \int_{\Omega} |\mathcal{N}(u(x), \nu(x)) - \mathcal{N}(v(x), \nu(x))|^2 dx \\ &= \int_{\Omega} |\mathcal{N}_0(u_{R_0}(x), \nu(x)) - \mathcal{N}_0(v_{R_0}(x), \nu(x))|^2 dx. \end{aligned} \tag{4.47}$$

Since \mathcal{N}_0 is continuous on \mathbb{R}^{m+2} , we have

$$\sup_{x \in \Omega} |\mathcal{N}_0(u_{R_0}(x), \nu(x)) - \mathcal{N}_0(v_{R_0}(x), \nu(x))|^2 \leq \sup_{s_1, s_2 \in \mathcal{K}_1, \zeta \in \mathcal{K}_2} |\mathcal{N}_0(s_1, \zeta) - \mathcal{N}_0(s_2, \zeta)|^2 =: M_1 < \infty. \tag{4.48}$$

Note that M_1 does not depend on the choice of u and v in K . Moreover, \mathcal{N}_0 is uniformly continuous on the compact set $\mathcal{K}_1 \times \mathcal{K}_2$. Thus, there exists a $\delta' > 0$, independent of u and v , such that

$$\begin{aligned} & (s_1, \zeta_1)^\top, (s_2, \zeta_2)^\top \in \mathcal{K}_1 \times \mathcal{K}_2, \quad \|(s_1, \zeta_1)^\top - (s_2, \zeta_2)^\top\| \leq \delta' \\ & \Rightarrow |\mathcal{N}_0(s_1, \zeta_1) - \mathcal{N}_0(s_2, \zeta_2)| < \frac{\varepsilon'}{(2|\Omega|)^{1/2}}. \end{aligned} \tag{4.49}$$

Denote the set $E'_{u,v} := \{x \in \Omega : |u_{R_0}(x) - v_{R_0}(x)| \geq \delta'\}$ for any $u, v \in K$. By Chebyshev's inequality, we have

$$|E'_{u,v}| \leq \frac{1}{(\delta')^2} \|u_{R_0} - v_{R_0}\|_{L^2(\Omega)}^2 \leq \frac{1}{(\delta')^2} \|u - v\|_{L^2(\Omega)}^2, \quad \forall u, v \in K. \quad (4.50)$$

It follows from (4.47)–(4.50) and the definition of $E'_{u,v}$ that

$$\begin{aligned} \|\mathcal{G}(u) - \mathcal{G}(v)\|_{L^2(\Omega)}^2 &= \int_{E'_{u,v}} |\mathcal{N}_0(u_{R_0}(x), \nu(x)) - \mathcal{N}_0(v_{R_0}(x), \nu(x))|^2 dx \\ &\quad + \int_{\Omega \setminus E'_{u,v}} |\mathcal{N}_0(u_{R_0}(x), \nu(x)) - \mathcal{N}_0(v_{R_0}(x), \nu(x))|^2 dx \\ &\leq \frac{M_1}{(\delta')^2} \|u - v\|_{L^2(\Omega)}^2 + \frac{(\varepsilon')^2}{2}. \end{aligned}$$

Hence, there exists $\delta := (\varepsilon' \delta')/(2M_1)^{1/2}$ such that for any $u, v \in K$ with $\|u - v\|_{L^2(\Omega)} < \delta$, we have $\|\mathcal{G}(u) - \mathcal{G}(v)\|_{L^2(\Omega)} < \varepsilon'$. Note that the constant δ does not depend on u or v . Since $\varepsilon' > 0$ is taken arbitrarily, we conclude that \mathcal{G} is uniformly continuous on K . In particular, $\mathcal{G}(K)$ is compact. \square

Proposition 4.11. *Let $N : L^2(\Omega) \rightarrow L^2(\Omega)$ and $\theta : L^2(\Omega) \rightarrow \mathbb{R} \cup \{+\infty\}$ satisfy Assumptions 2.2 and 4.7. For any compact set $K \subset L^2(\Omega)$ and $\varepsilon > 0$, there exists a neural network \mathcal{Q}_A defined in (2.11) such that*

$$\sup_{v \in K} \|(N + \tau I + \partial\theta)^{-1}(v) - \mathcal{Q}_A(v)\|_{L^2(\Omega)} < \varepsilon.$$

Moreover, the image $\mathcal{Q}_A(K)$ is compact in $L^2(\Omega)$.

Proof. This follows immediately by first applying Lemma 4.9 and then applying Lemma 4.10 with $\nu(x) = (\mu(x), \lambda(x))^\top$ and $G = (N + \tau I + \partial\theta)^{-1}$. \square

4.3 The iUzawa-Net as Inexact Iterations of (1.5)

In this subsection, we show that the iUzawa-Net (1.7) can be embedded into the abstract framework (4.1). Specifically, we prove that the conditions (4.1c)–(4.1d) can be satisfied with arbitrary $\delta > 0$ by choosing sufficiently accurate neural network surrogates \mathcal{Q}_S , \mathcal{Q}_A , \mathcal{S} , and \mathcal{A} for the corresponding operators.

Proposition 4.12. *Assume that Assumptions 2.2 and 4.7 hold. Let $K \subset U \times Y$ be any compact sets, and denote by K_U and K_Y the projections of K onto U and Y , respectively. For any $\delta > 0$, there exist FNOs \mathcal{S} , \mathcal{A} , neural networks \mathcal{Q}_A defined in (2.11) and \mathcal{Q}_S defined in (2.7), and compact sets $K_{\mathcal{A}} \subset Y$ and $K_{\mathcal{Q}_A}, K_{\mathcal{S}} \subset U$, such that*

- (i) \mathcal{Q}_S is bounded, linear, and $\mathcal{Q}_S - (I + SN^{-1}S^*)$ is positive definite.
- (ii) The following approximation bounds hold:

$$\begin{aligned} K_{\mathcal{A}} &:= K_Y, \quad \sup_{p \in K_{\mathcal{A}}} \|S^*p - \mathcal{A}(p)\|_U < \min \left\{ \frac{1}{2}, \frac{1}{4\|S\|}, (c_0 + \tau)^{-1} \right\} (c_0 + \tau)\delta, \\ K_{\mathcal{Q}_A} &:= \tau K_U - \mathcal{A}(K_{\mathcal{A}}), \quad \sup_{v \in K_{\mathcal{Q}_A}} \|(N + \tau I + \partial\theta)^{-1}(v) - \mathcal{Q}_A(v)\|_U < \min \left\{ \frac{1}{2}, \frac{1}{4\|S\|} \right\} \delta, \\ K_{\mathcal{S}} &:= \mathcal{Q}_A(K_{\mathcal{Q}_A}) + K_U, \quad \sup_{v \in K_{\mathcal{S}}} \|Sv - \mathcal{S}(v)\|_Y < \frac{1}{2}\delta. \end{aligned} \quad (4.51)$$

Moreover, for any $(f, y_d)^\top \in K$ and $w^k = (u^k, p^k)^\top \in K$, let \mathcal{S} , \mathcal{A} , \mathcal{Q}_A and \mathcal{Q}_S satisfy the conditions above. Let $\bar{w}^{k+1} = (\bar{u}^{k+1}, \bar{p}^{k+1})^\top$ be defined by (4.1a)–(4.1b) with $Q_A = N + \tau I$ and $Q_S = \mathcal{Q}_S$, and $w^{k+1} = (u^{k+1}, p^{k+1})^\top$ be the output of the $(k+1)$ -th layer of the iUzawa-Net (1.7) with inputs y_d , f , u^k , p^k and neural networks $\mathcal{S}^k = \mathcal{S}$, $\mathcal{A}^k = \mathcal{A}$, $\mathcal{Q}_A^k = \mathcal{Q}_A$, $\mathcal{Q}_S^k = \mathcal{Q}_S$. Then we have

$$\max \{ \|u^{k+1} - \bar{u}^{k+1}\|_U, \|p^{k+1} - \bar{p}^{k+1}\|_Y \} < \delta, \quad (4.52)$$

and the image set $\{w^{k+1} : w^k \in K, (f, y_d)^\top \in K\}$ is compact.

Proof. By Proposition 3.7, there exists a neural network \mathcal{Q}_S defined in (2.7) such that \mathcal{Q}_S is linear, bounded, and $\mathcal{Q}_S - (I + SN^{-1}S^*)$ is positive semidefinite. In particular, we have $\sigma_0(\mathcal{Q}_S) \geq 1$. Note that K_U and K_Y are compact, hence the existence of \mathcal{A} , \mathcal{Q}_A and \mathcal{S} satisfying (4.51) and the compactness of $K_{\mathcal{A}}$, $K_{\mathcal{Q}_A}$, and $K_{\mathcal{S}}$ follow from Propositions 3.5 and 4.11. Moreover, the compactness of $\{w^{k+1} : w^k \in K, (f, y_d)^\top \in K\}$ follows from the continuity of \mathcal{S} , \mathcal{A} , \mathcal{Q}_A , and \mathcal{Q}_S in $L^2(\Omega)$ -norm.

To verify (4.52), note that $p^k \in K_Y = K_{\mathcal{A}}$, $u^k \in K_U$, and $\sigma_0(\mathcal{Q}_S) \geq 1$. Hence

$$\|S^*p^k - \mathcal{A}(p^k)\|_U < \min \left\{ \frac{1}{2}, \frac{1}{4\|S\|} \sigma_0(\mathcal{Q}_S) \right\} (c_0 + \tau) \delta.$$

$$\|(N + \tau I + \partial\theta)^{-1}(\tau u^k - \mathcal{A}(p^k)) - \mathcal{Q}_A(\tau u^k - \mathcal{A}(p^k))\|_U < \min \left\{ \frac{1}{2}, \frac{1}{4\|S\|} \sigma_0(\mathcal{Q}_S) \right\} \delta.$$

Applying Lemma 3.1 to $N + \tau I$ yields that $(N + \tau I + \partial\theta)^{-1}$ is Lipschitz continuous with constant $(c_0 + \tau)^{-1}$. Therefore, we have

$$\begin{aligned} \|u^{k+1} - \bar{u}^{k+1}\|_U &\leq \|\mathcal{Q}_A(\tau u^k - \mathcal{A}(p^k)) - (N + \tau I + \partial\theta)^{-1}(\tau u^k - \mathcal{A}(p^k))\|_U \\ &\quad + \|(N + \tau I + \partial\theta)^{-1}(\tau u^k - \mathcal{A}(p^k)) - (N + \tau I + \partial\theta)^{-1}(\tau u^k - S^*p^k)\|_U \\ &< \min \left\{ \frac{1}{2}, \frac{1}{4\|S\|} \sigma_0(\mathcal{Q}_S) \right\} \delta + (c_0 + \tau)^{-1} \|S^*p^k - \mathcal{A}(p^k)\|_U \\ &< \min \left\{ 1, \frac{1}{2\|S\|} \sigma_0(\mathcal{Q}_S) \right\} \delta \leq \delta. \end{aligned} \tag{4.53}$$

Note that $u^{k+1} \in \mathcal{Q}_A(K_{\mathcal{Q}_A})$, hence $u^{k+1} + f \in K_{\mathcal{S}}$. Thus,

$$\|\mathcal{S}(u^{k+1} + f) - S(u^{k+1} + f)\|_Y < \frac{1}{2} \sigma_0(\mathcal{Q}_S) \delta.$$

Utilizing $Q_S = \mathcal{Q}_S$ and the boundedness of \mathcal{Q}_S^{-1} , we obtain

$$\begin{aligned} \|p^{k+1} - \bar{p}^{k+1}\|_Y &\leq \|\mathcal{Q}_S^{-1}(\mathcal{S}(u^{k+1} + f) - y_d - p^k) - \mathcal{Q}_S^{-1}(S(\bar{u}^{k+1} + f) - y_d - p^k)\|_Y \\ &< \|\mathcal{Q}_S^{-1}\| (\|\mathcal{S}(u^{k+1} + f) - S(u^{k+1} + f)\|_Y + \|S\bar{u}^{k+1} - S\bar{u}^{k+1}\|_Y) \\ &< \sigma_0(\mathcal{Q}_S)^{-1} \left(\frac{1}{2} \sigma_0(\mathcal{Q}_S) \delta + \|S\| \cdot \frac{1}{2\|S\|} \sigma_0(\mathcal{Q}_S) \delta \right) = \delta, \end{aligned}$$

where the last inequality follows from the bound in (4.53). \square

4.4 Asymptotic ε -Optimality of the iUzawa-Net Layer Outputs

We are now ready to establish the following asymptotic ε -optimality of the iUzawa-Net layer outputs, which can also be viewed as a new universal approximation property of the iUzawa-Net.

Theorem 4.13. *Given Assumptions 2.2 and 4.7, for any compact set $K \subset Y \times U$ and $\varepsilon > 0$, there exist $\delta_0 = C\varepsilon$ with $C > 0$ independent of ε and $L_0 = O(\log(1/\varepsilon))$, such that for any $\delta < \delta_0$ and $L \geq L_0$, there exists an iUzawa-Net $\mathcal{T}(y_d, f; \theta_{\mathcal{T}})$ with L layers that is algorithm tracking with respect to K and δ in the sense of Definition 4.1. Moreover, for any $(y_d, f)^\top \in K$, the layer outputs $\{(u^k, p^k)^\top\}_{k=1}^L$ of $\mathcal{T}(y_d, f; \theta_{\mathcal{T}})$ satisfy*

$$\|T(y_d, f) - u^k\|_U < \varepsilon, \quad \forall k \geq L_0. \tag{4.54}$$

Proof. Denote $K^{\text{perm}} := \{(z, v) \in U \times Y : (v, z) \in K\}$, which corresponds to K up to a permutation of coordinates. By Proposition 4.12, there exists \mathcal{Q}_S of the architecture (2.7) such that \mathcal{Q}_S is bounded, linear, and $\mathcal{Q}_S - (I + SN^{-1}S^*)$ is positive semidefinite. Take $\mathcal{Q}_S^k = \mathcal{Q}_S$ for all $k = 0, \dots, L-1$. For any $\delta > 0$ and $L \geq 1$, we apply Proposition 4.12 recursively on k to obtain the neural networks \mathcal{S}^k , \mathcal{A}^k , and \mathcal{Q}_A^k in \mathcal{T} and compact sets $K_S^{(k)}$, $K_{\mathcal{Q}_A}^{(k)}$, and $K_{\mathcal{A}}^{(k)}$. Specifically,

- For $k = 0$, apply Proposition 4.12 with $K = \{(0, 0)^\top\} \cup K^{\text{perm}}$ and δ to obtain neural networks \mathcal{S}^0 , \mathcal{A}^0 , \mathcal{Q}_A^0 , and compact sets $K_S^{(0)}$, $K_{\mathcal{A}}^{(0)}$ and $K_{\mathcal{Q}_A}^{(0)}$. Denote the image $\{w^1 : w^0 = K, (y_d, f)^\top \in K\}$ as K_1 .

- For each $k = 1, \dots, L-1$, apply Proposition 4.12 with $K = K_k \cup K^{\text{perm}}$ and δ to obtain neural networks $\mathcal{S}^k, \mathcal{A}^k, \mathcal{Q}_A^k$ and compact sets $K_{\mathcal{S}}^{(k)}, K_{\mathcal{A}}^{(k)}$ and $K_{\mathcal{Q}_A}^{(k)}$. Denote the image $\{w^1 : w^0 = 0, (y_d, f)^\top \in K\}$ as K_{k+1} .

Define an **iUzawa-Net** $\mathcal{T}(y_d, f; \theta_{\mathcal{T}})$ of the form (1.7) with the constructed neural networks $\mathcal{S}^k, \mathcal{A}^k, \mathcal{Q}_A^k$, and \mathcal{Q}_S^k . For any $(y_d, f)^\top \in K$, denote the k -th layer output of \mathcal{T} as $(u^k, p^k)^\top$. For each $k = 1, \dots, L$, let $(\bar{u}^k, \bar{p}^k)^\top$ be defined from $(u^{k-1}, p^{k-1})^\top$ by (4.1a)–(4.1b) with the choice $Q_A = (N + \tau I + \partial\theta)$ and $Q_S = \mathcal{Q}_S$. By the above construction and (4.52), we have

$$\|u^{k+1} - \bar{u}^{k+1}\|_U < \delta, \quad \|p^{k+1} - \bar{p}^{k+1}\|_Y < \delta, \quad \forall k = 0, \dots, L-1,$$

and hence (4.1) is satisfied by $\{(u^k, p^k)^\top\}_{k=0}^L$ and $\{(\bar{u}^k, \bar{p}^k)^\top\}_{k=1}^L$. Note that Q_A and Q_S does not depend on δ in the above construction. Hence, it follows from Proposition 4.5 and Remark 4.6 that there exist $\delta_0 = C\varepsilon$ with C independent of ε and $L_0 = O(\log(1/\varepsilon))$, both do not depend on $(y_d, f)^\top$, such that for any $\delta < \delta_0$ and $L \geq L_0$, the layer outputs $\{(u^k, p^k)^\top\}_{k=1}^L$ of $\mathcal{T}(y_d, f; \theta_{\mathcal{T}})$ satisfies

$$\|T(y_d, f) - u^k\|_U \leq \|(u^k, p^k)^\top - (u^*, p^*)^\top\|_{U \times Y} < \varepsilon, \quad \forall k \geq L_0.$$

□

By setting $k = L$ and taking supremum over K in (4.54), Theorem 4.13 yields a new universal approximation theorem for the **iUzawa-Net**. This result is distinguished from Theorem 3.8 in that it guarantees the constructed **iUzawa-Net** to be (K, δ) -tracking. Moreover, Theorem 4.13 extends naturally to the dual variables $\{p^k\}_{k=0}^L$ in the layer outputs, establishing the asymptotic ε -optimality of $\{p^k\}_{k=0}^L$ with respect to the dual optimal solution p^* of (1.3). It is worth remarking that the asymptotic ε -optimality result presented in Theorem 4.13 does not, in itself, imply convergence, which requires the error to vanish as $k \rightarrow \infty$. The convergence of the inexact iterates (4.1) can be achieved by forcing the inexactness δ to decrease sufficiently fast with respect to iterations. A careful analysis of the convergence shapes the direction of subsequent works.

5 Approximation Results under Additional Regularity

Since the underlying optimization algorithm (1.5) involves identical operations in each iteration, it is natural to expect the optimization-informed neural network **iUzawa-Net** to be *weight tying*, whose definition is formulated as follows.

Definition 5.1. An **iUzawa-Net** defined in (1.7) is called *weight tying* if each layer consists of identical neural network parameters. Specifically, we have $\mathcal{S}^k = \mathcal{S}$, $\mathcal{A}^k = \mathcal{A}$, $\mathcal{Q}_A^k = \mathcal{Q}_A$ and $\mathcal{Q}_S^k = \mathcal{Q}_S$ for some fixed neural networks $\mathcal{S}, \mathcal{A}, \mathcal{Q}_A$ and \mathcal{Q}_S for any $k = 0, \dots, L-1$.

Note that Theorem 4.13 does not guarantee that the constructed **iUzawa-Net** \mathcal{T} is weight tying. This theoretical inconsistency motivates us to establish a universal approximation theorem for the **iUzawa-Net** that possesses both the weight tying and algorithm tracking properties. In this section, we show that this is achievable if additional regularity is imposed on the problem (1.1). Our approach relies heavily on an analysis that allows neural network approximation on *bounded* subsets of Sobolev spaces $H^s(\Omega)$ with $s > 0$, thereby bypassing the restrictive compactness assumption required in the previous sections. The core assumption is stated in Assumption 5.2.

Assumption 5.2. There exists a regularity exponent $0 < s \leq 1$ such that

- (i) The operator $S : L^2(\Omega) \rightarrow L^2(\Omega)$ takes the form

$$S = \iota^* \circ \tilde{S} \circ \iota, \tag{5.1}$$

where $\tilde{S} : H^{-s}(\Omega) \rightarrow H^s(\Omega)$ is a bounded linear operator, and $\iota : L^2(\Omega) \hookrightarrow H^{-s}(\Omega)$ is the canonical embedding, whose adjoint is given by another canonical embedding $\iota^* : H^s(\Omega) \hookrightarrow L^2(\Omega)$.

- (ii) The operator N and functional θ satisfy Assumption 2.2 with parameters $\lambda, \mu \in H^s(\Omega) \cap L^\infty(\Omega)$.
- (iii) For the function ψ_ξ and the set E defined in Assumption 2.2, the set-valued mapping $\xi \mapsto \text{gph } \partial\psi_\xi$ is sub-Lipschitz on E in the sense of [52, Definition 9.27]; or equivalently, for any $\xi_1, \xi_2 \in E$ and any $\rho > 0$, there exists $\kappa_\rho > 0$ such that

$$d_\rho(\text{gph } \partial\psi_{\xi_1}, \text{gph } \partial\psi_{\xi_2}) \leq \kappa_\rho \|\xi_1 - \xi_2\|,$$

where d_ρ is the Attouch–Wets distance between two sets, defined by

$$d_\rho(C, D) = \max_{|x| \leq \rho} |d(x, C) - d(x, D)| = \max_{|x| \leq \rho} \left| \inf_{y \in C} \|x - y\| - \inf_{z \in D} \|x - z\| \right|$$

for any sets $C, D \subset \mathbb{R}^n$ [3, 52].

Remark 5.3.

- (i) Assumption 5.2 (i) covers many important cases of (1.1), e.g., we have $s = 1$ for distributed control of elliptic equations. With minor modifications, it also applies to the boundary control of elliptic equations or even parabolic equations; we refer to [66, Sections 2.13 and 3.9] for more details.
- (ii) The requirement $0 < s \leq 1$ is just for simplicity in analysis. Our main theoretical result can be easily generalized to any $s > 0$; see the discussion after Theorem 5.11.
- (iii) Note that Assumption 5.2 (ii) and (iii) mildly strengthen Assumptions 2.2 and 4.7, which were applied in the analysis in Sections 3 and 4. In particular, Assumption 5.2 (ii) is satisfied for any function $\lambda, \mu \in C^1(\Omega) \cap C(\bar{\Omega})$, which holds for the important examples in Section 2.3 if $u_a, u_b \in C^1(\Omega) \cap C(\bar{\Omega})$. The notion of sub-Lipschitz continuity is ubiquitous in variational analysis. Though it is generally stronger than the continuity assumption in Assumption 4.7, it is still valid for the cases in Section 2.3.

The observation that additional regularity avoids the compactness assumption is grounded in the classical Rellich–Kondrachov theorem and its generalizations [38, Theorems 6.13 and 8.5], which can be summarized as the following proposition.

Proposition 5.4 (Rellich–Kondrachov). *Assume that $\Omega \subset \mathbb{R}^d$ is bounded with Lipschitz boundary. For any $0 \leq s_2 < s_1 \leq 1$, the embedding $H^{s_1}(\Omega) \hookrightarrow H^{s_2}(\Omega)$ is compact. Consequently, for any bounded set $B \subset H^{s_1}(\Omega)$, the closure of B in the topology of $H^{s_2}(\Omega)$ is compact.*

However, our setting requires a more delicate analysis than a direct application of Proposition 5.4. Our argument proceeds as follows. We first show that FNOs can approximate any continuous mappings from $H^{s_1}(\Omega)$ to $H^{s_2}(\Omega)$ on bounded subsets of $H^s(\Omega)$ for any $s > s_1$. For \mathcal{Q}_A^k defined in (2.11), we show that it achieves L^2 -approximation on any bounded subset of $H^s(\Omega)$, and the image of such a set is also bounded in $H^s(\Omega)$. Utilizing these results, for any bounded $B \subset H^s(\Omega)$, $\delta > 0$, and $R > 0$, we construct neural networks \mathcal{S} , \mathcal{A} , \mathcal{Q}_A and \mathcal{Q}_S that achieve accuracy δ on a sufficiently large approximation domain $B' \subset H^s(\Omega)$, an iUzawa–Net $\mathcal{T}(y_d, f; \theta_T)$ with each layer consisting of these neural networks, and show that the outputs of the first L layers of \mathcal{T} stay inside B' . Finally, we apply Proposition 4.5 to conclude the existence of an iUzawa–Net that achieves desirable approximation error, (B, δ) -tracking, and weight tying properties.

The technical details are specified in the remaining subsections.

5.1 Universal Approximation of FNOs and \mathcal{Q}_A^k on Bounded Sets

We begin with verifying the following refined approximation result of FNOs.

Proposition 5.5. *Let $0 \leq s_1 < 1$ and $s_2 \geq 0$. Let $\Omega \subset \mathbb{R}^d$ be a bounded domain with Lipschitz boundary such that $\bar{\Omega} \subset (0, 2\pi)^d$. Let $G : H^{s_1}(\Omega) \rightarrow H^{s_2}(\Omega)$ be a continuous mapping and $B \subset H^s(\Omega)$ be a bounded set for some $s_1 < s \leq 1$. Then for any $\varepsilon > 0$, there exist a continuous embedding $\mathcal{E} : H^{s_1}(\Omega) \rightarrow H^{s_1}(\mathbb{T}^d)$ and an FNO $\mathcal{G} : H^{s_1}(\mathbb{T}^d) \rightarrow H^{s_2}(\mathbb{T}^d)$, such that*

$$\sup_{u \in B} \|G(u) - (\mathcal{G} \circ \mathcal{E}(u))|_\Omega\|_{H^{s_2}(\Omega)} < \varepsilon. \quad (5.2)$$

Proof. By Proposition 5.4, there exists a compact set $K \subset H^{s_1}(\Omega)$ such that $B \subset K$. The desired result follows immediately from Proposition 3.5. \square

Next, we prove the approximation properties of \mathcal{Q}_A^k for $(N + \tau I + \partial\theta)^{-1}$ over bounded subsets. The following proposition is a weaker version of [73, Theorem 1] that suffices for our purpose.

Proposition 5.6 (c.f. [73, Theorem 1]). *Let $K = [a_1, b_1] \times \cdots \times [a_m, b_m] \subset \mathbb{R}^m$ be a cube. Let $B := \{g \in W^{1,\infty}(K) : \|g\|_{W^{1,\infty}(K)} \leq 1\}$. Then there exists an FCNN $\mathcal{N} : K \rightarrow \mathbb{R}$ with ReLU activation function, such that*

$$\sup_{g \in B} \|g - \mathcal{N}\|_{W^{1,\infty}(K)} < \varepsilon. \quad (5.3)$$

By Assumption 5.2 (ii) and Lemma 4.9, the operator $(N + \tau I + \partial\theta)^{-1}$ satisfies (4.30). We now show by a variational analysis approach that Assumption 5.2 (iii) guarantees that the function ϕ defined in (4.30) is locally Lipschitz continuous on $\mathbb{R} \times E \times [c_0, \infty)$, which is crucial for estimating the $H^s(\Omega)$ norm of the output of \mathcal{Q}_A^k .

Lemma 5.7. *Assume that Assumption 5.2 (ii) holds, and let $\phi : \mathbb{R} \times E \times [c_0, \infty)$ be defined as in (4.30). Then $\phi(s, \xi, \eta)$ is locally Lipschitz on $\mathbb{R} \times E \times [c_0, \infty)$ if Assumption 5.2 (iii) holds.*

Proof. For any $\xi \in E$ and $\eta \in [c_0, \infty)$, denote the set-valued mappings $\Xi_\xi := \partial\psi_\xi$ and $H_\eta := (\eta + \tau)I$. Note that Assumption 5.2 (ii) implies Assumption 4.7 (see e.g., [52, Theorem 5.50]), hence by Lemma 4.9, we have

$$\phi(s, \xi, \eta) = (\Xi_\xi + H_\eta)^{-1}(s). \quad (5.4)$$

In particular, the mapping $(s, \xi, \eta)^\top \mapsto (\Xi_\xi + H_\eta)^{-1}(s) \in \mathbb{R}$ is single-valued, continuous jointly in $(s, \xi, \eta)^\top$ on $\mathbb{R} \times E \times [c_0, \infty)$, and Lipschitz continuous in s with a uniform Lipschitz constant $L_\phi > 0$ for any $\xi \in E$ and $\eta \in [c_0, \infty)$. It suffices to show that ϕ is Lipschitz on any compact subset of $\mathbb{R} \times E \times [c_0, \infty)$. Fix any compact $K \subset \mathbb{R} \times E \times [c_0, \infty)$. Without loss of generality, assume that $K = [-R_0, R_0] \times ([-R_1, R_1]^m \cap E) \times [c_0, R_2]$ for some $R_0, R_1 \geq 0$ and $R_2 \geq c_0$.

We first show that for any $\rho > 0$, there exists $\bar{\kappa}_\rho > 0$ such that for any $\xi_1, \xi_2 \in E$ and $\eta_1, \eta_2 \in [c_0, R_2]$, we have

$$\hat{d}_\rho(\text{gph}(\Xi_{\xi_1} + H_{\eta_1}), \text{gph}(\Xi_{\xi_2} + H_{\eta_2})) \leq \bar{\kappa}_\rho \|(\xi_1, \eta_1)^\top - (\xi_2, \eta_2)^\top\|, \quad (5.5)$$

where \hat{d}_ρ denotes the truncated Hausdorff distance, which is defined by [47, 52]

$$\hat{d}_\rho(C, D) = \inf \{\eta \geq 0 : C \cap \overline{B}(0, \rho) \subset D + \overline{B}(0, \eta), D \cap \overline{B}(0, \rho) \subset C + \overline{B}(0, \eta)\}, \quad \text{for any sets } C, D.$$

Clearly, the mappings H_{η_1} and H_{η_2} are single-valued and Lipschitz continuous with common modulus $R_2 + \tau$. By Assumption 5.2 (ii), which implies Assumption 2.2, the function ψ_ξ is convex, lower semicontinuous, and proper for all $\xi \in E$, hence Ξ_{ξ_1} and Ξ_{ξ_2} have nonempty graphs. Thus by [53, Theorem 5.2], for any $\rho > 0$, there exists a sufficiently large $\bar{\rho} \geq \rho$ such that

$$\begin{aligned} \hat{d}_\rho(\text{gph}(\Xi_{\xi_1} + H_{\eta_1}), \text{gph}(\Xi_{\xi_2} + H_{\eta_2})) &\leq \sup_{r \in \overline{B}(0, \rho)} \hat{d}_\infty(H_{\eta_1}(r), H_{\eta_2}(r)) + (1 + R_2 + \tau) \hat{d}_{\bar{\rho}}(\text{gph}(\Xi_{\xi_1}), \text{gph}(\Xi_{\xi_2})) \\ &\leq \sup_{r \in \overline{B}(0, \rho)} \hat{d}_\infty(H_{\eta_1}(r), H_{\eta_2}(r)) + (1 + R_2 + \tau) \hat{d}_{\bar{\rho}}(\text{gph}(\Xi_{\xi_1}), \text{gph}(\Xi_{\xi_2})) \\ &\leq \rho \|\eta_1 - \eta_2\| + (1 + R_2 + \tau) \kappa_{\bar{\rho}} \|\xi_1 - \xi_2\| \\ &\leq \bar{\kappa}_\rho \|(\xi_1, \eta_1)^\top - (\xi_2, \eta_2)^\top\|, \end{aligned}$$

for some $\bar{\kappa}_\rho > 0$ that depends only on ρ . Note that the second inequality follows from the fact that

$$\hat{d}_{\bar{\rho}}(\text{gph}(\Xi_{\xi_1}), \text{gph}(\Xi_{\xi_2})) \leq \hat{d}_{\bar{\rho}}(\text{gph}(\Xi_{\xi_1}), \text{gph}(\Xi_{\xi_2})),$$

see e.g., [52]; and the third inequality follows from Assumption 5.2 (iii).

Then, by (5.5) and [53, Theorem 5.1], for any $\rho \geq R_0$ and $s \in [-R_0, R_0]$, we have

$$\text{exs} \left((\Xi_{\xi_1} + H_{\eta_1})^{-1}(s) \cap \overline{B}(0, \rho), (\Xi_{\xi_2} + H_{\eta_2})^{-1}(\overline{B}(s, \delta)) \right) \leq \hat{d}_\rho(\text{gph}(\Xi_{\xi_1} + H_{\eta_1}), \text{gph}(\Xi_{\xi_2} + H_{\eta_2})), \quad (5.6)$$

provided that $\delta \geq \hat{d}_\rho(\text{gph}(\Xi_{\xi_1} + H_{\eta_1}), \text{gph}(\Xi_{\xi_2} + H_{\eta_2}))$. Here, $\text{exs}(C, D)$ denotes the excess of C over D and satisfies $\text{exs}(C, D) = \sup_{x \in C} \text{dist}(x, D)$ if C, D are nonempty. As $(\Xi_\xi + H_\eta)^{-1}(s)$ is continuous in s , ξ and η , there exists a sufficiently large ρ_0 such that

$$(\Xi_\xi + H_\eta)^{-1}(s) \subset \overline{B}(0, \rho_0), \quad \forall s \in [-R_0, R_0], \quad \xi \in -[R_1, R_1]^m \cap E, \quad \eta \in [c_0, R_2].$$

Recall that $(\Xi_{\xi_1} + H_{\eta_1})^{-1}(s)$ is single-valued. Hence, for the choice

$$\rho_1 = \max\{\rho_0, R_0\}, \quad \delta = \hat{d}_{\rho_1}(\text{gph}(\Xi_{\xi_1} + H_{\eta_1}), \text{gph}(\Xi_{\xi_2} + H_{\eta_2})),$$

the inequality (5.6) reduces to

$$\text{dist}\left((\Xi_{\xi_1} + H_{\eta_1})^{-1}(s), (\Xi_{\xi_2} + H_{\eta_2})^{-1}(\overline{B}(s, \delta))\right) \leq \hat{d}_{\rho_1}(\text{gph}(\Xi_{\xi_1} + H_{\eta_1}), \text{gph}(\Xi_{\xi_2} + H_{\eta_2})).$$

Since $(\Xi_{\xi_2} + H_{\eta_2})^{-1}(s)$ is Lipschitz in s , it follows that

$$\begin{aligned} |\phi(s, \xi_1, \eta_1) - \phi(s, \xi_2, \eta_2)| &\leq \text{dist}\left((\Xi_{\xi_1} + H_{\eta_1})^{-1}(s), (\Xi_{\xi_2} + H_{\eta_2})^{-1}(\overline{B}(s, \delta))\right) + 2L_\phi\delta \\ &\leq (1 + 2L_\phi) \cdot \hat{d}_{\rho_1}(\text{gph}(\Xi_{\xi_1} + H_{\eta_1}), \text{gph}(\Xi_{\xi_2} + H_{\eta_2})) \\ &\leq (1 + 2L_\phi)\bar{\kappa}_{\rho_1} \|(\xi_1, \eta_1)^\top - (\xi_2, \eta_2)^\top\|. \end{aligned}$$

Note that $\bar{\kappa}_{\rho_1}$ depends only on ρ_1 , which is determined by the choice of K . Since any compact set of $\mathbb{R} \times E \times [c_0, \infty)$ is contained in some set of the form $[-R_0, R_0] \times ([-R_1, R_1]^m \cap E) \times [-R_2, R_2]$, it follows that ϕ is Lipschitz continuous on any compact subset of $\mathbb{R} \times E \times [c_0, \infty)$. We thus conclude that ϕ is locally Lipschitz on $\mathbb{R} \times E \times [c_0, \infty)$. \square

Lemma 5.8. *Assume that Assumption 5.2 holds, and let λ, μ, E and c_0 be defined as in Assumption 2.2. Let $\phi : \mathbb{R} \times E \times [c_0, \infty) \rightarrow \mathbb{R}$ be a locally Lipschitz continuous function. Assume that $G : L^2(\Omega) \rightarrow L^2(\Omega)$ satisfies*

$$G(u)(x) = \phi(u(x), \mu(x), \lambda(x)), \quad \text{a.e. in } \Omega, \quad \forall u \in L^2(\Omega). \quad (5.7)$$

Then for any bounded subset $B \subset H^s(\Omega)$ and $\varepsilon > 0$, there exists a neural network $\mathcal{N} : \mathbb{R}^{m+2} \rightarrow \mathbb{R}$ defined in (2.12), such that the neural network $\mathcal{G} : L^2(\Omega) \rightarrow L^2(\Omega)$ defined by

$$\mathcal{G}(u(x)) = \mathcal{N}(u(x), \mu(x), \lambda(x)) \quad \text{a.e. in } \Omega, \quad \forall u \in L^2(\Omega). \quad (5.8)$$

satisfies

$$\sup_{u \in B} \|G(u) - \mathcal{G}(u)\|_{L^2(\Omega)} < \varepsilon, \quad (5.9)$$

and

$$\|\mathcal{G}(u)\|_{H^s(\Omega)} \leq C(1 + \|u\|_{H^s(\Omega)}), \quad \forall u \in B \quad (5.10)$$

for some constant $C > 0$ independent of u , B , and ε .

Proof. Fix any bounded $B \subset H^s(\Omega)$ and $\varepsilon > 0$. Denote by $\nu(x) = (\mu(x), \lambda(x))^\top \in L^\infty(\Omega; \mathbb{R}^{m+1})$. Define the truncated function u_r of u as in (4.43) for all $u \in H^s(\Omega)$ and $r > 0$. By Proposition 5.4, there exists a compact set $K \subset L^2(\Omega)$ such that $u \in B$ implies $u \in K$. Thus, following a similar argument to the proof of Lemma 4.10, there exists an $R_0 > 0$ such that $R_0 \geq \|\nu\|_{L^\infty(\Omega; \mathbb{R}^{m+1})}$ and

$$\|u - u_{R_0}\|_{L^2(\Omega)}^2 < \frac{\varepsilon^2}{4L_\phi^2}, \quad \text{for all } u \in B. \quad (5.11)$$

Note that $u_{R_0} \in H^s(\Omega)$ by [38, Remark 6.28].

We now approximate $G(u)$ by a neural network of the form (5.8). Define constants

$$R_1 := \|\nu\|_{L^\infty(\Omega; \mathbb{R}^{m+1})}, \quad M_0 := \text{ess sup}_{x \in \Omega} |\phi(0, \mu(x), \lambda(x))|,$$

and three compact sets

$$\mathcal{K}_1 := [-R_0, R_0] \subset \mathbb{R}, \quad \mathcal{K}_2 := ([-R_1, R_1]^m \cap E) \times [c_0, R_1] \subset \mathbb{R}^{m+1}, \quad \tilde{\mathcal{K}}_2 = [-R_1, R_1]^{m+1} \subset \mathbb{R}^{m+1}.$$

Note that $R_1 \leq R_0$, $\mathcal{K}_2 \subset \tilde{\mathcal{K}}_2$, $u_{R_0}(x) \in \mathcal{K}_1$ a.e. in Ω for all $u \in K$, $\nu(x) \in \mathcal{K}_2$ a.e. in Ω , and $M_0 < \infty$ (since $\phi(0, \cdot)$ is continuous on the compact set \mathcal{K}_2 by assumption). By Assumption 5.2 and Lemma 5.7, ϕ is locally Lipschitz on $\mathbb{R} \times E \times [c_0, \infty)$. Since $\mathcal{K}_1 \times \mathcal{K}_2$ is compact, ϕ is Lipschitz on $\mathcal{K}_1 \times \mathcal{K}_2$. By the Kirschbraun theorem, the Lipschitz continuous function ϕ on $\mathcal{K}_1 \times \mathcal{K}_2$ admits a Lipschitz continuous extension $\tilde{\phi}$ on $\mathcal{K}_1 \times \tilde{\mathcal{K}}_2$ with the same Lipschitz constant L_ϕ . Note that $\mathcal{K}_1 \times \tilde{\mathcal{K}}_2$ is convex, and hence by [28, Theorem 4.1 and Remark 4.2] that $W^{1,\infty}(\mathcal{K}_1 \times \tilde{\mathcal{K}}_2) = C^{0,1}(\mathcal{K}_1 \times \tilde{\mathcal{K}}_2)$. In particular, $\tilde{\phi} \in W^{1,\infty}(\mathcal{K}_1 \times \tilde{\mathcal{K}}_2)$ with $\|D\tilde{\phi}\|_{L^\infty(\mathcal{K}_1 \times \tilde{\mathcal{K}}_2)} \leq L_\phi$, where $D\tilde{\phi}$ is the derivative of $\tilde{\phi}$ in the distributional sense. By Proposition 5.6 and scaling $\tilde{\phi}$ if necessary, there exists a fully connected neural network $\mathcal{N}_0 : \mathbb{R}^{m+2} \rightarrow \mathbb{R}$ with ReLU activation function, such that

$$\|\tilde{\phi} - \mathcal{N}_0\|_{W^{1,\infty}(\mathcal{K}_1 \times \tilde{\mathcal{K}}_2)} < \min \left\{ \frac{\varepsilon}{\sqrt{2|\Omega|}}, L_\phi \right\}. \quad (5.12)$$

In particular, $\tilde{\phi} - \mathcal{N}_0$ is Lipschitz continuous on $\mathcal{K}_1 \times \tilde{\mathcal{K}}_2$ with the Lipschitz constant $L_{\tilde{\phi} - \mathcal{N}_0}$ satisfying

$$L_{\tilde{\phi} - \mathcal{N}_0} \leq \|D(\tilde{\phi} - \mathcal{N}_0)\|_{L^\infty(\mathcal{K}_1 \times \tilde{\mathcal{K}}_2)} \leq \|\tilde{\phi} - \mathcal{N}_0\|_{W^{1,\infty}(\mathcal{K}_1 \times \tilde{\mathcal{K}}_2)} < L_\phi.$$

Hence \mathcal{N}_0 is Lipschitz continuous on $\mathcal{K}_1 \times \tilde{\mathcal{K}}_2$ with the Lipschitz constant $L_{\mathcal{N}_0} \leq 2L_\phi$, and

$$\sup_{(s,\zeta)^\top \in \mathcal{K}_1 \times \tilde{\mathcal{K}}_2} \left| \tilde{\phi}(s, \zeta) - \mathcal{N}_0(s, \zeta) \right|^2 < \frac{\varepsilon^2}{2|\Omega|}. \quad (5.13)$$

Restricting \mathcal{N}_0 back to the set $\mathcal{K}_1 \times \mathcal{K}_2$, and using the identity $\tilde{\phi} = \phi$ on $\mathcal{K}_1 \times \mathcal{K}_2$, it follows that \mathcal{N}_0 is Lipschitz continuous on $\mathcal{K}_1 \times \mathcal{K}_2$ with a Lipschitz constant $L_{\mathcal{N}_0} \leq 2L_\phi$, and

$$\sup_{(s,\zeta)^\top \in \mathcal{K}_1 \times \mathcal{K}_2} |\phi(s, \zeta) - \mathcal{N}_0(s, \zeta)|^2 < \frac{\varepsilon^2}{2|\Omega|}. \quad (5.14)$$

Clearly, there exists a neural network of the structure (2.12) that equals the FCNN \mathcal{N}_0 . Without loss of generality, denote this neural network also as \mathcal{N}_0 . Then, from (5.11) and (5.14), one can apply the same argument in the proof of Lemma 4.10 to show that there exists a neural network \mathcal{N} of the form (2.12), such that

$$\mathcal{N}(s, \zeta) = \mathcal{N}_0(\text{proj}_{\mathcal{K}_1}(s), \zeta), \quad \forall s \in \mathbb{R}, \zeta \in \mathcal{K}_2,$$

and the $\mathcal{G}(u)$ defined in (5.8) satisfies

$$\|G(u) - \mathcal{G}(u)\|_{L^2(\Omega)} < \varepsilon, \quad \forall u \in B,$$

which establishes (5.9).

We now prove (5.10). For any $u_{R_0} \in H^s(\Omega)$, recall that $u_{R_0} \in H^s(\Omega)$. If $s = 0$ or 1 , clearly we have $\|u_{R_0}\|_{H^s(\Omega)} \leq \|u\|_{H^s(\Omega)}$. For $0 < s < 1$, we have

$$\begin{aligned} \|u_{R_0}\|_{H^s(\Omega)} &= \|u_{R_0}\|_{L^2(\Omega)} + \int_{\Omega} \int_{\Omega} \frac{|u_{R_0}(x) - u_{R_0}(y)|^2}{|x - y|^{d+2s}} dx dy \\ &\leq \|u\|_{L^2(\Omega)} + \int_{\Omega} \int_{\Omega} \frac{|u(x) - u(y)|^2}{|x - y|^{d+2s}} dx dy \\ &= \|u\|_{H^s(\Omega)}. \end{aligned}$$

Since $\nu \in H^s(\Omega; \mathbb{R}^{m+1})$, we have $(u_{R_0}, \nu)^\top \in H^s(\Omega; \mathbb{R}^{m+2})$. Recall that \mathcal{N}_0 is Lipschitz continuous on $\mathcal{K}_1 \times \mathcal{K}_2$ with $L_{\mathcal{N}_0} \leq 2L_\phi$. Thus, a simple extension of [38, Theorem 6.27] yields

$$\mathcal{G}(u)(\cdot) = \mathcal{N}(u(\cdot), \nu(\cdot)) = \mathcal{N}_0(u_{R_0}(\cdot), \nu(\cdot)) \in H^s(\Omega), \quad (5.15)$$

and, in particular,

$$\|\mathcal{G}(u)\|_{H^s(\Omega)} \leq 2L_\phi \|(u_{R_0}, \nu)^\top\|_{H^s(\Omega; \mathbb{R}^{m+2})} \leq 2\sqrt{2}L_\phi (\|\nu\|_{H^s(\Omega; \mathbb{R}^{m+1})} + \|u\|_{H^s(\Omega)}) \leq C (1 + \|u\|_{H^s(\Omega)}),$$

where $C > 0$ is a constant depending only on L_ϕ , $\|\nu\|_{H^s(\Omega; \mathbb{R}^{m+1})}$ but independent of u , B , and ε . \square

Proposition 5.9. *Let $N : L^2(\Omega) \rightarrow L^2(\Omega)$ and $\theta : L^2(\Omega) \rightarrow \mathbb{R} \cup \{+\infty\}$ satisfy Assumption 5.2. For any $s > 0$, bounded subset $B \subset H^s(\Omega)$, and $\varepsilon > 0$, there exists a neural network \mathcal{Q}_A defined in (2.11) such that*

$$\sup_{v \in B} \|(N + \tau I + \partial\theta)^{-1}(v) - \mathcal{Q}_A(v)\|_{L^2(\Omega)} < \varepsilon,$$

and

$$\|\mathcal{Q}_A(v)\|_{H^s(\Omega)} \leq C(1 + \|v\|_{H^s(\Omega)}), \quad \forall v \in B,$$

for some constant $C > 0$ independent of u , B , and ε .

Proof. The desired result follows directly from Assumption 5.2 and Lemma 5.8 with $\nu(x) = (\mu(x), \lambda(x))^\top$ and $G = (N + \tau I + \partial\theta)^{-1}$. \square

5.2 A New Universal Approximation Theorem of the iUzawa-Net

We now prove that given sufficiently large approximation domains of \mathcal{S} , \mathcal{A} , and \mathcal{Q}_A , a single layer of the iUzawa-Net maps bounded sets in $H^s(\Omega)$ to bounded images in $H^s(\Omega)$. Moreover, the radius of the image is bounded uniformly independent of the size of the approximation domains. For notational convenience, denote by $\overline{B}_{H^s(\Omega)}(v, R)$ the closed ball in $H^s(\Omega)$ centered at v with radius $R > 0$.

Proposition 5.10. *Let Assumption 5.2 hold with regularity exponent $0 < s \leq 1$. Then*

- (i) *There exists \mathcal{Q}_S defined in (2.7) that is bounded, linear, and maps $H^s(\Omega)$ continuously into $H^s(\Omega)$. The operator $\mathcal{Q}_S - (I + SN^{-1}S^*)$ is positive semidefinite.*

Moreover, for any $\delta > 0$, $R_1 > 0$ and $B := \overline{B}_{H^s(\Omega)}(0, R_1)$, there exists a critical radius $R_0 > 0$ such that for any $R_2 > R_0$, there exists two FNOs \mathcal{S} , \mathcal{A} , and a neural network \mathcal{Q}_A defined in (2.11), such that

- (ii) *The following approximation bounds hold:*

$$\begin{aligned} \sup_{p \in \overline{B}_{H^s(\Omega)}(0, R_2)} \|S^*p - \mathcal{A}(p)\|_{L^2(\Omega)} &< \min \left\{ \frac{1}{2}, \frac{1}{4\|S\|}, (c_0 + \tau) \right\} (c_0 + \tau)^{-1} \delta, \\ \sup_{v \in \overline{B}_{H^s(\Omega)}(0, R_2)} \|(N + \tau I + \partial\theta)^{-1}(v) - \mathcal{Q}_A(v)\|_{L^2(\Omega)} &< \min \left\{ \frac{1}{2}, \frac{1}{4\|S\|} \right\} \delta, \\ \sup_{v \in \overline{B}_{H^s(\Omega)}(0, R_2)} \|Sv - \mathcal{S}(v)\|_{L^2(\Omega)} &< \frac{1}{2} \delta. \end{aligned} \quad (5.16)$$

- (iii) *For any $(y_d, f)^\top \in B \times B$, $(u^k, p^k)^\top \in B \times B$, and \mathcal{Q}_S satisfying (i), if $(u^{k+1}, p^{k+1})^\top$ is the $(k+1)$ -th layer output of the iUzawa-Net (1.7) with inputs y_d , f , u^k , p^k and neural networks $\mathcal{S}^k = \mathcal{S}$, $\mathcal{A}^k = \mathcal{A}$, $\mathcal{Q}_A^k = \mathcal{Q}_A$ and $\mathcal{Q}_S^k = \mathcal{Q}_S$, then we have $u^{k+1} \in H^s(\Omega)$, $p^{k+1} \in H^s(\Omega)$, and*

$$\max \{ \|u^{k+1}\|_{H^s(\Omega)}, \|p^{k+1}\|_{H^s(\Omega)} \} \leq C(1 + \delta + \|u^k\|_{H^s(\Omega)} + \|p^k\|_{H^s(\Omega)} + \|y_d\|_{H^s(\Omega)} + \|f\|_{H^s(\Omega)}) \leq R_0, \quad (5.17)$$

for some constant $C > 0$ independent of u^k , p^k , y_d , f , δ , R_1 and R_2 .

Proof. By Proposition 3.7, there exists a neural network $\mathcal{Q}_S : L^2(\Omega) \rightarrow L^2(\Omega)$ defined in (2.7) such that \mathcal{Q}_S is linear, bounded, maps $H^s(\Omega)$ into $H^s(\Omega)$ continuously, and $\mathcal{Q}_S - (I + SN^{-1}S^*)$ is positive semidefinite, thus (i) is verified. In particular, we have $\sigma_0(\mathcal{Q}_S) \geq 1$. Now fix arbitrary $\delta > 0$ and $R_2 > 0$. Let $\tilde{S} : H^{-s} \rightarrow H^s$ and $\iota : L^2(\Omega) \rightarrow H^{-s}(\Omega)$ be defined as in Assumption 5.2. By Proposition 5.5, there exist FNOs $\mathcal{S} : L^2(\Omega) \rightarrow H^s(\Omega)$ and $\mathcal{A} : L^2(\Omega) \rightarrow H^s(\Omega)$ such that

$$\begin{aligned} \sup_{p \in \overline{B}_{H^s(\Omega)}(0, R_2)} \|(\tilde{S}^* \circ \iota)p - \mathcal{A}(p)\|_{H^s(\Omega)} &< \min \left\{ \frac{1}{2}, \frac{1}{4\|S\|}, (c_0 + \tau) \right\} (c_0 + \tau)^{-1} \delta, \\ \sup_{v \in \overline{B}_{H^s(\Omega)}(0, R_2)} \|(\tilde{S} \circ \iota)v - \mathcal{S}(v)\|_{H^s(\Omega)} &< \frac{1}{2} \delta. \end{aligned} \quad (5.18)$$

Identify \mathcal{S} , \mathcal{A} as mappings from $L^2(\Omega)$ to $L^2(\Omega)$ via the continuous embedding $\iota^* : H^s(\Omega) \rightarrow L^2(\Omega)$. Clearly, we have $\|\iota^*\| \leq 1$. It follows from (5.18) that

$$\begin{aligned} \sup_{p \in \overline{B}_{H^s(\Omega)}(0, R_2)} \|S^*p - \mathcal{A}(p)\|_{L^2(\Omega)} &< \min \left\{ \frac{1}{2}, \frac{1}{4\|S\|}, (c_0 + \tau) \right\} (c_0 + \tau)^{-1} \delta, \\ \sup_{v \in \overline{B}_{H^s(\Omega)}(0, R_2)} \|Sv - \mathcal{S}(v)\|_{L^2(\Omega)} &< \frac{1}{2} \delta. \end{aligned} \quad (5.19)$$

Applying Proposition 5.9 to $(N + \tau I + \partial\theta)^{-1}$, we obtain a neural network \mathcal{Q}_A of the form (2.11) such that

$$\sup_{v \in \overline{B}_{H^s(\Omega)}(0, R_2)} \|(N + \tau I + \partial\theta)^{-1}(v) - \mathcal{Q}_A(v)\|_{L^2(\Omega)} < \min \left\{ \frac{1}{2}, \frac{1}{4\|S\|} \right\} \delta, \quad (5.20)$$

and

$$\|\mathcal{Q}_A(v)\|_{H^s(\Omega)} \leq C_1(1 + \|v\|_{H^s(\Omega)}), \quad \forall v \in \overline{B}_{H^s(\Omega)}(0, R_2) \quad (5.21)$$

for some constant C_1 independent of u , R_1 , R_2 , and δ . Note that $\|\cdot\|_{L^2(\Omega)} \leq \|\cdot\|_{H^s(\Omega)}$. Thus, (5.16) follows from (5.19) and (5.20).

Now, for any $R_1 > 0$, we show the existence of a critical radius $R_0 > 0$ by starting from a small value and enlarging it step-by-step to satisfy our approximation purpose. We initialize $R_0 = R_1$ and consider any $R_2 > R_0$. We have $p^k \in \overline{B}_{H^s(\Omega)}(0, R_1) \subset \overline{B}_{H^s(\Omega)}(0, R_2)$. By the already proved results, there exists an FNO \mathcal{A} satisfying (5.16) and (5.18). It follows that

$$\begin{aligned} \|\tau u^k - \mathcal{A}(p^k)\|_{H^s(\Omega)} &\leq \tau \|u^k\|_{H^s(\Omega)} + \|\mathcal{A}(p^k)\|_{H^s(\Omega)} \\ &\leq \tau \|u^k\|_{H^s(\Omega)} + \|\tilde{S}^* \circ \iota\| \|p^k\|_{H^s(\Omega)} + C_3 \delta \\ &\leq C_2 \|u^k\|_{H^s(\Omega)} + C_3 \|p^k\|_{H^s(\Omega)} + C_4 \delta \end{aligned} \quad (5.22)$$

for some constants $C_2, C_3, C_4 > 0$ independent of u^k, p^k, δ, R_1 and R_2 . Now we take $R_0 = \max\{R_1, \sqrt{2}C_2R_1 + C_3\delta\}$ and consider any $R_2 > R_0$. For such a choice, there exist \mathcal{A} and \mathcal{Q}_A satisfying (5.16), (5.21) and (5.22). Thus, we have

$$\begin{aligned} \|u^{k+1}\|_{H^s(\Omega)} &\leq \|\mathcal{Q}_A(\tau u^k - \mathcal{A}(p^k))\|_{H^s(\Omega)} \\ &\leq C_1 (1 + \|\tau u^k - \mathcal{A}(p^k)\|_{H^s(\Omega)}) \\ &\leq C_1 (1 + C_2 \|u^k\|_{H^s(\Omega)} + C_3 \|p^k\|_{H^s(\Omega)} + C_4 \delta), \end{aligned} \quad (5.23)$$

and hence

$$\|u^{k+1} + f\|_{H^s(\Omega)} \leq C_1 (1 + C_2 \|u^k\|_{H^s(\Omega)} + C_3 \|p^k\|_{H^s(\Omega)} + C_4 \delta) + \|f\|_{H^s(\Omega)}. \quad (5.24)$$

Now we take

$$R_0 = \max \left\{ R_1, \sqrt{2}C_2R_1 + C_3\delta, C_1 (1 + C_2 \|u^k\|_{H^s(\Omega)} + C_3 \|p^k\|_{H^s(\Omega)} + C_4 \delta) + \|f\|_{H^s(\Omega)} \right\}$$

and consider any $R_2 > R_0$. From the above, there exist \mathcal{S} , \mathcal{A} , \mathcal{Q}_A and \mathcal{Q}_S satisfying (i) and (ii), (5.18) and (5.24). As a result, we have $\|u^{k+1}\|_{H^s(\Omega)} \leq R_0$. Recall that \mathcal{Q}_S maps $H^s(\Omega)$ into $H^s(\Omega)$ continuously, and we have fixed \mathcal{Q}_S before choosing δ and R_2 . Hence, (5.18) implies

$$\begin{aligned} \|p^{k+1}\|_{H^s(\Omega)} &\leq \|p^k\|_{H^s(\Omega)} + \|\mathcal{Q}_S\| (\|\mathcal{S}(u^{k+1} + f)\|_{H^s(\Omega)} + \|p^k\|_{H^s(\Omega)} + \|y_d\|_{H^s(\Omega)}) \\ &\leq \|p^k\|_{H^s(\Omega)} + \|\mathcal{Q}_S\| \left(\|(\tilde{S} \circ \iota)\| \|u^{k+1} + f\|_{H^s(\Omega)} + \frac{1}{2} \delta + \|p^k\|_{H^s(\Omega)} + \|y_d\|_{H^s(\Omega)} \right) \\ &\leq C_5 (1 + \delta + \|u^k\|_{H^s(\Omega)} + \|p^k\|_{H^s(\Omega)} + \|y_d\|_{H^s(\Omega)} + \|f\|_{H^s(\Omega)}), \end{aligned} \quad (5.25)$$

for some $C_5 > 0$ independent of $u^k, p^k, y_d, f, \delta, R_1$ and R_2 . Therefore, it follows from (5.23) and (5.25) that there exists

$$\begin{aligned} R_0 &= \max \left\{ R_1, \sqrt{2}C_2R_1 + C_3\delta, C_1 (1 + C_2 \|u^k\|_{H^s(\Omega)} + C_3 \|p^k\|_{H^s(\Omega)} + C_4 \delta) + \|f\|_{H^s(\Omega)}, \right. \\ &\quad \left. C_5 (1 + \delta + \|u^k\|_{H^s(\Omega)} + \|p^k\|_{H^s(\Omega)} + \|y_d\|_{H^s(\Omega)} + \|f\|_{H^s(\Omega)}) \right\}, \end{aligned} \quad (5.26)$$

such that for any $R_2 > R_0$, there exists a $C > 0$ constructed by $C_i, 1 \leq i \leq 5$ such that (5.17) holds. Moreover, C is independent of $u^k, p^k, y_d, f, \delta, R_1$ and R_2 (although the construction of R_0 utilized the value of $C_i, 1 \leq i \leq 5$). \square

We are finally at the position to prove a universal approximation theorem for the **iUzawa-Net** with shared layer parameters over any bounded set under Assumption 5.2.

Theorem 5.11. *Given Assumption 5.2 with the regularity exponent $0 < s \leq 1$. For any $\varepsilon > 0$, $R > 0$, and $B := \overline{B}_{H^s(\Omega)}(0, R)$, there exists $\delta_0 = C\varepsilon$ with $C > 0$ independent of ε and $L_0 = O(\log(1/\varepsilon))$, such that for any $\delta < \delta_0$ and $L \geq L_0$, there exists an **iUzawa-Net** $\mathcal{T}(y_d, f; \theta_{\mathcal{T}})$ with L layers that is weight tying and algorithm tracking with respect to $B \times B$ and δ . Moreover, for any $(y_d, f)^\top \in B \times B$, the layer outputs $\{(u^k, p^k)^\top\}_{k=1}^L$ of $\mathcal{T}(y_d, f; \theta_{\mathcal{T}})$ satisfy*

$$\|T(y_d, f) - u^k\|_{L^2(\Omega)} < \varepsilon, \quad \forall k \geq L_0. \quad (5.27)$$

Proof. By Proposition 5.10, there exists \mathcal{Q}_S of the architecture (2.7) such that \mathcal{Q}_S is bounded, linear, maps $H^s(\Omega)$ continuously into $H^s(\Omega)$, and $\mathcal{Q}_S - (I + SN^{-1}S^*)$ is positive semidefinite. In view of Proposition 4.5, it suffices to construct \mathcal{S} , \mathcal{A} , and \mathcal{Q}_A , such that the layer outputs of the **iUzawa-Net** (1.7) satisfy (4.1) for $Q_A = (N + \tau I + \partial\theta)^{-1}$, $Q_S = \mathcal{Q}_S$ and sufficiently small δ . To this end, we recursively apply Proposition 5.10 for $k = 0, \dots, L-1$ to construct a series of critical radii $\{R_0^{(k)}\}_{k=0}^{L-1}$ and neural networks. Specifically, fix arbitrary $\delta > 0$ and formally denote $R_0^{(-1)} = 0$,

- For $k = 0, 1, \dots, L-1$, take $R_1 := \max\{R_0^{(k-1)}, R\}$, apply Proposition 5.10 with R_1 and δ to obtain a critical radius $R_0^{(k)} > 0$. Take $R_2^{(k)} = 2R_0^{(k)}$ and let $\mathcal{S}^{(k)}$, $\mathcal{A}^{(k)}$, and $\mathcal{Q}_A^{(k)}$ be any neural network satisfying Proposition 5.10 (ii) and (iii).

Now consider the **iUzawa-Net** $\mathcal{T}(y_d, f; \theta_{\mathcal{T}})$ with each layer sharing the neural networks $\mathcal{S} := \mathcal{S}^{(L-1)}$, $\mathcal{A} := \mathcal{A}^{(L-1)}$, $\mathcal{Q}_A := \mathcal{Q}_A^{(L-1)}$ and $\mathcal{Q}_S := \mathcal{Q}_S^{(L-1)}$. Denote $R_0 := R_0^{(L-1)}$, and consider any $(y_d, f)^\top \in B \times B$. Let $\{(u^k, p^k)^\top\}_{k=0}^L$ be the corresponding layer outputs of $\mathcal{T}(y_d, f; \theta_{\mathcal{T}})$. By the above construction and the independence of the constant C in (5.17) from $u^k, p^k, y_d, f, \delta, R_1$ and R_2 , we have for all $k = 0, \dots, L-1$ that

$$\max\{\|u^{k+1}\|_{H^s(\Omega)}, \|p^{k+1}\|_{H^s(\Omega)}\} \leq R_0^{(k)} \leq R_0.$$

Note in particular that $\max\{\|u^{k+1}\|_{H^s(\Omega)}, \|p^{k+1}\|_{H^s(\Omega)}\} \subset \overline{B}_{H^s(\Omega)}(R_2^{(k)})$. Hence, by (5.16) and the argument in the proof of Proposition 4.12, we have

$$\max\left\{\|u^{k+1} - \bar{u}^{k+1}\|_{L^2(\Omega)}, \|p^{k+1} - \bar{p}^{k+1}\|_{L^2(\Omega)}\right\} \leq \delta, \quad \forall k = 0, \dots, L-1, \quad (5.28)$$

for the sequences $\{\bar{u}^{k+1}\}$ and $\{\bar{p}^{k+1}\}$ satisfying (4.1) with $Q_A = (N + \tau I + \partial\theta)^{-1}$ and $Q_S = \mathcal{Q}_S$. Note that Q_S does not depend on δ . In view of (5.28), Proposition 4.5 guarantees that for any $\varepsilon > 0$, there exists a $\delta_0 = C\varepsilon$ where C is independent of ε , and $L_0 = O(1/\log(\varepsilon))$, such that for any $\delta < \delta_0$ and $L \geq L_0$, the above specified \mathcal{T} satisfies

$$\|T(y_d, f) - u^k\|_{L^2(\Omega)} \leq \|w^k - w^*\|_{L^2(\Omega) \times L^2(\Omega)} < \varepsilon, \quad \forall k \geq L_0. \quad (5.29)$$

\square

We remark that Theorem 5.11 holds even for $s > 1$. Specifically, given any bounded $B \subset H^s(\Omega)$ with $s > 1$, it is bounded (and even compact) in $H^{\lfloor s \rfloor}(\Omega)$ by [38, Theorem 11.8], and hence bounded (and even compact) in $H^1(\Omega)$ by applying the Rellich-Kondrachov theorem for integer regularity exponents [66, Theorem 7.4] if necessary. Using the same argument, one can show that the parameters λ, μ in Assumption 2.2 belong to $H^1(\Omega) \cap L^\infty(\Omega)$. Moreover, $S : L^2(\Omega) \hookrightarrow H^{-s}(\Omega) \rightarrow H^s(\Omega) \hookrightarrow L^2(\Omega)$ can be treated as a continuous mapping $L^2(\Omega) \hookrightarrow H^{-1}(\Omega) \rightarrow H^1(\Omega) \hookrightarrow L^2(\Omega)$. Hence, we are completely reduced to the case where Assumption 5.2 holds with $s = 1$, and thus Theorem 5.11 remains valid.

6 Numerical Experiments

In this section, we demonstrate the application of the proposed **iUzawa-Net** to several representative instances of the optimal control problem (1.1). A series of numerical results is presented to illustrate the effectiveness and efficiency of the **iUzawa-Net**. The codes were written in Python, and all the deep learning methods are implemented with PyTorch. The numerical experiments were conducted on a Linux server equipped with an Intel i7-14700K processor and two NVIDIA GeForce RTX 4090 GPUs. All the codes and generated data are available at <https://github.com/tianyouzeng/iUzawa-Net>.

6.1 Elliptic Optimal Control: Isotropic Case

We consider the following elliptic optimal control problem defined on the bounded domain $\Omega := (0, 1) \times (0, 1) \subset \mathbb{R}^2$:

$$\begin{aligned} \min_{y \in L^2(\Omega), u \in L^2(\Omega)} \quad & \frac{1}{2} \|y - y_d\|_{L^2(\Omega)}^2 + \frac{\alpha}{2} \|u\|_{L^2(\Omega)}^2 + I_{U_{ad}}(u), \\ \text{s.t.} \quad & \begin{cases} -\Delta y = u + f & \text{in } \Omega, \\ y = 0 & \text{on } \partial\Omega, \end{cases} \end{aligned} \quad (6.1)$$

where $\alpha > 0$ is a regularization parameter and $I_{U_{ad}}(\cdot)$ is the indicator functional of the admissible set

$$U_{ad} = \{u \in L^2(\Omega) \mid u_a(x) \leq u(x) \leq u_b(x) \text{ a.e. in } \Omega\}$$

for some given $u_a, u_b \in L^\infty(\Omega)$. Note that $I_{U_{ad}}(\cdot)$ equivalently imposes a control constraint $u \in U_{ad}$.

In this example, we consider the even more challenging case where u_a and u_b are also treated as parameters of (6.1) and vary across instances. This is allowed in implementation, since the neural network \mathcal{Q}_A^k in the **iUzawa-Net** admits u_a and u_b as inputs. We fix the regularization parameter $\alpha = 0.01$ and apply the **iUzawa-Net** to learn the solution operator that maps the problem data (y_d, f, u_a, u_b) to the optimal control u^* . To generate the training and testing datasets, we first discretize the domain $\overline{\Omega}$ as a uniform $m \times m$ grid denoted by $\overline{\mathcal{D}}$. For training, we set $m = 64$ and sample $N = 16384$ functions $\{(y_d)_i\}_{i=1}^N$ and $\{f_i\}_{i=1}^N$ independently from the following Gaussian random fields (GRFs) with Matérn covariance kernels [41]:

$$\begin{aligned} (y_d)_i &\sim \mathcal{GR}(0, (-\Delta_D + 9I)^{-1.5}), \\ f_i &\sim \frac{1}{\sqrt{2}} (\mathcal{GR}(0, (-\Delta_D + 9I)^{-1.5}) + \mathcal{GR}(0, (-\Delta_N + 9I)^{-1.5})), \end{aligned}$$

where Δ_D and Δ_N denote the Laplacian operators on Ω with homogeneous Dirichlet and Neumann boundary conditions, respectively. The control constraints $\{(u_a)_i\}_{i=1}^N$ and $\{(u_b)_i\}_{i=1}^N$ are generated as $(u_a)_i = \min\{a_i + v_i, 0\}$ and $(u_b)_i = \max\{b_i + w_i, 0\}$ for $i = 1, \dots, N$, with

$$\begin{aligned} a_i &\sim \text{Unif}(-10, -1), \quad b_i \sim \text{Unif}(1, 10), \\ v_i, w_i &\sim \frac{1}{\sqrt{2}} (\mathcal{GR}(0, (-\Delta_D + 9I)^{-2}) + \mathcal{GR}(0, (-\Delta_N + 9I)^{-2})). \end{aligned}$$

For each generated data tuple $((y_d)_i, f_i, (u_a)_i, (u_b)_i)$, we compute the corresponding optimal control u_i^* of (1.1) using the SSN method detailed in [67]. The training set is thus formulated as $\{((y_d)_i, f_i, (u_a)_i, (u_b)_i; u_i^*)\}_{i=1}^N$. A testing set of size $N = 2048$ is generated following the same procedure. To evaluate the generalization ability of the trained **iUzawa-Net** across different resolutions, we further generate two additional testing sets from the same distributions, each of size $N = 2048$, on finer grids of resolutions $m = 128$ and 256 , respectively. For each generated dataset, the number of active optimal controls u_i^* and the measure ratio $|A(u_i^*)|/|\Omega|$ for each active set $A(u_i^*)$ of each active⁶ u_i^* are summarized in Table 6.1. The presence of both active and inactive instances in the dataset ensures a comprehensive evaluation of **iUzawa-Net** across problems with active or redundant control constraint $u \in U_{ad}$.

We construct two **iUzawa-Nets**, called **iUzawa-Net-F** and **iUzawa-Net-S**, respectively. The **iUzawa-Net-F** uses different neural networks \mathcal{S}^k , \mathcal{A}^k , \mathcal{Q}_A^k , and \mathcal{Q}_S^k for each different layer k (hence the suffix **-F** for free),

⁶An optimal control u^* is considered active if $u^*(x) = u_a(x)$ or $u^*(x) = u_b(x)$ for some $x \in \overline{\mathcal{D}}$. For each active u^* , its active set is defined by $A(u^*) := \{x \in \Omega : u^*(x) = u_a(x) \text{ or } u^*(x) = u_b(x)\}$.

m	# of active u_i^*		$ A(u_i^*) / \Omega $ for active u_i^*	
	Training	Testing	Training Mean	Testing Mean
64	11450	1422	0.2116	0.2128
128	—	1419	—	0.2130
256	—	1433	—	0.2256

Table 6.1: Statistics of active optimal control and active sets in the training and testing datasets of different resolutions m . A dash (—) indicates that the corresponding data is not applicable.

while the **iUzawa-Net-S** employs weight tying across all layers (hence the suffix -S for shared). The rationality of the weight tying construction is theoretically guaranteed by Theorem 5.11: Note that Assumption 5.2 (i) and (iii) follow from the discussions in Remark 5.3, and Assumption 5.2 (ii) follows from the regularity of $(y_d)_i$, f_i , $(u_a)_i$, and $(u_b)_i$ induced by the Laplacian operators in the Matérn covariance kernels. We denote the two **iUzawa-Nets** uniformly as $\mathcal{T}(y_d, f, u_a, u_b; \theta_{\mathcal{T}})$, which shall not cause confusion by context. We take $L = 6$ layers for the **iUzawa-Net-F** and $L = 10$ layers for the **iUzawa-Net-S**. The configurations for the neural sub-networks are identical for the **iUzawa-Net-F** and **iUzawa-Net-S**, which are detailed as follows. Each of \mathcal{S}^k , \mathcal{A}^k , and \mathcal{Q}_S^k admits a lifting dimension of $m_p = 8$ and a maximum of $k_{\max} = 8$ truncated Fourier modes in each coordinate. We apply 4 Fourier layers in \mathcal{S}^k and \mathcal{A}^k with the GeLU activation function. We set $\gamma = 10^{-6}$ in \mathcal{Q}_S^k . For \mathcal{Q}_A^k , all hidden layers admit a width of 64, and we take $\tau = 10^{-4}$. All inputs are padded to a resolution of 72 for handling non-periodic cases. These configurations lead to a total of 272,094 trainable parameters for the **iUzawa-Net-F** and 45,349 parameters for the **iUzawa-Net-S**.

We train the **iUzawa-Net-F** and **iUzawa-Net-S** by minimizing the following empirical loss function of (2.15):

$$\mathcal{L}(\theta_{\mathcal{T}}) = \frac{1}{N} \sum_{i=1}^N \frac{\sum_{x \in \bar{\mathcal{D}}} |\mathcal{T}((y_d)_i, f_i, (u_a)_i, (u_b)_i; \theta_{\mathcal{T}})(x) - u_i^*(x)|}{\max \{ \sum_{x \in \bar{\mathcal{D}}} |u_i^*(x)|, \varepsilon_L \}}, \quad (6.2)$$

where we set $\varepsilon_L = 10^{-8}$. We employ the **AdamW** optimizer [43] with a batch size of 64 and train the networks for 300 epochs. The learning rate is initialized to 0.001 and is decayed by a factor of 0.6 every 30 epochs. The training process takes approximately 8×10^3 seconds for both the **iUzawa-Net-F** and **iUzawa-Net-S**.

To evaluate the performance of the trained models, we compute the following absolute and relative L^2 -errors of the predicted optimal control \hat{u} :

$$\varepsilon_{\text{abs}}(\hat{u}) = \|\hat{u} - u^*\|_{L^2(\Omega)}, \quad \varepsilon_{\text{rel}}(\hat{u}) = \frac{\varepsilon_{\text{abs}}(\hat{u})}{\|u^*\|_{L^2(\Omega)}}. \quad (6.3)$$

Furthermore, for comparison with benchmark operator learning methods for approximating the solution operator T , we test the numerical accuracy of two standard FNOs in [40] for approximating the solution operator of (6.1). One FNO is constructed with 3 Fourier layers, 10 Fourier modes, and a lifting dimension of 8; and the other employs 4 Fourier layers, 12 Fourier modes, and a lifting dimension of 15. The two FNOs contain 45,881 and 295,682 neural network parameters, which are slightly higher than the **iUzawa-Net-S** and the **iUzawa-Net-F**, respectively. The numerical results are reported in Table 6.2. Additionally, Figure 6.1 displays the computed control and the pointwise error relative to the reference solution for a randomly selected instance from the testing set.

The results in Table 6.2 demonstrate that the **iUzawa-Net-F** and **iUzawa-Net-S** achieve satisfactory accuracy with few layers. Compared with the FNOs, the proposed **iUzawa-Nets** yield significantly higher accuracy, highlighting the advantage of the optimization-informed network design. Furthermore, the results confirm the excellent generalization capability of the **iUzawa-Net-F** and **iUzawa-Net-S** in a zero-shot super-resolution setting, i.e., a model trained on low-resolution data can output accurate predictions for high-resolution inputs without any retraining or fine-tuning.

To evaluate the computational efficiency, we compare the inference time of the trained **iUzawa-Nets** with the runtimes of three established FEM-based methods: the SSN method in [50], the primal-dual method in [11, 26], and the inexact Uzawa method (1.5). For the primal-dual method, the stepsizes of 3.5×10^2 and 1

Method	m	$\varepsilon_{\text{rel}}(\hat{u})$		$\varepsilon_{\text{abs}}(\hat{u})$	
		Mean	SD	Mean	SD
iUzawa-Net-F	64	2.06×10^{-3}	1.03×10^{-3}	4.15×10^{-3}	1.91×10^{-3}
	128	2.31×10^{-3}	0.85×10^{-3}	4.87×10^{-3}	1.76×10^{-3}
	256	2.31×10^{-3}	0.79×10^{-3}	4.83×10^{-3}	1.61×10^{-3}
iUzawa-Net-S	64	3.58×10^{-3}	2.98×10^{-3}	6.85×10^{-3}	3.72×10^{-3}
	128	3.66×10^{-3}	2.76×10^{-3}	7.03×10^{-3}	3.69×10^{-3}
	256	3.69×10^{-3}	2.57×10^{-3}	7.33×10^{-3}	3.90×10^{-3}
3-layer FNO	64	1.44×10^{-2}	1.11×10^{-2}	2.97×10^{-2}	2.10×10^{-2}
	128	1.43×10^{-2}	1.08×10^{-2}	2.95×10^{-2}	2.15×10^{-2}
	256	1.44×10^{-2}	1.06×10^{-2}	3.05×10^{-2}	2.18×10^{-2}
4-layer FNO	64	1.07×10^{-2}	0.88×10^{-2}	1.58×10^{-2}	2.10×10^{-2}
	128	1.12×10^{-2}	0.82×10^{-2}	2.29×10^{-2}	1.56×10^{-2}
	256	1.12×10^{-2}	0.79×10^{-2}	2.23×10^{-2}	1.58×10^{-2}

Table 6.2: Comparison of numerical results for solving (6.1).

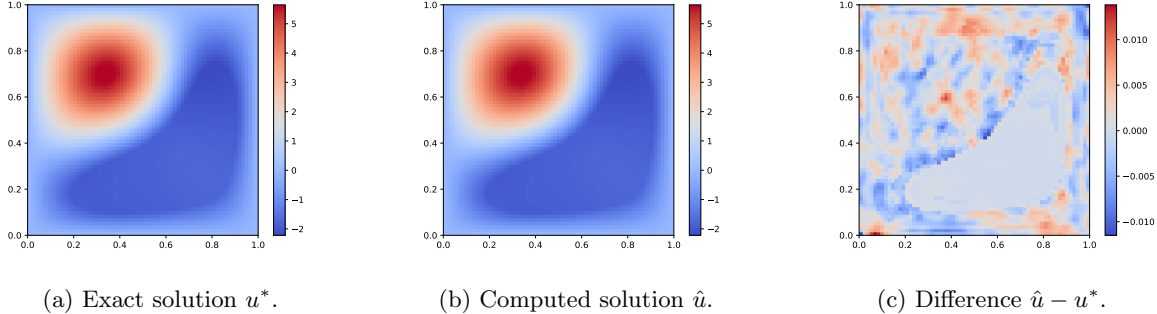


Figure 6.1: Computed optimal control for a single instance of (6.1) with $m = 64$.

are taken in each primal and dual update, respectively. The SSN method and the inexact Uzawa method do not require specific stepsize tuning. For the inexact Uzawa method, we adopt the preconditioning strategy from [59, Section 5]. To ensure a fair comparison, matrices in the linear systems are pre-factorized prior to timing for all compared methods where applicable. The termination criteria for each method are set as $\varepsilon_{\text{rel}} \leq \varepsilon_{\text{rtol}}$, where ε_{rel} is defined in (6.3). We take $\varepsilon_{\text{rtol}} = 2 \times 10^{-3}$, which matches the accuracy achieved by the trained **iUzawa-Net-F** and **iUzawa-Net-S**. The average computation time per instance for various resolutions m is reported in Table 6.3. In addition, we present the number of iterations or layer required for each numerical method in Table 6.4.

For $m = 64$, the performance of the **iUzawa-Net-F** and **iUzawa-Net-S** is comparable to that of the traditional iterative methods. However, as the resolution increases, the inference time of both the **iUzawa-Net-F** and **iUzawa-Net-S** remains nearly constant, whereas the computational cost of the iterative solvers grows significantly. Consequently, the two **iUzawa-Nets** demonstrate superior efficiency on finer resolutions for achieving a comparable level of accuracy.

6.2 Elliptic Optimal Control: Anisotropic Case

To further demonstrate the advantages of data-driven preconditioner training in the **iUzawa-Net**, we consider an ill-conditioned elliptic optimal control problem governed by an anisotropic elliptic operator. Specifically,

m	SSN	Primal-Dual	Inexact Uzawa	iUzawa-Net-F	iUzawa-Net-S
64	0.0792	0.0251	0.0427	0.0327	0.0546
128	0.1767	0.2187	0.1771	0.0348	0.0547
256	0.7739	0.9660	0.3550	0.0439	0.0547

Table 6.3: Computation time (seconds) of the SSN method, the primal-dual method, the inexact Uzawa method, the iUzawa-Net-F, and the iUzawa-Net-S for solving (6.1) under different resolutions m (averaged over instances in the testing sets).

m	SSN	Primal-Dual	Inexact Uzawa	iUzawa-Net-F	iUzawa-Net-S
64	2.59	10.77	17.94	6	10
128	1.91	10.78	7.71	6	10
256	1.94	10.78	6.57	6	10

Table 6.4: Number of iterations or layers of the SSN method, the primal-dual method, the inexact Uzawa method, the iUzawa-Net-F, and the iUzawa-Net-S for solving (6.1) under different resolutions m (averaged over instances in the testing sets).

let $\Omega = (0, 1) \times (0, 1) \subset \mathbb{R}^2$ and consider the following problem with a Neumann boundary condition:

$$\begin{aligned} \min_{y \in L^2(\Omega), u \in L^2(\Omega)} \quad & \frac{1}{2} \|y - y_d\|_{L^2(\Omega)}^2 + \frac{\alpha}{2} \|u\|_{L^2(\Omega)}^2 + I_{U_{ad}}(u), \\ \text{s.t.} \quad & \begin{cases} -\nabla \cdot (a \nabla y) + cy = u + f & \text{in } \Omega, \\ \frac{\partial y}{\partial \mathbf{n}} = 0 & \text{on } \partial\Omega, \end{cases} \end{aligned} \quad (6.4)$$

where $a \in \mathbb{R}^{2 \times 2}$ is a symmetric and positive definite matrix, $c > 0$ is a constant, and \mathbf{n} denotes the outward unit normal vector to $\partial\Omega$. Other symbols are defined as in Section 6.1. In this example, we set

$$a = \begin{pmatrix} 1 & 0 \\ 0 & 100 \end{pmatrix}, \quad c = 1, \quad \text{and } \alpha = 0.01.$$

The large contrast in the eigenvalues of the coefficient matrix a introduces strong anisotropy, making the problem ill-conditioned and numerically challenging.

As in Section 6.1, we treat u_a and u_b as problem parameters alongside y_d and f . The training and testing data are generated using the strategy described in Section 6.1, with the exception that $(y_d)_i$ is sampled from a Gaussian random field constructed to have non-vanishing boundary values:

$$(y_d)_i \sim \frac{1}{\sqrt{2}} (\mathcal{GR}(0, (-\Delta_D + 9I)^{-1.5}) + \mathcal{GR}(0, (-\Delta_N + 9I)^{-1.5})),$$

We generate a training set of size $N = 16384$ with resolution $m = 64$. The testing set consists of three groups with resolutions $m = 64, 128, 256$ and sizes $N = 2048, 64, 64$, respectively.

Two neural networks, iUzawa-Net-F and iUzawa-Net-S, are constructed using the same configuration as described in Section 6.1. We train the iUzawa-Net-F and iUzawa-Net-S by minimizing the empirical loss function defined in (6.2) using the AdamW optimizer with a batch size of 64 for 300 epochs. The learning rate is initialized as 0.002 and decays by a factor of 0.6 every 30 epochs. The total training time is approximately 8×10^3 seconds for each model.

We include in Figure 6.2 the computed control and the pointwise difference relative to the reference solution for a randomly selected instance from the testing set. The numerical errors of the computed solutions defined in (6.3) are reported in Table 6.5, which demonstrate that both the iUzawa-Net-F and iUzawa-Net-S achieve satisfactory accuracy despite the anisotropy of the problem. We compare the inference time of the iUzawa-Nets with the runtimes of the SSN method in [50], the primal-dual method in [11, 26],

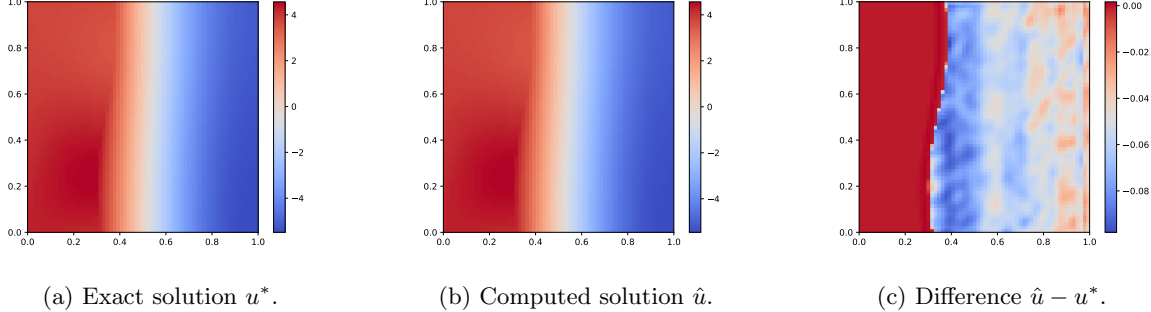


Figure 6.2: Computed optimal control for a single instance of (6.4) with $m = 64$.

and the inexact Uzawa method in [59]. The termination criteria are set to be the same as those in Section 6.1 with $\varepsilon_{\text{rtol}} = 4 \times 10^{-3}$, matching the relative accuracy of the trained neural networks. For the primal-dual method, we observe that small stepsizes are necessary to ensure convergence, and we take 2.0 for each primal update and 0.4 for each dual update. The results are reported in Table 6.6. The performance of both the SSN method and the primal-dual method deteriorates significantly under the ill-conditioned setting. The inexact Uzawa method, despite using a multigrid-based preconditioner, also suffers from the anisotropy. However, the inference time of the two **iUzawa-Nets** is nearly identical to that reported in Section 6.1. This confirms that the superiority in efficiency of the **iUzawa-Net** is even more substantial for the ill-conditioned case.

Method	m	$\varepsilon_{\text{rel}}(\hat{u})$		$\varepsilon_{\text{abs}}(\hat{u})$	
		Mean	SD	Mean	SD
iUzawa-Net-F	64	7.05×10^{-3}	9.29×10^{-3}	1.86×10^{-2}	1.91×10^{-2}
	128	6.41×10^{-3}	6.11×10^{-3}	1.72×10^{-2}	1.64×10^{-2}
	256	5.48×10^{-3}	3.84×10^{-3}	1.45×10^{-2}	1.02×10^{-2}
iUzawa-Net-S	64	4.60×10^{-3}	5.47×10^{-3}	1.12×10^{-2}	8.82×10^{-3}
	128	4.21×10^{-3}	3.00×10^{-3}	1.06×10^{-2}	7.60×10^{-3}
	256	3.95×10^{-3}	1.83×10^{-3}	9.93×10^{-3}	4.88×10^{-3}

Table 6.5: Numerical results for solving (6.4).

m	SSN	Primal-Dual	Inexact Uzawa	iUzawa-Net-F	iUzawa-Net-S
64	4.2924	1.1408	0.1711	0.0314	0.0521
128	21.3961	8.7064	1.1660	0.0356	0.0561
256	60.6969	23.0420	4.9387	0.0421	0.0564

Table 6.6: Computation time (seconds) of the SSN method, the primal-dual method, the inexact Uzawa method, the **iUzawa-Net-F**, and the **iUzawa-Net-S** for solving (6.4) with different grid resolutions m (averaged over instances in the testing sets).

Finally, we demonstrate the number of iterations (averaged over testing sets) required for the compared methods in Table 6.7. For achieving the same level of accuracy, the **iUzawa-Nets** requires significantly fewer layers than the number of outer iterations required by the primal-dual method (without preconditioner) and the inexact Uzawa method (with manually-designed multigrid-based preconditioner). This verifies the numerical advantages of the data-driven and automatic preconditioner-training mechanism of the **iUzawa-Net**. It is noteworthy that the SSN method requires fewer outer iterations due to its superlinear convergence property; however, this is at the cost of more computationally demanding inner iterations for solving the

resulting algebraic systems, as reflected by the computation time in Table 6.6.

m	SSN	Primal-Dual	Inexact Uzawa	iUzawa-Net-F	iUzawa-Net-S
64	3.64	209.23	29.06	6	10
128	2.86	214.19	21.61	6	10
256	3.08	215.75	22.02	6	10

Table 6.7: Number of iterations or layers of the SSN method, the primal-dual method, the inexact Uzawa method, the iUzawa-Net-F, and the iUzawa-Net-S for solving (6.4) under different resolutions m (averaged over instances in the testing sets).

6.3 Parabolic Optimal Control

We now extend our investigation to the following parabolic optimal control problem defined on the spatial-temporal domain $\Omega_T := \Omega \times [0, T_f]$ with $\Omega := (0, 1) \times (0, 1) \subset \mathbb{R}^2$ and $T_f = 1$:

$$\begin{aligned} \min_{y \in L^2(\Omega_T), u \in L^2(\Omega_T)} \quad & \frac{1}{2} \|y - y_d\|_{L^2(\Omega_T)}^2 + \frac{\alpha}{2} \|u\|_{L^2(\Omega_T)}^2 + \beta \|u\|_{L^1(\Omega_T)} + I_{U_{ad}}(u), \\ \text{s.t.} \quad & \begin{cases} \frac{\partial y}{\partial t} - \Delta y = u + f & \text{in } \Omega_T, \\ y = 0 & \text{on } \partial\Omega_T, \\ y(0) = 0 & \text{in } \Omega, \end{cases} \end{aligned} \quad (6.5)$$

where $\alpha > 0$, $\beta \geq 0$ are regularization parameters. The term $\beta \|u\|_{L^1(\Omega_T)}$ introduces sparsity in the optimal control, and the indicator functional $I_{U_{ad}}$ imposes a control constraint $u \in U_{ad}$, where the admissible set U_{ad} is defined by

$$U_{ad} = \{u \in L^2(\Omega_T) \mid u_a(x, t) \leq u(x, t) \leq u_b(x, t) \text{ a.e. in } \Omega \times [0, T_f]\} \quad (6.6)$$

for some $u_a, u_b \in L^\infty(\Omega_T)$.

In this numerical example, we set the parameters as $\alpha = 0.01$, $\beta = 0.01$, $u_a = -6$, and $u_b = 6$. We then apply the iUzawa-Net to learn the solution operator that maps the problem data (y_d, f) to the sparse optimal control u^* . For data generation, the spacial domain Ω is discretized as a uniform grid with a resolution of $m \times m$, and the time interval $[0, T_f]$ is discretized as m_T uniform time steps. We generate a training set of $N = 16384$ samples with $m = m_T = 32$ by drawing functions $\{(y_d)_i\}_{i=1}^N$ and $\{f_i\}_{i=1}^N$ independently from the GRF

$$(y_d)_i, f_i \sim \frac{1}{\sqrt{2}} (\mathcal{GR}(0, (-\Delta_D + 9I)^{-1.5}) + \mathcal{GR}(0, (-\Delta_N + 9I)^{-1.5})),$$

where Δ_D and Δ_N now denote the Laplacian operators on Ω_T with homogeneous Dirichlet and Neumann boundary conditions, respectively. For each data pair $((y_d)_i, f_i)$, the corresponding optimal control u_i^* is computed using a high-fidelity SSN algorithm [67], providing reference solutions for training. A testing set of $N = 2048$ samples with $m = m_T = 32$ is generated following the same procedure. To assess the model's zero-shot super-resolution generalization capability, we construct three additional testing sets of sizes $N = 64, 64, 16$ with finer resolutions $m = m_T = 64, 128, 256$, respectively.

We construct two iUzawa-Nets, named iUzawa-Net-F and iUzawa-Net-S, and denote them uniformly by $\mathcal{T}(y_d, f; \theta_T)$. The iUzawa-Net-F employs distinct weights for the neural networks \mathcal{S}^k , \mathcal{A}^k , \mathcal{Q}_A^k , and \mathcal{Q}_S^k in each layer k , while the iUzawa-Net-S uses shared weights across all layers. We take $L = 5$ layers for both the iUzawa-Net-F and the iUzawa-Net-S. The architecture of the modules is specified as follows. We adopt 3 layers in the FNOs \mathcal{S}^k and \mathcal{A}^k with a lifting dimension $m_p = 8$. For each Fourier layer, the truncated Fourier modes are set to $k_{\max} = 8$ in each coordinate, and the GeLU activation function is applied. For \mathcal{Q}_S^k , the lifting dimension is set to $m_p = 8$, the truncated Fourier modes are set to $k_{\max} = 8$ in each coordinate, and $\gamma = 10^{-6}$. We set the width of all hidden layers of \mathcal{Q}_A to $m_p = 64$. We take $\tau = 10^{-4}$ for both the iUzawa-Net-F and the iUzawa-Net-S. All inputs are padded to a resolution of 36 for accommodating

non-periodic boundary conditions. The total number of trainable parameters are 3,360,225 and 672,045 for the **iUzawa-Net-F** and the **iUzawa-Net-S**, respectively. All the learnable parameters are initialized using the default settings of PyTorch.

The networks are trained by minimizing the following empirical loss function of (2.15):

$$\mathcal{L}(\theta_{\mathcal{T}}) = \frac{1}{N} \sum_{i=1}^N \frac{\sum_{x \in \bar{\mathcal{D}}} |\mathcal{T}((y_d)_i, f_i; \theta_{\mathcal{T}})(x) - u_i^*(x)|}{\max \left\{ \sum_{x \in \bar{\mathcal{D}}} |u_i^*(x)|, \varepsilon_L \right\}}$$

with $\varepsilon_L = 10^{-8}$. We use the **AdamW** optimizer for 300 epochs with a batch size of 32. The learning rate is initialized to 5×10^{-4} and is decayed by a factor of 0.6 every 30 epochs. The training process takes approximately 2.8×10^4 seconds for both the **iUzawa-Net-F** and **iUzawa-Net-S**.

After training, the performance of the trained models are evaluated on the testing sets using the following absolute and relative L^2 -errors:

$$\varepsilon_{\text{abs}}(\hat{u}) = \|\hat{u} - u^*\|_{L^2(\Omega_T)}, \quad \varepsilon_{\text{rel}}(\hat{u}) = \frac{\varepsilon_{\text{abs}}(\hat{u})}{\|u^*\|_{L^2(\Omega_T)}}.$$

The numerical results are summarized in Table 6.8, and the solution of a randomly chosen instance from the testing set is visualized in Figure 6.3. These results affirm that both the **iUzawa-Net-F** and the **iUzawa-Net-S** achieve high accuracy for solving the parabolic optimal control problem (6.5). Notably, the data presented in Table 6.8 highlights the models' zero-shot generalization capability, as they perform well on spatial and temporal resolutions unseen during training.

Method	$m = m_T$	$\varepsilon_{\text{rel}}(\hat{u})$		$\varepsilon_{\text{abs}}(\hat{u})$	
		Mean	SD	Mean	SD
iUzawa-Net-F	32	3.39×10^{-3}	1.64×10^{-3}	7.14×10^{-3}	2.08×10^{-3}
	64	1.41×10^{-2}	3.39×10^{-3}	3.00×10^{-2}	8.97×10^{-3}
	128	1.99×10^{-2}	3.88×10^{-3}	4.72×10^{-2}	1.44×10^{-2}
	256	2.19×10^{-2}	3.37×10^{-3}	5.96×10^{-2}	2.19×10^{-2}
iUzawa-Net-S	32	4.97×10^{-3}	2.84×10^{-3}	1.02×10^{-2}	3.19×10^{-3}
	64	1.52×10^{-2}	4.12×10^{-3}	3.31×10^{-2}	9.84×10^{-3}
	128	2.11×10^{-2}	3.86×10^{-3}	4.77×10^{-2}	1.43×10^{-2}
	256	2.25×10^{-2}	3.46×10^{-3}	6.07×10^{-2}	2.11×10^{-2}

Table 6.8: Numerical results of **iUzawa-Net-F** and **iUzawa-Net-S** for solving (6.5).

Finally, we compare the computational efficiency between the trained **iUzawa-Nets** and an SSN method, the primal-dual method in [11, 26], and an inexact Uzawa method. For the SSN method, we employ a modified version of the implementation in [69, Section 4], solving the resulting linear systems with a preconditioned conjugate gradient method and multigrid cycles. The inexact Uzawa method is a straightforward extension of the approach in [59] to the parabolic setting. To ensure a fair comparison, matrices in the linear systems are pre-factorized prior to timing where applicable. The algorithms are terminated once any iteration \hat{u} satisfies $\varepsilon_{\text{rel}}(\hat{u}) \leq \varepsilon_{\text{rtol}}$, where we set $\varepsilon_{\text{rtol}} = 3 \times 10^{-3}$ to match the accuracy achieved by the trained **iUzawa-Nets**.

The computation time of different numerical methods is reported in Table 6.9. The results clearly indicate that the **iUzawa-Net-F** and **iUzawa-Net-S** significantly outperform the traditional numerical methods across all tested resolutions. This further validates the **iUzawa-Net** as a highly efficient solver for nonsmooth optimal control problems, underscoring the advantage of our approach where a forward-pass neural network architecture replaces a computationally costly iterative procedure. We observe that the computation time of the **iUzawa-Net-F** and **iUzawa-Net-S** increases less noticeably when the grid resolution is raised from 32 to 64 than when it is increased from 64 to 128. This behavior is mainly attributed to the fact that, for small m , the inference time is dominated by non-computational overheads, such as data transfer between the CPU and the GPU. This observation suggests that, when m is small, the efficiency of the **iUzawa-Net** could be further improved by optimizing hardware utilization, which we leave for future investigation.

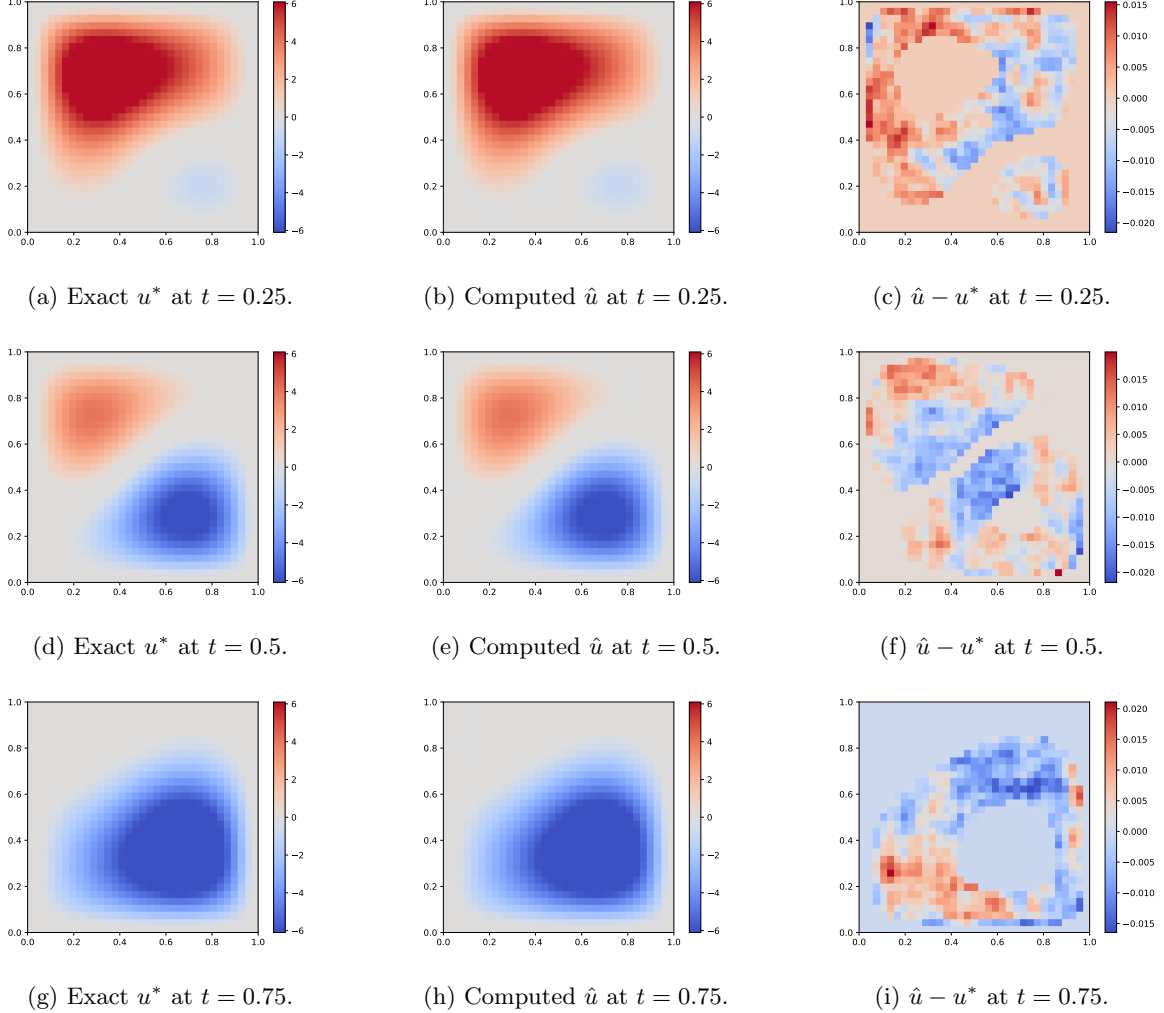


Figure 6.3: Computed optimal control for a single instance of (6.5) with $m = m_T = 32$.

7 Conclusions

We propose the **iUzawa-Net**, an optimization-informed deep neural network architecture that unrolls an inexact Uzawa method, for a general class of parameterized nonsmooth optimal control problems of linear PDEs. The proposed **iUzawa-Net** is capable of learning the solution operator that maps parameters defining the problem to the corresponding solution, effectively replacing iterations of a traditional solver with a forward pass of the neural network and hence making real-time solutions possible. Theoretically, we prove both universal approximation properties and the asymptotic ε -optimality with respect to network depth, notably extending these guarantees to the weight-tying setting under mild regularity assumptions. Numerical experiments for solving nonsmooth elliptic and parabolic optimal control problems demonstrate that the **iUzawa-Net** both achieves high accuracy with few layers and exhibits excellent generalization capability in zero-shot super-resolution scenarios. With real-time solvability, ease of implementation, structural interpretability, and theoretical guarantees, the **iUzawa-Net** is a new and powerful tool for solving optimal control problems of PDEs.

$m = m_T$	SSN	Primal-Dual	Inexact Uzawa	iUzawa-Net-F	iUzawa-Net-S
32	3.2701	0.3554	0.1800	0.0434	0.0411
64	7.8134	2.0814	0.4576	0.0564	0.0474
128	36.3343	8.7503	2.6888	0.3204	0.2584
256	278.5647	77.9398	28.5403	2.0640	2.0609

Table 6.9: Computation time (seconds) of the SSN method, the primal-dual method, the inexact Uzawa method, the iUzawa-Net-F, and the iUzawa-Net-S for solving (6.5) with different resolutions m and m_T (averaged over instances in the testing sets).

References

- [1] J. ADLER AND O. ÖKTEM, *Learned primal-dual reconstruction*, IEEE Transactions on Medical Imaging, 37 (2018), pp. 1322–1332.
- [2] H. ANTIL, *Mathematical opportunities in digital twins (MATH-DT)*, preprint, arXiv:2402.10326, 2024.
- [3] H. ATTTOUCH, R. LUCCHETTI, AND R. J.-B. WETS, *The topology of the ρ -Hausdorff distance*, Annali di Matematica Pura ed Applicata, 160 (1991), pp. 303–320.
- [4] H. H. BAUSCHKE AND P. L. COMBETTES, *Convex Analysis and Monotone Operator Theory in Hilbert Spaces*, CMS Books in Mathematics, Springer Cham, 2 ed., 2017.
- [5] H. H. BAUSCHKE, X. WANG, AND L. YAO, *General resolvents for monotone operators: characterization and extension*, preprint, arXiv:0810.3905, 2008.
- [6] M. BEHRENS, H. G. BOCK, S. ENGELL, P. KHOBKHUN, AND A. POTSCHKA, *Real-time PDE constrained optimal control of a periodic multicomponent separation process*, Trends in PDE Constrained Optimization, (2014), pp. 521–537.
- [7] M. BERGGREN, R. GLOWINSKJ, AND J.-L. LIONS, *A computational approach to controllability issues for flow-related models. (II): Control of two-dimensional, linear advection-diffusion and Stokes models*, International Journal of Computational Fluid Dynamics, 6 (1996), pp. 253–274.
- [8] L. T. BIEGLER, O. GHATTAS, M. HEINKENSCHLOSS, D. KEYES, AND B. VAN BLOEMEN WAANDERS, *Real-time PDE-constrained Optimization*, SIAM, 2007.
- [9] J. H. BRAMBLE, J. E. PASCIAK, AND A. T. VASSILEV, *Analysis of the inexact Uzawa algorithm for saddle point problems*, SIAM Journal on Numerical Analysis, 34 (1997), pp. 1072–1092.
- [10] S. P. CHAKRABARTY AND F. B. HANSON, *Optimal control of drug delivery to brain tumors for a test of PDE driven models using the Galerkin finite element method*, in Proceedings of the 44th IEEE Conference on Decision and Control, IEEE, 2005, pp. 1613–1618.
- [11] A. CHAMBOLLE AND T. POCK, *A first-order primal-dual algorithm for convex problems with applications to imaging*, Journal of Mathematical Imaging and Vision, 40 (2011), pp. 120–145.
- [12] P. D. CHRISTOFIDES AND J. CHOW, *Nonlinear and robust control of PDE systems: Methods and applications to transport-reaction processes*, Applied Mechanics Reviews, 55 (2002), pp. B29–B30.
- [13] S. DUBLJEVIC, N. H. EL-FARRA, P. MHASKAR, AND P. D. CHRISTOFIDES, *Predictive control of parabolic PDEs with state and control constraints*, International Journal of Robust and Nonlinear Control: IFAC-Affiliated Journal, 16 (2006), pp. 749–772.
- [14] S. DUBLJEVIC, P. MHASKAR, N. H. EL-FARRA, AND P. D. CHRISTOFIDES, *Predictive control of transport-reaction processes*, Computers & Chemical Engineering, 29 (2005), pp. 2335–2345.
- [15] J. ECKSTEIN, *Nonlinear proximal point algorithms using Bregman functions, with applications to convex programming*, Mathematics of Operations Research, 18 (1993), pp. 202–226.
- [16] H. C. ELMAN AND G. H. GOLUB, *Inexact and preconditioned Uzawa algorithms for saddle point problems*, SIAM Journal on Numerical Analysis, 31 (1994), pp. 1645–1661.
- [17] M. FISHER, J. NOCEDAL, Y. TRÉMOLET, AND S. J. WRIGHT, *Data assimilation in weather forecasting: a case study in PDE-constrained optimization*, Optimization and Engineering, 10 (2009), pp. 409–426.

- [18] Y. GAO, Y. SONG, Z. TAN, H. YUE, AND S. ZENG, *Prox-PINNs: A deep learning algorithmic framework for elliptic variational inequalities*, preprint, arXiv:2505.14430, 2025.
- [19] R. GLOWINSKI AND J.-L. LIONS, *Exact and approximate controllability for distributed parameter systems*, Acta Numerica, 3 (1994), pp. 269–378.
- [20] R. GLOWINSKI, Y. SONG, X. YUAN, AND H. YUE, *Application of the alternating direction method of multipliers to control constrained parabolic optimal control problems and beyond*, Annals of Applied Mathematics, 38 (2022), pp. 115–158.
- [21] K. GREGOR AND Y. LECUN, *Learning fast approximations of sparse coding*, in Proceedings of the 27th International Conference on Machine Learning, 2010, pp. 399–406.
- [22] M. GRIEVES AND J. VICKERS, *Digital twin: Mitigating unpredictable, undesirable emergent behavior in complex systems*, in Transdisciplinary Perspectives on Complex Systems: New Findings and Approaches, Springer, 2016, pp. 85–113.
- [23] M. W. GRIEVES, *Digital twins: Past, present, and future*, in The Digital Twin, Springer, 2023, pp. 97–121.
- [24] A. HAUPTMANN AND O. ÖKTEM, *Learned iterative networks: An operator learning perspective*, preprint, arXiv:2512.08444, 2025.
- [25] B. HE, Y. YOU, AND X. YUAN, *On the convergence of primal-dual hybrid gradient algorithm*, SIAM Journal on Imaging Sciences, 7 (2014), pp. 2526–2537.
- [26] B. HE AND X. YUAN, *Convergence analysis of primal-dual algorithms for a saddle-point problem: From contraction perspective*, SIAM Journal on Imaging Sciences, 5 (2012), pp. 119–149.
- [27] K. HE, X. ZHANG, S. REN, AND J. SUN, *Deep residual learning for image recognition*, in Proceedings of the IEEE Conference on Computer Vision and Pattern Recognition (CVPR), 2016.
- [28] J. HEINONEN, *Lectures on Lipschitz analysis*, Lecture Notes, University of Jyväskylä, 2005.
- [29] R. HERZOG AND E. SACHS, *Preconditioned conjugate gradient method for optimal control problems with control and state constraints*, SIAM Journal on Matrix Analysis and Applications, 31 (2010), pp. 2291–2317.
- [30] M. HINZE, R. PINNAU, M. ULRICH, AND S. ULRICH, *Optimization with PDE Constraints*, Mathematical Modelling: Theory and Applications, Springer Dordrecht, 2009.
- [31] S. A. H. HOSSEINI, B. YAMAN, S. MOELLER, M. HONG, AND M. AKÇAKAYA, *Dense recurrent neural networks for accelerated MRI: History-cognizant unrolling of optimization algorithms*, IEEE Journal of Selected Topics in Signal Processing, 14 (2020), pp. 1280–1291.
- [32] G. HUANG, Z. LIU, L. VAN DER MAATEN, AND K. Q. WEINBERGER, *Densely connected convolutional networks*, in Proceedings of the IEEE Conference on Computer Vision and Pattern Recognition (CVPR), July 2017.
- [33] N. KOVACHKI, S. LANTHALER, AND S. MISHRA, *On universal approximation and error bounds for Fourier neural operators*, Journal of Machine Learning Research, 22 (2021), pp. 1–76.
- [34] N. KOVACHKI, Z. LI, B. LIU, K. AZIZZADENESHeli, K. BHATTACHARYA, A. STUART, AND A. ANANDKUMAR, *Neural operator: Learning maps between function spaces with applications to PDEs*, Journal of Machine Learning Research, 24 (2023), pp. 1–97.
- [35] A. KRATSIOS, A. NEUFELD, AND P. SCHMOCKER, *Generative neural operators of log-complexity can simultaneously solve infinitely many convex programs*, preprint, arXiv:2508.14995, 2025.
- [36] K. KUNISCH AND A. RÖSCH, *Primal-dual active set strategy for a general class of constrained optimal control problems*, SIAM Journal on Optimization, 13 (2002), pp. 321–334.
- [37] M.-C. LAI, Y. SONG, X. YUAN, H. YUE, AND T. ZENG, *The hard-constraint PINNs for interface optimal control problems*, SIAM Journal on Scientific Computing, 47 (2025), pp. C601–C629.
- [38] G. LEONI, *A First Course in Fractional Sobolev Spaces*, no. 229 in Graduate Studies in Mathematics, American Mathematical Society, 2023.
- [39] B. LI, L. YANG, Y. CHEN, S. WANG, Q. CHEN, H. MAO, Y. MA, A. WANG, T. DING, J. TANG, AND R. SUN, *PDHG-unrolled learning-to-optimize method for large-scale linear programming*, preprint, arXiv:2406.01908, 2024.
- [40] Z. LI, N. B. KOVACHKI, K. AZIZZADENESHeli, B. LIU, K. BHATTACHARYA, A. STUART, AND A. ANANDKUMAR, *Fourier neural operator for parametric partial differential equations*, in International Conference on Learning Representations, 2021.

[41] F. LINDGREN, H. RUE, AND J. LINDSTRÖM, *An explicit link between Gaussian fields and Gaussian Markov random fields: the stochastic partial differential equation approach*, Journal of the Royal Statistical Society Series B: Statistical Methodology, 73 (2011), pp. 423–498.

[42] J. L. LIONS, *Optimal control of systems governed by partial differential equations*, vol. 170, Springer, 1971.

[43] I. LOSHCHILOV AND F. HUTTER, *Decoupled weight decay regularization*, in International Conference on Learning Representations, 2019.

[44] L. LU, P. JIN, G. PANG, Z. ZHANG, AND G. E. KARNIADAKIS, *Learning nonlinear operators via DeepONet based on the universal approximation theorem of operators*, Nature Machine Intelligence, 3 (2021), pp. 218–229.

[45] A. MANZONI, A. QUARTERONI, AND S. SALSA, *Optimal Control of Partial Differential Equations: Analysis, Approximation, and Applications*, Springer, 2021.

[46] J. R. MARTINS, *Aerodynamic design optimization: Challenges and perspectives*, Computers & Fluids, 239 (2022), p. 105391.

[47] U. MOSCO, *Convergence of convex sets and of solutions of variational inequalities*, Advances in Mathematics, 3 (1969), pp. 510–585.

[48] J. W. PEARSON, M. STOLL, AND A. J. WATHEN, *Regularization-robust preconditioners for time-dependent PDE-constrained optimization problems*, SIAM Journal on Matrix Analysis and Applications, 33 (2012), pp. 1126–1152.

[49] A. PINKUS, *Approximation theory of the MLP model in neural networks*, Acta Numerica, 8 (1999), pp. 143–195.

[50] M. PORCELLI, V. SIMONCINI, AND M. TANI, *Preconditioning of active-set Newton methods for PDE-constrained optimal control problems*, SIAM Journal on Scientific Computing, 37 (2015), pp. S472–S502.

[51] R. T. ROCKAFELLAR, *Convex Analysis*, Princeton University Press, 1970.

[52] R. T. ROCKAFELLAR AND R. J. B. WETS, *Variational Analysis*, no. 317 in Grundlehren Der Mathematischen Wissenschaften, Springer Berlin, 1998.

[53] J. O. ROYSET, *Stability and error analysis for optimization and generalized equations*, SIAM Journal on Optimization, 30 (2020), pp. 752–780.

[54] A. SCHIELA AND S. ULRICH, *Operator preconditioning for a class of inequality constrained optimal control problems*, SIAM Journal on Optimization, 24 (2014), pp. 435–466.

[55] A. SCHINDELE AND A. BORZÌ, *Proximal methods for elliptic optimal control problems with sparsity cost functional*, Applied Mathematics, 7 (2016), p. 967.

[56] A. SCHINDELE AND A. BORZÌ, *Proximal schemes for parabolic optimal control problems with sparsity promoting cost functionals*, International Journal of Control, 90 (2017), pp. 2349–2367.

[57] N. SHLEZINGER AND Y. C. ELDAR, *Model-based deep learning*, Foundations and Trends in Signal Processing, 17 (2023), pp. 291–416.

[58] N. SHLEZINGER, J. WHANG, Y. C. ELDAR, AND A. G. DIMAKIS, *Model-based deep learning*, Proceedings of the IEEE, 111 (2023), pp. 465–499.

[59] Y. SONG, X. YUAN, AND H. YUE, *An inexact Uzawa algorithmic framework for nonlinear saddle point problems with applications to elliptic optimal control problem*, SIAM Journal on Numerical Analysis, 57 (2019), pp. 2656–2684.

[60] Y. SONG, X. YUAN, AND H. YUE, *Accelerated primal-dual methods with enlarged step sizes and operator learning for nonsmooth optimal control problems*, preprint, arXiv:2307.00296, 2023.

[61] Y. SONG, X. YUAN, AND H. YUE, *The ADMM-PINNs algorithmic framework for nonsmooth PDE-constrained optimization: A deep learning approach*, SIAM Journal on Scientific Computing, 46 (2024), pp. C659–C687.

[62] Y. SONG, X. YUAN, H. YUE, AND T. ZENG, *An operator learning approach to nonsmooth optimal control of nonlinear PDEs*, preprint, arXiv:2409.14417, 2024.

[63] G. STADLER, *Elliptic optimal control problems with L^1 -control cost and applications for the placement of control devices*, Computational Optimization and Applications, 44 (2009), pp. 159–181.

[64] M. STOLL, *One-shot solution of a time-dependent time-periodic PDE-constrained optimization problem*, IMA Journal of Numerical Analysis, 34 (2014), pp. 1554–1577.

[65] M. STOLL AND A. WATHEN, *Preconditioning for partial differential equation constrained optimization with control constraints*, Numerical Linear Algebra with Applications, 19 (2012), pp. 53–71.

- [66] F. TRÖLTZSCH, *Optimal Control of Partial Differential Equations: Theory, Methods, and Applications*, no. 112 in Graduate Studies in Mathematics, American Mathematical Society, 2010.
- [67] M. ULRICH, *Semismooth Newton methods for operator equations in function spaces*, SIAM Journal on Optimization, 13 (2002), pp. 805–841.
- [68] M. ULRICH AND S. ULRICH, *Primal-dual interior-point methods for PDE-constrained optimization*, Mathematical Programming, 117 (2009), pp. 435–485.
- [69] H. WANG, C. YU, AND Y. SONG, *An augmented Lagrangian method for state constrained linear parabolic optimal control problems*, Journal of Optimization Theory and Applications, 203 (2024), pp. 196–226.
- [70] D. XIU AND D. M. TARTAKOVSKY, *Computational framework for real-time digital twins*, in Thermopedia, Begell House, 2025.
- [71] Y. YANG, J. SUN, H. LI, AND Z. XU, *Deep ADMM-Net for compressive sensing MRI*, in Advances in Neural Information Processing Systems, vol. 29, 2016.
- [72] Y. YANG, J. SUN, H. LI, AND Z. XU, *ADMM-CSNet: A deep learning approach for image compressive sensing*, IEEE Transactions on Pattern Analysis and Machine Intelligence, 42 (2018), pp. 521–538.
- [73] D. YAROTSKY, *Error bounds for approximations with deep ReLU networks*, Neural Networks, 94 (2017), pp. 103–114.
- [74] X. ZHANG, W. XU, S. S. NAIR, AND V. CHELLABOINA, *PDE modeling and control of a flexible two-link manipulator*, IEEE Transactions on Control Systems Technology, 13 (2005), pp. 301–312.